Molecular organization of tubular post-Golgi intermediates forming at the *trans*-Golgi network exit sites

Thesis

Molecular organization of tubular post-Golgi intermediates forming at the *trans*-Golgi network exit sites

Renato Gaibisso

Discipline: Life Sciences
Sponsoring Establishment: Consorzio Mario Negri Sud

Thesis submitted in accordance with the requirements of the Open University for the degree of Doctor of Philosophy
January 2009

To Filippo, my son
and to the memory of my grandfather

"The weakest things in this world
can overcome the strongest things"
Lao Tze

Abstract

The ability of cells to export proteins is essential for numerous cellular functions. Proteins for export are synthesised in the endoplasmic reticulum (ER) and move through the Golgi complex to the trans-Golgi network (TGN), from where they are shipped to various final destinations, including the plasma membrane (PM) (apical or basolateral, in polarized cells), early and late endosomes, and secretory granules.

The membranous carriers involved in the trafficking step from the TGN directly to the PM are much larger than vesicles, and are pleiomorphic rather than vesicular. They also do not possess an external coat, as has been seen with other types of carriers (e.g. clathrin, COPI and COPII vesicles). At present, the molecular mechanisms of the formation of these large pleiomorphic carriers are completely unknown.

I built up a thematic interactome to look at interactions between the many players involved in TGN-to-PM trafficking, and I have added some newly discovered interesting interactions through use of a two-hybrid matrix system. I thus focused my attention on some key elements such as the Arf1 and Arl1 interacting protein Arfaptin, the TRAnsport Protein Particle (TRAPP) complex, protein kinase D (PKD) and C-terminal binding protein/BFA-ribosylated substrate (Ctbp1-S/BARS) since these were revealed as being important nodes into this thematic interactome.

Arfaptin is a protein specifically recruited to the TGN through a BAR domain which can interact with membranes, possibly bending them; thus, Arfaptin might be relevant in the initial formation of carriers. We have discovered that PKD (a protein

involved in fission) phosphorylates and displaces Arfaptin from the Golgi complex, regulating its action in time, since the fission-mediated action of PKD occurs later. The fission activity of PKD can occur via Ctbp1-S/BARS, which is already known to be involved in membrane fission. Moreover, we have identified Ctbp1-S/BARS as a PKD phosphorylation substrate.

A possible role for the mammalian TRAPP complex in the exit of VSVG from the Golgi to the PM (TGN-to-PM), comes from the study of interaction networks after our two-hybrid screening. This has shown some links between TRAPP and other relevant players, such as PKD and 14-3-3γ. In yeast, TRAPPII has been characterized as being relevant for post-Golgi exocytic trafficking. The TRAPPII complex comprises TRAPPI (Bet5p, Trs20p, Bet3p, Trs23p, Trs31p, Trs33p, Trs85p) plus three TRAPPII-specific components (Trs65p, Trs120p, Trs130p). In yeast, as in mammals, Bet3 is an essential component, since it can anchor the rest of the complex to Golgi membranes. The removal of Bet3 both chronically, with specific siRNA and acutely, with microinjection of specific antibodies, shows for the first time a role for TRAPP in TGN-to-PM trafficking: Bet3 removal strongly delays the transport of VSVG specifically from the TGN to the PM, without affecting its ER-to-Golgi trafficking.

INDEX

Abbreviations

AP	Adaptor protein
ARF	ADP-ribosylation factor
ATTC	American tissue type collection
BSA	Bovine serum albumin
CGN	*Cis*-Golgi network
CtBP1-S/BARS	C-terminal binding protein/Brefeldin A-ribosylated substrate
DAG	Diacylglycerol
DMEM	Dulbecco's modified Eagles medium
DMSO	Dimethylsulfoxide
DTT	DL-dithiothreitol
EDTA	Ethilene diamine tetra-acetic acid
EM	Electron microscopy
ER	Endoplasmic reticulum
ERGIC	Endoplasmic reticulum–Golgi intermediate compartment
FCS	Foetal calf serum
GAP	GTP-ase activating protein
GDP	Guanosine diphosphate
GEF	Guanine nucleotide exchange factor
GERL	Golgi–endoplasmic reticulum–lysosomes
GFP	Green fluorescent protein
GPC	Golgi-to-plasma membrane carrier
GST	Glutatione-S-transferase
GTP	Guanosine triphosphate
HA	Haemagglutinin

HeLa	Henrietta Lacks
HEPES	4-(2-Hydroxy-ethyl)-piperazine-1-ethane-sulfonic acid
IF	Immunofluorescence
IgG	Immunoglobulin G
IPTG	Isopropyl-β-D-1-thiogalactopyranoside
LB	Luria-Bertani
MDCK	Madin-Darby canine kidney
M6PR	Mannose-6-phosphate receptor
NBD	Nucleotide-binding domain
O/N	Overnight
ORF	Open reading frame
PBS	Phosphate-buffered saline
PCR	Polymerase chain reaction
PH	Pleckstrin homology
PITP	Phosphatidylinositol transfer proteins
PKC	Protein kinase C
PKD	Protein kinase D
PLD	Phospholipase D
PM	Plasma membrane
SBD	Substrate binding domain
SDS-PAGE	Sodium dodecyl sulphate-polyacrylamide gel electrophoresis
siRNA	Small-interfering RNA
TGN	*Trans*-Golgi network
ts	Temperature sensitive
VSV	Vesicular stomatitis virus
VSVG	Vesicular stomatitis virus glycoprotein

VTCs Vesicular tubular clusters

List of Figures

List of Tables

Preface

One of the major characteristics that distinguishes living beings from inanimate things is homeostasis, conceived as the ability to maintain an internal composition distinct from the external, surrounding environment. Biological membranes provide the very boundaries within which life can exist, separating the panoply of biochemical reactions that define a living cell from the extracellular world. The plasma membrane (PM) is present in all living organisms, as it was surely present as a necessary condition for life in the first living organisms, which is started with the last universal common ancestor (LUCA) that has been estimated to have lived some 3- 4 billion years ago (Doolittle, 2000).

Compartmentalization is a mandatory condition for the maintenance of the chemical and osmotic conditions inside the cell. Nevertheless, phospholipid bilayers have many different functions other than compartmentalization, such as the selective import of nutrients and catabolite discarding, along with signalling and membrane trafficking events. These are the more evident functions of biological membranes. Over millions of years of evolution, compartmentalization has become more elaborate, since in eukaryotic cells, internal membranes have restricted specific cellular functions into specific, physically delimited compartments, such as mitochondria and chloroplasts, with the last in plants. The intracellular organelles have thus developed in the eukaryotic cell to allow specialized functions in specific areas of the cell.

Among all of the intracellular organelles, the Golgi complex is probably the most dynamic and complex organelle, and the more fascinating from the morphological point of view. However, the Golgi complex is also the most difficult to

understand from the molecular and physiological point of view. One reason for this complexity comes from the presence of many roads going to and coming from many different compartments of the secretory pathway.

Membrane trafficking is an equilibrium between fluxes of:

- Membrane lipids and 'cargo' proteins that have to move to their final destinations (PM, endosomes, vacuoles, lysosomes);
- Membrane lipids and resident enzymes that have to remain in their 'local' positions to maintain the subcompartment identity.

These two (in and out) fluxes both pass through the Golgi complex, which occupies a central position in the physiology of membrane trafficking, maintaining this equilibrium. Moreover, although membrane trafficking is extensive, it does not compromise the identity of the compartments involved.

The exit from the Golgi requires the fine sorting of several pathways, which occurs at the trans-Golgi network (TGN), among which the route starting from the TGN and destined directly to reach and fuse with the PM (TGN-to-PM trafficking) is the topic of this PhD project.

1 Introduction

1.1 Background

1.1.1 The discovery of a complex organelle

In 1898, the Italian histologist Camillo Golgi firstly described the "apparato reticolare interno", which literally means the 'internal reticular apparatus'. He used a cytochemical staining procedure based on silver nitrate that was originally set up for the study of the organization of the central nervous system. However, it was not until the early 1950s, with the introduction of the electron microscope, that the existence of the Golgi apparatus was fully accepted by the scientific community.

At that time, it became immediately clear how complex this organelle is. The collective electron microscopy studies carried out over the following years established that the Golgi complex consist of a morphologically heterogeneous set of membrane-limited compartments that have common recognizable features, and they are interposed between the endoplasmic reticulum (ER) and the PM. The constant and most characteristic structural component of the Golgi apparatus is a stack of smooth-surfaced cisternae (or saccules), which usually have a flattened, plate-like centre and more dilated rims. Another constant characteristic of the Golgi complex is the absence of ribosomes, which are instead confined in the rough endoplasmic reticulum (RER).

It is now clear that in addition to specific Golgi elements, the juxtanuclear Golgi region is crowded with other cellular structures, such as coated vesicles, lysosomes, and in many cases, centrioles with their associated microtubules.

The current vision presents the Golgi complex as separated into distinct components: the flattened cisternal saccules that are organised into stacks of cisternae closely apposed to one another; the vesicular (or round profiles) tubular network; and sometimes vacuolar profiles. Variations in the form, amount, and disposition of these components occur in different cell types and in different functional states of the cell. The cisternal profiles are divided into *cis*- medial- and *trans*-cisternae, starting from the beginning of the secretory pathway, moving towards the exit from the Golgi. The distal cisternae at both the *cis* and *trans* sides are less flattened and more tubulated, and they are generally budded and have curved profiles (Fig. 1). Vesicular profiles and tubular networks also characterize the extreme poles of these dynamic organelles.

Most plasma membrane and secretory proteins have one or more carbohydrate chains, and one of the main functions of the Golgi is to add these sugar moieties to these proteins. Some glycosylation reactions occur in the lumen of the ER, others in the lumina of the *cis*, medial-, or *trans*-Golgi cisternae. Thus the presence of certain carbohydrate residues on proteins provide useful markers for following their movement from the ER and through the Golgi cisternae (e.g. endo-H resistance).

In addition, over the last decade, it has become clear that beyond its primary biosynthetic, trafficking and sorting functions, the Golgi complex has an active role in global cell processes that are not necessarily and directly linked to membrane trafficking events, such as signalling, apoptosis and mitosis.

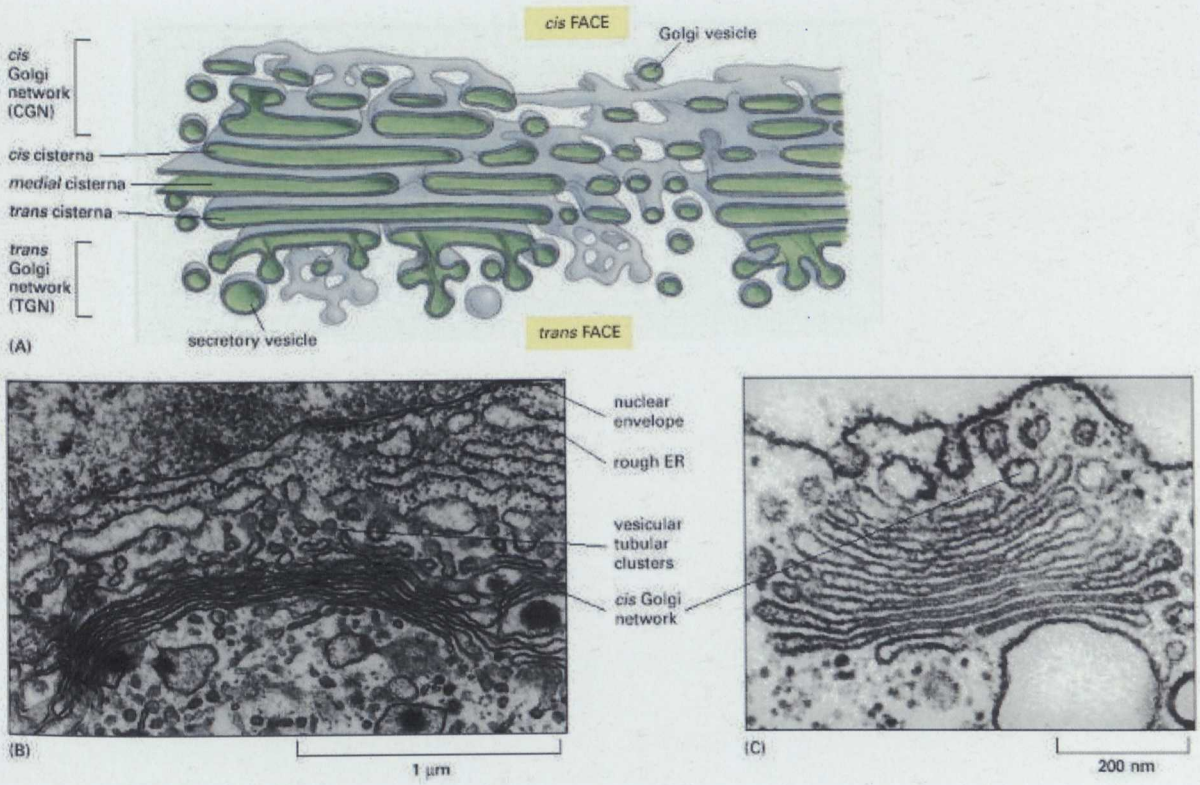

Figure 1. The Golgi complex
(A) Three-dimensional reconstruction from electron micrographs of the Golgi complex in a secretory animal cell. The *cis*-face of the Golgi stack is that closest to the ER. (B) A thin-section electron micrograph emphasizing the transitional zone between the ER and the Golgi complex in an animal cell. (C) An electron micrograph of a Golgi complex in a plant cell (the green alga *Chlamydomonas*) seen in cross section. In plant cells, the Golgi complex is generally more distinct and more clearly separated from other intracellular membranes than in animal cells. (A, redrawn from A. Rambourg and Y. Clermont, *Eur. J. Cell Biol.* 51:189–200, 1990; B, taken from Brij J. Gupta; C, taken from George Palade.)

1.1.2 The TGN

The TGN is the most complex among the membrane trafficking compartments, since it has the highest number of trafficking pathways that arrive and depart (discussed further in chapter 1.1.6), making it the most complicated sorting station in the cell (Fig. 2).

Novikoff and co-workers first described this compartment in 1964, and based on electron microscopy evidence and on the observation that acid phosphatase activity is often associated with this compartment, they postulated that these membranes constitute a link between the Golgi, the ER, and lysosomes. Accordingly, they introduced the acronym GERL as their designation (Novikoff and Novikoff, 1977). At that time, it became immediately evident that the *trans* side of many (but not all) Golgi stacks is often separated from the rest of the stack, and its characteristic morphology has been described as varying from straight (rigid lamellae) to tubular and tortuous.

Later on, a more detailed description of this trans-Golgi network (TGN) compartment was provided, indicating a system of tubules emanating from the *trans*-most Golgi cisterna that provides the exit sites for the processed glycoproteins (Griffiths and Simons, 1986).

Over the past few years, however, this model has been modified by observations based on electron microscopy tomography and cryofixation (Mogelsvang *et al.*, 2004), which have demonstrated that the TGN can derive not only from the last

Figure 2. Three-dimensional tomographic reconstruction of the Golgi complex, showing the *cis*-Golgi network (white) and the stack with the terminal three *trans*-cisternae in purple, red and blue. The TGN (purple) appears as a tubular network that emerges from the lateral part of one of the *trans*-cisternae, not necessarily the last *trans*-cisterna (blue). Bar, 200 nm.

trans cisterna, but also from the two adjacent *trans* cisternae, from which tubules project into the space overlying the Golgi stacks. Importantly, only the last cisterna and the tubules originating from it show clathrin-coated buds, indicating that potentially only the last cisterna is involved in transport to endosomes, which relies on clathrin-coated carriers (see below).

The current models of the Golgi complex do not usually incorporate the GERL structure. Its role has remained controversial for many years (Griffiths and Simons, 1986), despite documentation of the existence of this Golgi-associated structure in many morphological studies of different cell types. Then, the concept of the spatial relationship between the ER and the TGN was refined, particularly with more recent three-dimensional (3D) studies demonstrating that there are no continuities, whereby the membranes of these two compartments can appose each other instead, at the so-called ER-TGN contact sites, which are present in many different cell types (Levine and Loewen, 2006).

Taking into consideration our present knowledge, the term TGN is biased, as this organelle is composed of not only tubular networks, but also of disks, spheres and vacuolar structures. Nevertheless, for the sake of clarity, this term remains, since the TGN is still the most common term used to describe the Golgi exit sites among the scientific community.

The function of the TGN as an intersecting of many transport pathways means that it is the main sorting station. The TGN is important in this complicated situation, to insure that every cargo goes towards its correct destination, and hence not along the wrong pathway. The TGN functions as the main sorting station not only for newly synthesized proteins and lipids to their appropriate cellular destinations, but also for

the uptake of recycling proteins and lipids (Traub and Kornfeld, 1997; Bonifacino and Rojas, 2006). In the TGN, both anterograde and retrograde cargoes are re-sorted to at least two to six different destinations, depending on the cell type (Fig. 3). In many cells proteins are delivered to basolateral or apical PM endosomes, and to lysosomes or retrogradely to the Golgi complex (De Matteis and Luini, 2008). In regulated secretory cells, such as pancreatic acinar cells, there is an additional pathway directed through the storage and secretory granules.

The second main function of the TGN is participation in protein and lipid post-translational and post synthetic modifications. The TGN compartment contains a number of resident enzymes that are involved in the processing of the cargo molecules, such as sialylation and fucosylation of N-linked and O-linked glycans and sulphation of the glycosaminoglycans (GAGs). In addition, a number of proteins (e.g. albumin) are processed in the TGN from their pro-forms to their mature forms, via the cleavage of a pro-peptide, a process mediated by furin (Thomas, 2002).

1.1.3 Membrane trafficking

Generally speaking the term "membrane trafficking" describes the formation and the movement of specific membrane-bound compartments, together with their fluid-phase and protein contents (the "cargo") between and within intracellular subcompartments, or organelles. Membrane trafficking comprises: the secretory, endocytic and retrograde pathways.

In every eukaryotic cell, the huge number of proteins that pass thorough the Golgi system to reach the external environment make the secretory pathway of

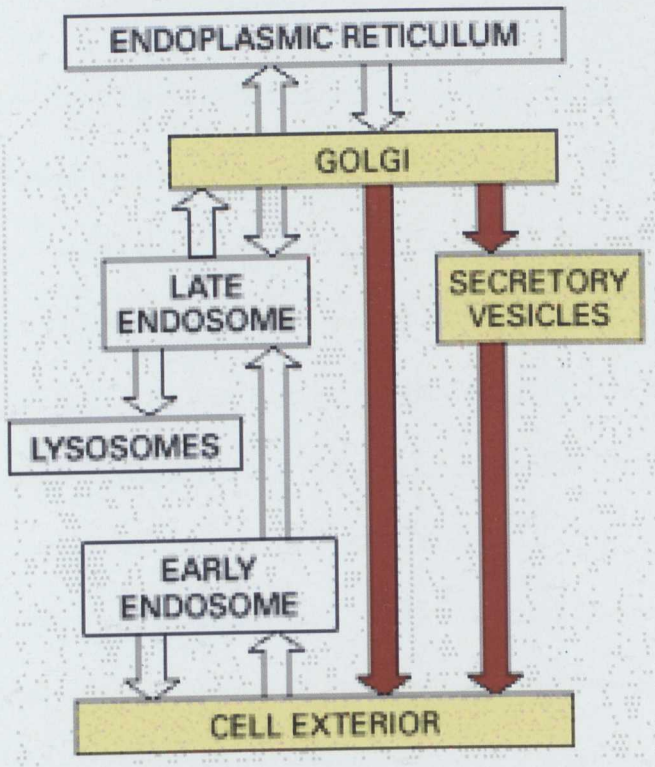

Figure 3 The endocytic and biosynthetic secretory pathways
In this "road map" of biosynthetic protein traffic, the endocytic and biosynthetic secretory pathways (red) are illustrated. In addition, the retrieval pathways by which the backflow of selected components is maintained are indicated.

absolute importance, such as cargo proteins involved in extracellular matrix construction/degradation, and receptors, signalling hormones, and so on.

All secretory and membrane proteins contain a leader or a signal peptide that can be segregated into the ER lumen or inserted into the ER membranes respectively. Cargo proteins move along the exocytic pathway in a vectorial way, which finally drives them to the external environment, and this is by definition the secretory pathway. Proteins that are not properly folded are retained in the ER by means of interactions with molecular chaperones, such as Bip, calreticulin and calnexin, that provide the correct "quality control" of proteins that exit the ER (Ellgaard and Helenius, 2003). Once synthesized and properly folded into the ER, the secretory proteins, membrane proteins of the PM or proteins that has to be retained in endosomes or lysosomes, pass thorough the ER-Golgi intermediate compartment (ERGIC), or vesicular-tubular clusters (VTCs), then they cross the cis-Golgi network (CGN), the *cis*-, the *medial*- and the *trans*-Golgi cisternae and the trans Golgi network (TGN), into which they are finally sorted and targeted to their final destination (Fig. 3). This last sorting step is remarkably complex.

The mechanisms by which proteins are synthesized or modified in one intracellular compartment and then transported to another intracellular organelle constitute one of the most challenging aspects for investigators in the field of membrane trafficking. Each step in the secretory pathway is characterized by a plethora of specific components that both regulate important processes, and provide temporal and spatial resolution. As the anterograde transport of cargo progresses through the secretory pathway, at the same time a large amount of membrane material is transferred retrogradely from one cellular compartment to another, thus implying

the existence of a highly regulated compensatory system of membrane recycling that maintains the identity of each organelle in terms of its lipid and protein composition (De Matteis and Luini, 2008).

1.1.4 ER-to-Golgi transport

Protein folding in the ER is triggered by a class of ER-resident proteins known as the chaperones. These proteins mediate both the folding of newly synthesized proteins, and the retention of misfolded proteins within the lumen of the ER. Among the chaperones, those that have been better characterised to date are the lectins calnexin and calreticulin, and other enzymes, such as BIP and protein disulphide isomerase (PDI) (Ellgaard and Helenius, 2003).

Once properly folded, newly synthesized proteins are sorted from the ER-resident proteins in the specialised zones known as ER exit sites, which are scattered over the surface of the ER. Here, the Ras-related small G protein Sar1 begins the process of the assembly of cytosolic COPII components for the formation of a complex sitting on the bilayer in a 'cage' form which promotes membrane budding and the subsequent formation of a transport carrier (Schekman and Orci, 1996). The COPII assembly on the membranes at the ER exit sites start with the Sec12-mediated nucleotide exchange of GTP (in place of GDP) on Sar1. This exchange is potentially triggered by cargo molecules or putative cargo receptors. The Sec23/24 and Sec13/31 heterodimers are then assembled on the cytoplasmic leaflet of the activated ER membrane, to form the COPII-coated bud (Fig. 4). This bud is generally believed to transform into a 50-nm vesicle, although it may not immediately sever, potentially allowing the formation of a tubule that could cluster with other adjacent COPII-derived tubules. ER exit sites observed at the electron microscope usually contain

multiple budding profiles, possibly representing budding vesicles that subsequently fuse locally to form pleiomorphic pre-Golgi transport intermediates (Stinchcombe *et al.*, 1995). An alternative possibility is that the budding profiles represent ER exit sites that transform directly into pre-Golgi intermediates without the need for small 50-nm vesicle intermediates (Mironov *et al.*, 2003), as happens in the classical view of ER-to-Golgi transport. What is clear from the molecular point of view is that the Sar1-COPII system is necessary to allow transport from the ER to the Golgi, since mutants of COPII components or Sar1 result in a block in protein exit from the ER (Kaiser and Schekman, 1990; Barlowe *et al.*, 1993).

1.1.5 Golgi-to-ER retrograde transport

Resident ER proteins, such as the chaperones mentioned above, can 'escape' from the ER along with anterograde cargoes. Then from their workplace (the ER) they 'fall' into VTC or Golgi compartments. Thus, to maintain the compartmental identity of both ER and Golgi these proteins need to be retrieved back from the Golgi via a transport system that is distinct from the COPII system.

COPI is an heptameric (α–, β–, β'–, γ–, δ–, ε–, ζ-COP) cytosolic protein complex that exists in a preassembled form in the cytosol (Bonifacino and Lippincott-Schwartz, 2003). In conjunction with the Ras-like GTP-binding protein Arf1, it assembles onto Golgi membranes to form an electron-dense coat that facilitates membrane budding (and probably also fission) of transport intermediates (Pepperkok *et al.*, 1993) (Fig. 4). Although initially the COPI system was believed to mediate anterograde cargo transport (Pepperkok *et al.*, 1993), these COPI vesicles are not enriched with anterograde cargoes. One possible explanation for the COPI-anterograde hypothesis could be that indirect effects on anterograde transport can

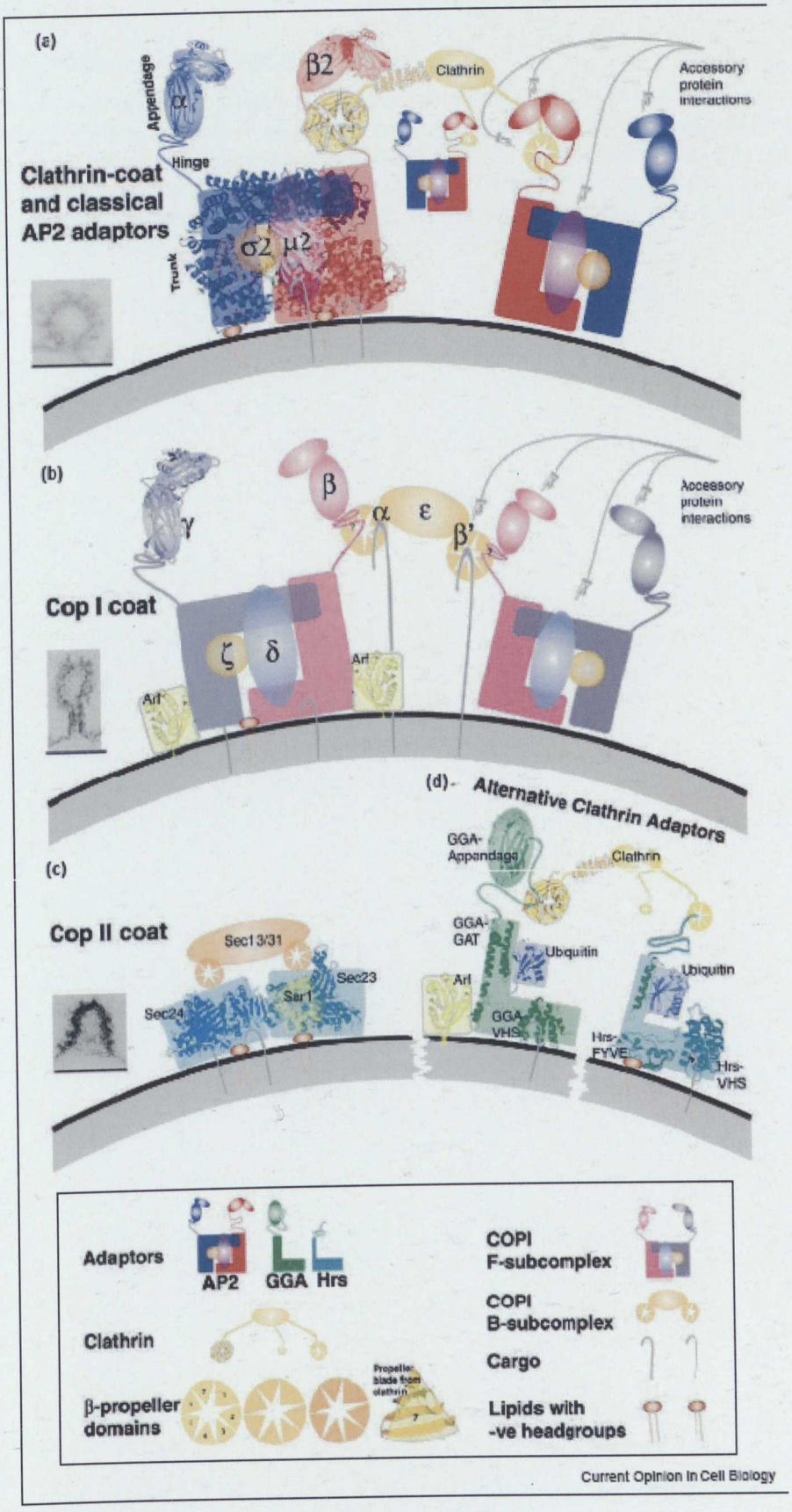

(See next page for legend)

PAGE

NUMBERING

AS ORIGINAL

Figure 4. COPI coats and clathrin-adaptor coats

(a) The 'classical' AP2 clathrin adaptor with its four subunits forms a complex that links cargo recruitment to clathrin. Clathrin is a trimer and each terminal domain is represented as being bound to a β2 adaptin appendage and hinge domain. (b) The COPI subunits (c) The COPII subcomplexes, Sec23/24 and Sec13/31. (a,b,c) Inset: EM image of relevant coated-vesicle budding. Scale bar, 100nm (d) Alternative clathrin adaptors GGAs and Hrs. (from McMahon et al. 2004)

occur due to disequilibrium between anterograde and retrograde transport, which are mutually dependent.

At present, one of the most accepted roles for the COPI machinery is to mediate the budding of retrograde vesicles, which would recycle proteins back from the Golgi complex to the ER, or from late Golgi compartments to early Golgi compartments (Pelham, 1994). The COPI subunits can bind dilysine residues in the motif KKXX, which is believed to function as an ER-retrieval sequence on proteins. Moreover, proteins that have mutations to these sequences are delivered to the cell surface (Letourneur *et al.*, 1994).This KKXX motif is present in the KDEL receptor, a recycling protein that is involved in the retrieval of ER-resident proteins containing the KDEL signal sequence, such as the chaperones (Griffiths *et al.*, 1994).

1.1.6 Many pathways to and from the TGN

The role of the TGN as a point of intersection of many transport pathways means that it is the main sorting station. The TGN is important to ensure that cargoes go towards their correct destinations, and not along the wrong pathways. Indeed, the TGN functions as the main sorting station not only for newly synthesized proteins and lipids, but also for recycling proteins and lipids (Traub and Kornfeld, 1997). In the TGN, both anterograde and retrograde cargoes are sorted to at least two to six different destinations, depending on the cell type. In ordinary cells, proteins are delivered to the basolateral or apical PM, or to endosomes, or lysosomes, or retrogradely to the Golgi complex (De Matteis and Luini, 2008). The TGN also receives proteins and lipids moving from the PM towards the ER, such as with the bacterial toxins, like the Shiga toxin family (Sannerud *et al.*, 2003). In regulated secretory cells there is an additional pathway directed to storage or secretory granules (Tooze, 1998) (Fig. 6).

Some of these cargo carriers that bud and are released from the TGN are clathrin-dependent. The formation of these clathrin-coated carriers is triggered by Arf1 which, via its GTP/GDP cycle promotes the recruitment and activation of adaptor proteins, such as the APs (AP1, AP3, AP4) or the 'atypical' adaptors Golgi-localized, γ-ear-containing Arf-binding proteins (GGAs) (Fig 4). APs (the acronym originally meant 'assembly polypeptides' although conveniently it also stands for 'adaptor protein') then mediate clathrin recruitment and cargo segregation (Robinson, 2004). Clathrin-coated carriers mediate the formation of vesicles containing the mannose-6-phosphate receptor (M6PR), which is destined to the late endosomes (LEs), and the formation of the secretory granules destined to the external surface in a regulated fashion.

1.2 TGN-to-PM transport

1.2.1 General view

The transport of membrane-bound or secreted proteins from the TGN directly to the external surface is generally considered as a constitutive pathway. This transport occurs in all known cell types and is divided into apical (AP), e.g. the GPI-anchored proteins, p75, and HA cargoes, and basolateral (BL) transport, e.g. the vesicular stomatitis virus G protein (VSVG) and LDL receptor cargo transport in epithelial (thus polarized) cells. For many years MDCK cells have been the model for targeted delivery since they have a clear epithelial polarity.

Apical and basolateral membrane domains can be recognized in all epithelial cells; indeed, they can also be recognized (with less confidence) in non-epithelial cells that have specialization of different PM domains, such as hepatocytes, retinal pigment epithelium cells, retinal rod photoreceptors, hippocampal neurons and osteoclasts. These cells thus show transport towards distinct domains of the plasma membrane

(Keller and Simons, 1997) (Fig 5). In some cases, the polarization of secretory cargoes can depend on the functional state of the cell, as in the case of human fibroblasts: when they are 'resting', the delivery of different cargoes occurs randomly towards all of the PM, while when they are in a functional state of movement instead, different cargoes appear to be segregated towards different PM domains, such as the leading edge of the cell.

Until a few years ago, it was believed that all intracellular carriers were small coat (e.g. clathrin, COPII and COPI)-derived vesicles, but it is now clear that the bulk of the traffic is carried by large pleiomorphic tubular-saccular intermediates. This is the case for the transport between the ER and the Golgi complex via VTCs (as mentioned above), and also for transport between the TGN and the PM, which is the topic of this thesis.

Although VTCs have a pleiomorphic structure that is to some extent comparable to the carriers that mediate TGN-to-PM transport, they also have COPI and COPII present on some part of their structure; TGN-to-PM carriers do not. Indeed, the biggest difference seen for TGN-to-PM transport, as compared to the above-mentioned trafficking routes, is the absence of clathrin or another type of coat, at least revelable by electron microscopy as an electrondense coat, as is the case for COPI-, COPII- and clathrin-coated structures (Polishchuk *et al.*, 2003).

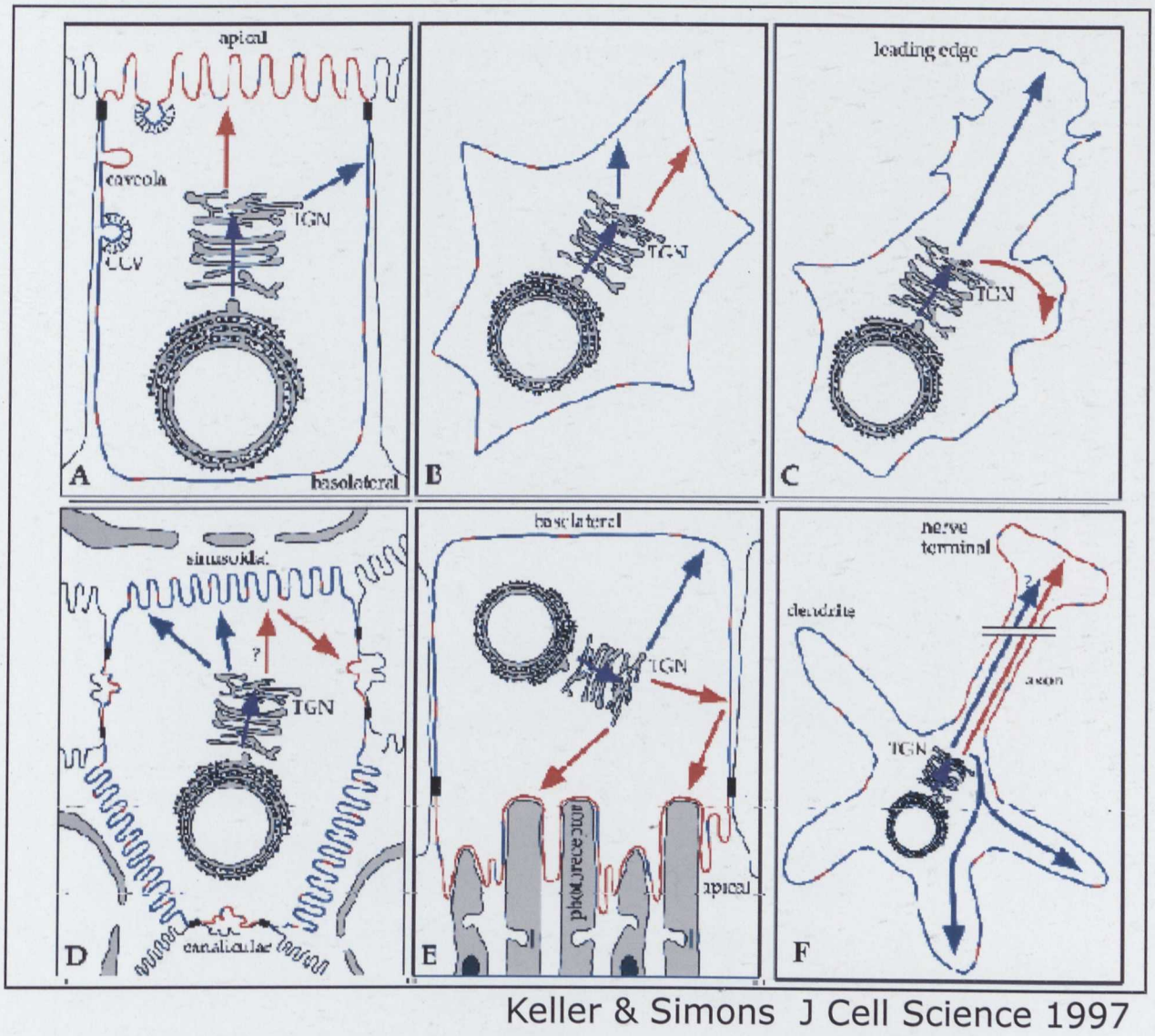

Figure 5. Apical and basolateral pathways in polarized and non-polarized cells

Membranes equivalent to the apical and basolateral surfaces of (A) MDCK cells are depicted in red and dark blue, respectively. (B) While in a resting fibroblast apical and basolateral pathways reach the cell surface randomly, (C) a migrating fibroblast uses the basolateral route to deliver newly synthesized proteins to the leading edge. (D) Hepatocytes contain at least two pathways to the basolateral surface. They, however, do not have a direct apical pathway,but instead use a transcytotic route. As indicated by the question mark, it is not known whether apical proteins use a raft-dependent mechanism to reach the basolateral surface in hepatocytes. (E) Retinal pigment epithelium cells use a direct as well as an indirect pathway for apical delivery. (F) In hippocampal neurons the axon and somatodendritic surfaces are equivalent to the apical and basolateral domains of MDCK cells, respectively.

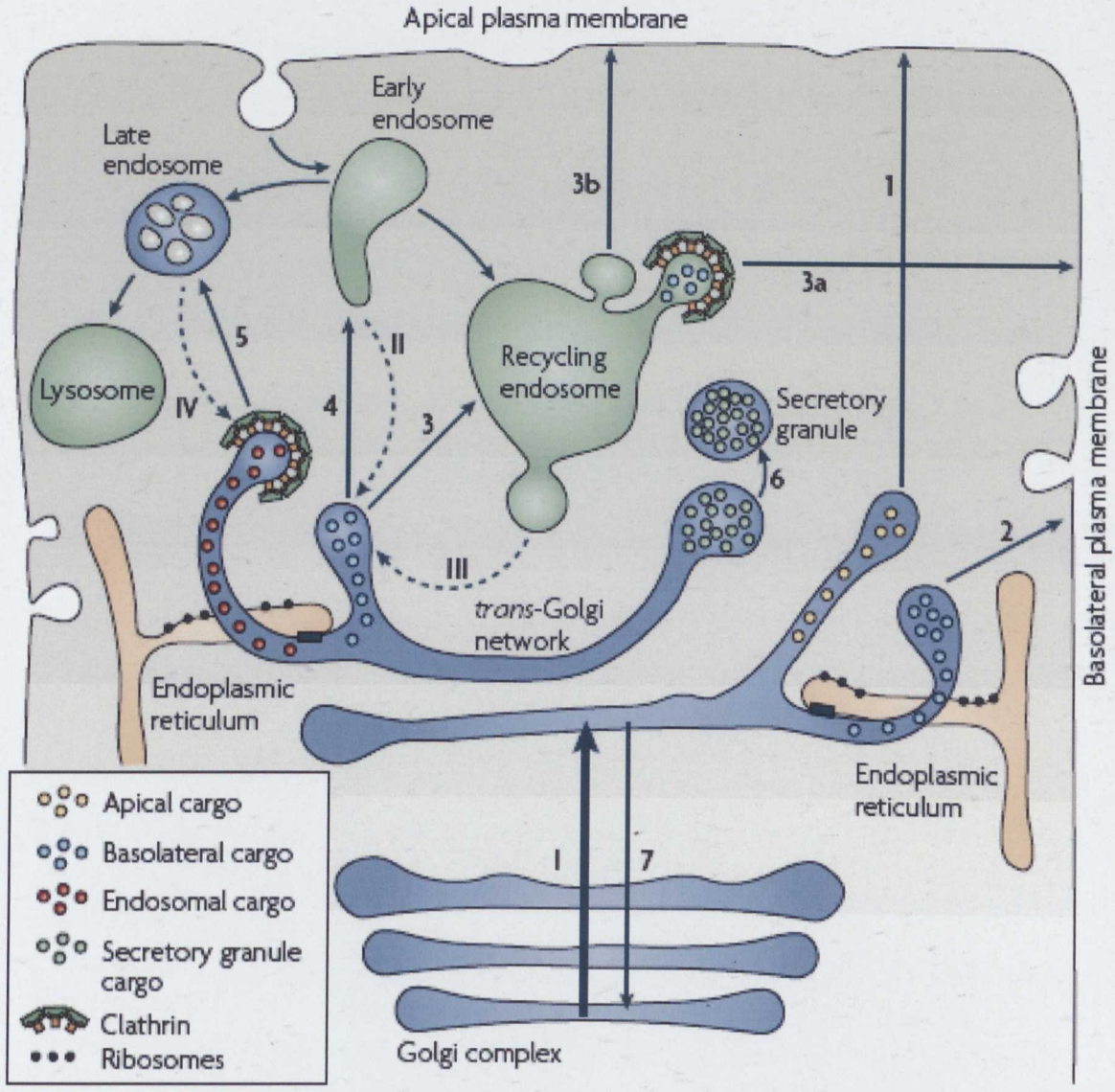

Figure 6. The *trans*-Golgi network (TGN) sorts newly synthesized proteins
The *trans*-Golgi network (TGN) sorts newly synthesized proteins that arrive from earlier Golgi compartments (I) towards different destinations (1–6). It also receives input from the endocytic pathway (II–IV) and sends back components to the earlier Golgi compartments (7). The exit routes from the TGN include those towards the apical plasma membrane (1), the basolateral plasma membrane (2), recycling endosomes (3), early endosomes (4), late endosomes (5) and specialized compartments such as secretory granules (6) in secretory cells. Secretory proteins can also use a transendosomal pathway through recycling endosomes to reach the basolateral (3, 3a) or apical surfaces (3, 3b). Golgi-resident proteins recycle back to the Golgi stack (7), as secretion consumes the last *trans*-Golgi cisternae. The endoplasmic reticulum makes close contact with the last two *trans*-Golgi cisternae (black boxes), through which lipid exchange can occur between these two organelles. Picture taken by (De Matteis and Luini *Nat Rev Mol Cell Biol* 2008).

The major characterisation of these so called 'pleiomorphic' carriers is due to morphological studies carried out over the past few years, which gave them the name of Golgi-to-plasma membrane carriers (GPCs) (Luini *et al.*, 2008).

GPCs are more easily seen after the release of a 20°C temperature block (allowing secretory proteins to reach the last compartment of the Golgi complex, but not to leave it, resulting in accumulation of cargo in the Golgi). After the temperature shift to 32°C the transport toward the PM occurs in the form of large (sometimes as much as half the length of a cisterna), pleiomorphic/tubular, sometimes fenestrated/anastomosed, membrane carriers. These bud, elongate, and then detach *en bloc* from the TGN, and finally follow microtubular tracks until they fuse with the PM (Polishchuk *et al.*, 2003).

The "lifecycle" of a GPC consists of four distinct stages: (i) the formation of TGN tubular export domains, where different cargoes are segregated from each other and from the Golgi enzymes; (ii) the docking of these tubular domains onto molecular motors and their extrusion towards the cell periphery along microtubules; (iii) the fission of the forming GPC from the donor membrane; and finally (iv) the delivery of the newly formed GPC to the plasma membrane (Fig. 7).

The first step (formation) includes the segregation of the cargo proteins from the Golgi-resident enzymes. These export domains usually contain TGN markers, such as TGN46; i.e. they are part of the TGN (Polishchuk *et al.*, 2003). As described above, the TGN derives not only from the last *trans* cisterna, but also from the three *trans*-most cisternae, from were tubules emanate into the *trans* space of the Golgi stacks. Remarkably, only the *trans*-most cisterna has clathrin-coated buds. Thus it is likely,

although yet to be formally demonstrated, that the carriers emanating from the clathrin-free cisternae are all contributing to the formation of GPCs that are constitutively directed to the PM.

The second step (extrusion) apparently requires the pulling force of molecular motors, such as kinesin (see below). This pulling force is applied to the TGN membranes, and it is important to facilitate the extension of GPC precursors from the Golgi body, and later for the fission step of the GPC (see below) (Kreitzer *et al.*, 2000; Polishchuk *et al.*, 2003). In cell-free systems, the addition of kinesin to Golgi membranes (and even to liposomes) together with microtubules induces the formation of tubule-like membranes that are similar to GPC precursors (Roux *et al.*, 2002), while a block of kinesin function by microinjection of an inhibitory antibody (Kreitzer *et al.*, 2000) or expression of the headless kinesin mutant (Nakata and Hirokawa, 2003) prevents GPC formation from the Golgi complex. Kinesin has been seen to be associated with the tip of the GPC precursors, although it can also attach to other points along the GPC precursor membrane (Polishchuk *et al.*, 2003).

Microtubular motors can have critical roles also in the third step (fission): the movement of kinesins along microtubules can create tension within a GPC precursor that facilitates the fission process. Indeed, based on *in-vitro* data, membranes under tension have recently been proposed to have an important role in fission (Roux *et al.*, 2006). *In vivo,* the stop-and-go characteristic movement of GPCs directed to the PM (Polishchuk *et al.*, 2003) might be due to a fission event that is concomitant to a pause in the movement, which reasonably corresponds to the time required for a tubular membrane to stretch and break under tension. The movement can then continue to bring the smaller, severed membrane carriers towards the PM.

What has been seen from this time-step analysis of the constitutive TGN-to-PM transport is indeed the important role of morphological knowledge in the understanding of such a complex process.

The morphology of the TGN is very dynamic and depends also on its secretory status. When exit from the TGN is blocked by a lowering of the temperature to 20°C in the presence of abundant cargo, the volume and surface area of the TGN increase greatly (Griffiths *et al.*, 1989); while in the absence of cargo, a 20°C block results in all three of the *trans*-most cisternae producing bulging exit domains (Ladinsky *et al.*, 2002). At physiological temperatures, three-dimensional (3D) analyses of the Golgi stacks have revealed well developed, tubular-reticular, TGN-like membranes at the *trans* side of the Golgi complex in actively secreting cells, while the TGN is nearly absent in quiescent cells (Trucco *et al.*, 2004).

From these observations, a model of the TGN emerges by which this organelle consists essentially of a dynamic assembly of tubular export domains that form on arrival of cargo and that are then consumed as export carriers. In this context, the questions that arise are: How is the segregation of cargo within the distinct tubular domains of the TGN achieved? How are the different tubular domains established? How are they converted into export carriers?

Below, I will describe the underlying mechanisms separately, although they might in fact operate concomitantly and in an integrated fashion. In the 'molecular players' section, I will list the individual entities, along with their known molecular roles, and in the 'molecular machineries' section, I will attempt to group them into

(relatively arbitrary) separate functional modules, based on the current models in the literature.

1.2.2 Molecular players

The transport of the G protein of vesicular stomatitis virus (VSVG) in its thermo-sensitive (ts) version is used as a reliable and potent marker of transport in the secretory pathway, as it is synchronizable by temperature blocks: at 40° C, VSVG is retained in the ER because the temperature sensitivity causes a folding problem, then at 32° C, VSVG can assume its correct conformation, and it can thus leave the ER. Another way to syncronize VSVG (as with many other molecules) is with a 20° C temperature block, which allows VSVG to reach the Golgi complex, but blocks its exit from the TGN. This is not due to a folding problem, but it depends on a still unclarified mechanism. Here, I will describe the molecular players that are responsible for TGN-to-PM traffic of VSVG, grouping them into functional classes.

Signalling proteins are involved in a series of signalling pathways, which are apparently unrelated to trafficking. In future work, signalling proteins and their pathways can put in relationship the external stimuli and the regulation of Golgi functions.

The $\beta1\gamma2$/ $\beta3\gamma2$ subunits of the heterotrimeric G-proteins can trigger the activation of PKCη, which in turn activates protein kinase D (PKD), promoting the fission of PM-directed carriers containing VSVG (Liljedahl *et al.*, 2001; Yeaman *et al.*, 2004; Diaz Anel and Malhotra, 2005). PKD is also responsible for a series of cellular processes, as it is a signalling protein that triggers cell survival, cancer, invasiveness and immune responses (Wang, 2006).

Src kinase is important in an endomembrane signalling circuit that is triggered by ER-to- Golgi trafficking, allowing the progression of VSVG out of the Golgi (Pulvirenti *et al.*, 2008). Src might thus provide regulation of the homeostasis between the arrival and departure membranes and cargoes.

Small G proteins and their related factors are fundamental regulators of membrane trafficking. The Arf1 protein acts in the multiple regulation of several pathways in membrane trafficking (Donaldson *et al.*, 2005) as briefly elucidated in the previous sections. In the TGN-to-PM trafficking of VSVG Arf1 acts via the recruitment and activation of PI4KIIIβ on the Golgi complex, thus triggering the production of phosphatidylinositol 4-phosphate (PtdIns4*P*), and thus acting on the local lipid composition, generating distinct TGN microdomains (De Matteis and Godi, 2004). Many Arf1 regulators and effectors are present at the TGN, including the brefeldin A (BFA)-sensitive GDP/GTP exchange factors (GEFs) BIG1 and BIG2 (Gillingham and Munro, 2007), and the GTPase-activating protein (GAP) ARAP1, which is enriched at the TGN (DeMatteis laboratory, unpublished observation).

The small GTPase Cdc42 is a regulator of actin polymerization that has been characterized as having important functions in signalling and cytoskeletal reorganization. Cdc42 binds to the Golgi complex in an Arf-dependent fashion (Erickson *et al.*, 1996; Egea *et al.*, 2006), and it regulates the dynamics of a local pool of short actin filaments at the Golgi complex (Cohen *et al.*, 2001; Musch *et al.*, 2001). Through this interaction Cdc42 might control the polarization of trafficking markers (Musch *et al.*, 2001). LIMK1 kinase can also regulate actin dynamics via cofilin at the

growth cones in neuronal cells, which receive a substantial transport of post-Golgi material for the developing neurons (Peter *et al.*, 2004; Rosso *et al.*, 2004).

The Arf-like protein Arl1 is exclusively located at the TGN, and, when in the active (GTP) form, its well characterized action consists of the recruitment of several GRIP-domain-containing proteins (Lu and Hong, 2003; Lu *et al.*, 2006). The GRIP domain is a coiled-coil structural feature of still obscure function that interacts specifically with TGN membranes also through homo-dimerization (Lu *et al.*, 2006). The GRIP-domain-containing proteins that are specifically recruited to the TGN are GCC185, GCC88, Golgin97 and p230/245 (Munro, 2005).

Recently a link between GRIP-containing proteins and Rab proteins has been shown (Burguete *et al.*, 2008).

Over 60 members of the Rab family of small G-proteins have been identified, among which there are Rab11, Rab6 and Rab8 that are interesting for post-Golgi trafficking. In particular, Rab6 is present on TGN-derived carriers and regulates exocytosis by enhancing the processive kinesin-dependent motion of secretory vesicles (Grigoriev *et al.*, 2007). Recently, Rab6 has been shown to interact with GCC185, a GRIP-domain-containing protein that is also an interactor of Arl1, and this interaction occurs in a non-exclusive way. Moreover the Rab6-GCC185 interaction is necessary for TGN recruitment of GCC185-Arl1 (Burguete *et al.*, 2008). Rab8 controls AP1B-dependent trafficking of basolateral carriers (Kroschewski *et al.*, 1999; Musch *et al.*, 2001; Ang *et al.*, 2003), and recent data from the Rab8 knockout mouse also indicate its involvement in apical trafficking in intestinal cells (Sato *et al.*, 2007). Regulation of carrier motility is the candidate sphere of action for Rab8, considering

that it associates with optineurin, which binds myosin VI and FIP2, the latter being responsible for the association with actin through hungtintin (Hattula and Peranen, 2000; Sahlender *et al.*, 2005; Au *et al.*, 2007). Rab11a is localized at the TGN, on recycling endosomes and in specialized membrane compartments in secretory cells (Goldenring *et al.*, 1996; Ullrich *et al.*, 1996). It has also been implicated in basolateral trafficking (Chen *et al.*, 1998; Lock and Stow, 2005).

Arfaptin is an effector of both Arf1 and Arl1, and it interacts with the GTP-bound forms of both proteins. Arfaptin1 is involved in the transport of matrix-degradation factors (Ho *et al.*, 2003). Arfaptins (1 and 2) are specifically localized at the TGN (DeMatteis laboratory, unpublished observations) and they have a BAR domain, which has been structurally determined to be a membrane-curvature sensor (Peter *et al.*, 2004).

Phospholipid metabolism proteins, can directly modify the phospholipids, e.g. phosphatidylinositol 4-kinases (PI4K) and phosphatases, or they can transfer specific lipid species from one intracellular compartment to another, where the enzymes for their metabolism are located. Activation of ARF can trigger the generation of distinct TGN microdomains through an action on the local lipid composition, since it stimulates the production of PtdIns4*P*, recruiting and activating PI4KIIIβ (see above). As with the phosphoinositides in general, PtdIns4*P* acts as a gathering point for the recruitment of a specific set of cytosolic proteins that contribute to the local specialization of the TGN membrane. Indeed, this Arf1–PtdIns4*P* pairing can be considered as a marker for TGN domains, as is the Rab5–PtdIns3*P* pairing for early endosomes (Shin and Nakayama, 2004). Neuronal calcium sensor (NCS)-

1/Frequenin interacts with PI4K and positively regulates its activity, although NCS-1/Frequenin also inhibits the Arf-mediated activation of PI4K (Haynes *et al.*, 2005).

The lipid-transfer proteins are another important class of proteins which include ceramide transfer protein (CERT), phosphatidylinositol-four-phosphate adaptor protein 2 (FAPP2) and oxysterol-binding protein1 (OSBP1) (Holthuis and Levine, 2005). FAPP has been visualized on tubular carrier precursors (Godi *et al.*, 2004) and FAPP2 has been proposed to transfer glucosylceramide from the Golgi complex into the TGN (D'Angelo *et al.*, 2007). Here, tubulation could result from the selective transfer of lipids into the cytosolic TGN membrane leaflet, creating transmembrane area asymmetry and hence curvature (Zimmerberg and Kozlov, 2006). The other transfer proteins CERT and OSBP1 might have important roles too, through their insertion of ceramide and cholesterol, respectively, into the TGN membranes (Levine and Loewen, 2006). This would also facilitate membrane curvature (Shemesh *et al.*, 2003; Zimmerberg and Kozlov, 2006).

The lipid-metabolizing enzyme phospholipase D1 (PLD1), which can be activated by Arf1 (Roth *et al.*, 1999) (and also by hormones and growth factors), converts the phospholipid phosphatidylcholine (PC) into phosphatidic acid (PA). Its product is a structural component of membranes that promotes membrane bending and/or recruits several proteins involved in membrane trafficking (Manifava *et al.*, 2001; Ktistakis *et al.*, 2003). Nir2 is a PI-transfer protein that is involved in TGN-to-PM trafficking, and its depletion results in a reduction of diacylglycerol (DAG) level in the Golgi complex (Litvak *et al.*, 2005).

Proteins involved in several **other functions,** such as scaffolds, tethering complexes and transmembrane proteins localized at TGN with unknown functions, might also be relevant in the understanding of TGN-to-PM transport. 14-3-3 is a scaffolding protein that interacts with PI4KIIIβ, in its S294 phosphorylated form following the kinase activity of PKD (Hausser *et al.*, 2005). The action of 14-3-3 is specifically to protect the S294 specific phospho-site from de-phosphorylation (Hausser *et al.*, 2006). Moreover, once 14-3-3γ isoforms are knocked-down by siRNA, the VSVG transport from TGN to plasma membrane is impaired (Luini laboratory, unpublished observations). C-terminal binding protein/Brefeldin A-ribosylated substrate (CtBP1-S/BARS) is a multifunctional protein that has key roles both as a transcription co-repressor in development and oncogenesis (Chinnadurai, 2002), and as a promoter of Golgi membrane fission (Weigert *et al.*, 1999). More recently BARS has been characterized as exerting its fissioning activity on VSVG-containing carriers in TGN-to-PM trafficking (Bonazzi *et al.*, 2005).

The TRAPP complex, and especially its most conserved subunit Bet3, has been characterized in mammals as being important for the homotypic-mediated fusion of COPII vesicles, and it is thus necessary for the progression of VSVG from the ER to the Golgi complex, according to the (although debated) homotypic-fusion model of transport (Yu *et al.*, 2006). There are many pieces of evidence implicating TRAPPII (TRAPPI plus Trs65p, Trs120p, Trs130p) in late-Golgi pathways in yeast, such as the synthetic lethality of Trs65p with the phosphoinositide 4-Kinase Pik1p (Sciorra *et al.*, 2005). Moreover, when Trs130p is knocked-out, invertase accumulates inside the Golgi (Cai *et al.*, 2005). TRAPPI is a GEF for Ypt1p and TRAPPII is a GEF for Ypt31/32p. Moreover, Trs65 is responsible for the GEF-specificity shift from Ypt1p to

Ypt31/32p, and this last Rab protein homologue is involved in post-Golgi traffic in yeast (Liang *et al.*, 2007).

TGN46 is a single-pass membrane protein, and it is probably the most well known specific marker of the TGN compartment; however, its function at the present time is unknown.

Clathrin (although never found on GPCs) has been recognized recently as being important for TGN-to-PM trafficking of basolateral cargo, even when it is blocked in an acute way (Deborde *et al.*, 2008). At the present time, it is impossible to understand the functional role of clathrin in transport of GPCs carriers that are completely devoid of this (and any other) coat.

1.2.3 Molecular machineries

In this section I will group the players described above into arbitrary and separated functional modules, based on the current models into the literature. I will refer to these functional modules as: *tubulation, fission* and *transport modules* and each will be associated with the corresponding temporal steps described above (Fig 7).

The *tubulation module* (Fig. 7a) starts its action with the GEFs BIG1 and BIG2, which activate Arf1, exchanging its GDP for GTP and allowing it to insert its hydrophobic moiety into the TGN membranes in a specific way. Thus BIG1, 2 act in the opposite way to GBF-1 (another Arf1 GEF), which instead restricts the activity of Arf1 on the intermediate compartment and *cis*-Golgi. Nothing else is known about the roles of BIG1,2, and the way they are recruited to their sites of action is completely unknown. Active Arf1 recruits PI4KIIIβ, which in turn enhances the local production

of PtdIns4*P*, and PtdIns4*P* recruits FAPP. FAPP is also directly Arf1 dependent, and at the TGN they promote the tubulation of VSVG-containing carriers (GPCs, see above), and its action can be directly related to the ability to maintain a local PtdIns4*P* population on tubulation sites via the PH domain (Godi *et al.*, 2004). The action of Arf1 on tubulation appear thus to be indirect; however the tubulation can be promoted by the direct Arf1 interactors Arfaptin1,2, which have a BAR domain structurally determined as a membrane-curvature promoting agent (Peter *et al.*, 2004). Moreover, Arfaptin1,2 also interact with active Arl1, which in contrast to Arf1, is specifically located at the TGN (Burd *et al.*, 2004). The action of Arfaptin1,2 on tubule formation has been verified *in vitro,* via a liposomal tubulation assay (Peter *et al.*, 2004).

The *fission module* (Fig. 7b) starts with Gβγ, which activate PKCη. Both PKCη and DAG activate PKD, and thus Nir2 can participate in the process activating the CDP-choline pathway, which in turn leads to increased DAG production (Luini *et al.*, 2005). The kinase activity of PKD is necessary for the fission of VSVG-containing GPCs (Liljedahl *et al.*, 2001). Active PKD then activates PI4KIIIβ via phosphorylation at serine 294, and this phosphorylation is relevant, but not strictly necessary, for fission (Hausser *et al.*, 2005).

PI4KIIIβ is probably not the only PKD substrate that is required for fission activity, since the PI4KIIIβ S294A mutant delays VSVG exit by only half the rate compared to a PKD kinase-dead (KD) mutant (Hausser *et al.*, 2005). A constitutively active (CA) PKD mutant fragments the Golgi as a consequence of the hyperactivation of the fissioning activity (Bossard *et al.*, 2007). This indicates the need for a regulating feedback that allows the fission machinery to act in the correct way in space and time, to produce the GPCs, according to details described above (fission can occur between

hot spots in which the VSVG cargo is more concentrated; see chapter 1.2.1) (Polishchuk *et al.*, 2003).

CERT provides ceramide to the TGN compartment, then Golgi-localized sphingomyelin (SM) synthase 1 uses ceramide and phosphatidylcholine (PC) to generate SM and DAG (Perry and Ridgway, 2005). DAG is a prerequisite for PKD recruitment and activation. The other side of the story is that CERT is inactivated by PKD phosphorylation, providing a lower amount of ceramide; consequently, it provides a lower amount of DAG to the TGN compartment. This mechanism was recently proposed in the regulation of PKD-mediated transport (Fugmann *et al.*, 2007).

CtBP1-S/BARS has been characterized as being important in the transport of VSVG from the TGN to the basolateral PM in COS7, HeLa and MDCK cells, and its role in the process has focused on membrane fission. This arises from the observations that VSVG-containing tubules are not impaired in their formation from the TGN membranes, but they are not able to detach, when specific siRNA were used and also using the dominant negative deletion mutant nucleotide-binding domain (NBD) of BARS and dominant negative point mutant D355 (Bonazzi *et al.*, 2005). However, neither the regulation of BARS, nor the fine molecular mechanism BARS exerts onto the GPCs to drive the fission activity, are clear to date.

Another player in fission is dynamin, a protein that is well known as having a key role in fission at several trafficking stages (Orth and McNiven, 2003). Dynamin is present in the Golgi complex (McNiven *et al.*, 2000) and is required for the export of p75 from the Golgi in polarized cells. BARS and dynamin act on different cargoes and pathways (Bonazzi *et al.*, 2005).

The *transport module* (Fig. 7) (which is probably the least clear) is mediated by cytoskeletal motors that drive moving forces in transporting cargo along cytoskeletal tracks, along with tethering factors that assure specificity of the final cargo delivery. The elongation of carrier precursors from the TGN and their translocation through the cytosol occurs along microtubules (Polishchuk *et al.*, 2003) by virtue of microtubule-based motors (usually kinesins), and this happens in nearly all animal species (Jaulin *et al.*, 2007). In mammalian cells, motors interact with transport carriers in a remarkably, but not completely, selective fashion.

Kinesin heavy chain-5B (KIF5B) is a well studied molecular motor, which mediates apical trafficking of p75 in MDCK cells (Jaulin *et al.*, 2007). However, these motors can also show a degree of promiscuity, as KIF1B has also been implicated in Rab6-dependent trafficking of VSVG in a non-polarized cell line (Grigoriev *et al.*, 2007).

The TRAPPII complex is considered to be a tethering factor, and at least in yeast its role as a GEF for Ypt31/32p has been established (Liang *et al.*, 2007). The functional homologue of Ypt31/32p in mammals can be Rab11, Rab6, and Rab8, which are involved in BL transport (see above: molecular players/small G-proteins). The TRAPP complex can be important for post-Golgi trafficking, at least into this last step of membrane targeting of GPCs.

2 Aim of the project

The aim of my PhD project consists first in the bioinformatic collection of interactions between thematically chosen players of TGN-to-PM trafficking in mammals, using web-based databases, such as STRING (http://string.embl.de//). Moreover, I have collected not only proteins that are functionally relevant in the process, but I have collected also proteins localizing specifically at the TGN, even if their function is still not clear, e.g. Arl1, Arfaptin and TGN46. This provides the hope of better defining the puzzling molecular machineries that have roles in the different temporal steps mentioned above, considering also the possibility that these roles can be overlapping. The need to better define these molecular machineries comes from the comparison between the high level of organization of the clathrin, COPI and COPII machineries on one side, and the lack of knowledge about consequentiality, temporal organization and regulation of the TGN-to-PM routes at the molecular level on the other side (Fig. 7). The concept is thus to look for new protein-protein interactions, with the aim of better defining the molecular aspect of the problem. Then the goal is the identification of new interactions between players mentioned above, which will be involved specifically in VSVG trafficking from the Golgi to the PM, making use of a two-hybrid system. This will finally focus my attention on the discovery of new players in TGN-to-PM trafficking, such as elements for which a role in TGN-to-PM trafficking might be suspected, but have not been characterized yet.

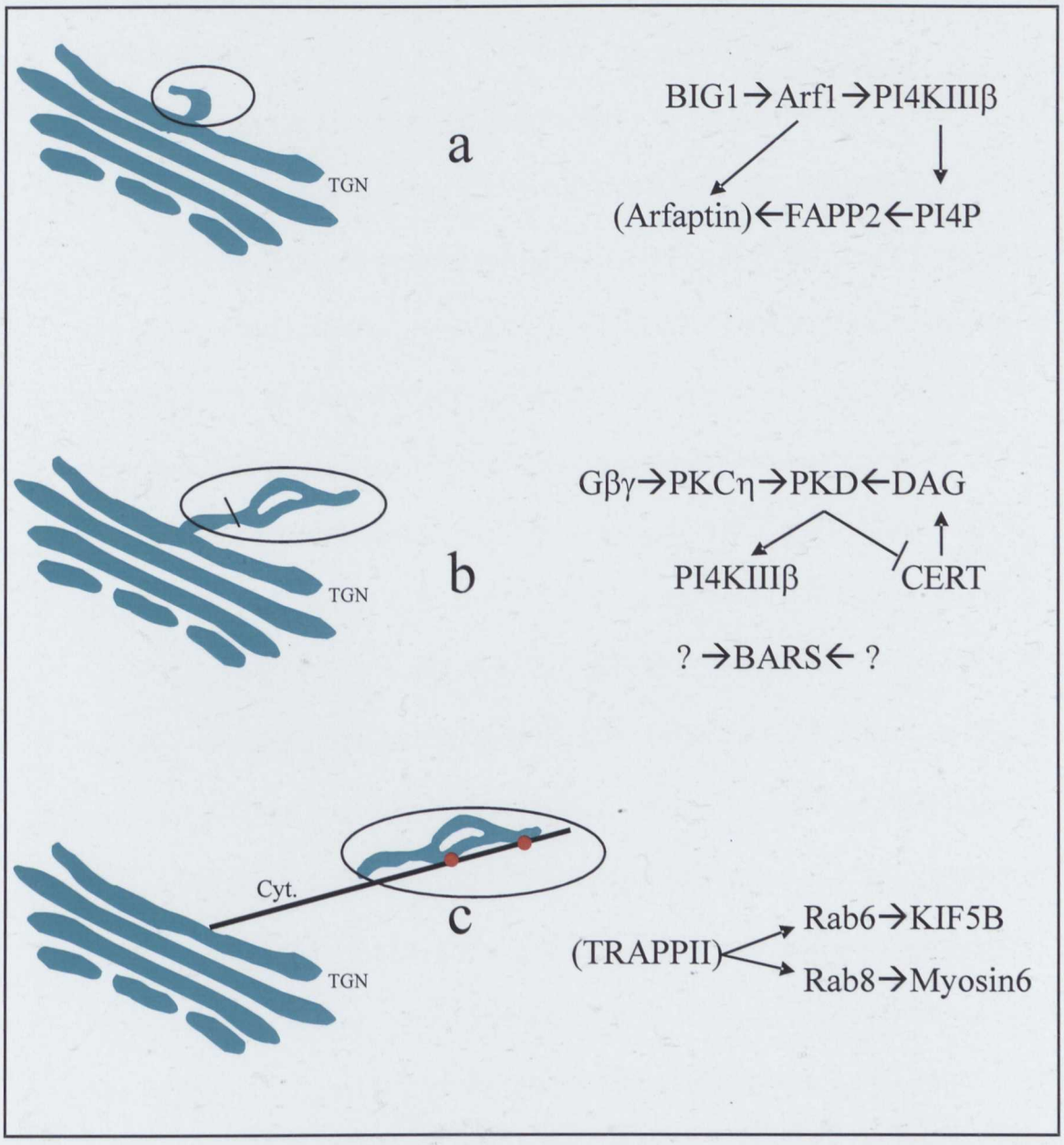

Figure 7. The temporal steps of post-Golgi carrier (PGC) formation:

a) Segregation of the 'export' membrane from the resident Golgi domains, with the inclusion of both cargo and machinery proteins. b) Extrusion in the form of tubules and irregular saccules and detachement c) Transport from the parent organelle. Cyt. = cytoskeletal tracks (MT or actin), red spots = motors. The molecular mechanisms and the exact temporal sequence within which the molecular players act on these processes are still unclear. On right side are shown the molecular pathways, see chapter 1.2.3 for details.

3 Materials and methods

3.1 Subcloning

3.1.1 Open reading frame (ORF) production

Five μg of each plasmid DNA were digested with the appropriate restriction enzymes (Amersham), to produce the following ORFs, that were ready to be inserted in-frame with the activation domain (AD) of pGAD-T7 and the binding domain (BD) of pGBK-T7 (Clontech). The restriction endonucleases were purchased from Amersham Pharmacia Bio-Tec (UK). The enzymes in their order of use are as follows: Synbindin was excised from the pEYFP-N1 plasmid with EcoRI and BamHI; the fragment of Arap1 from amino acid 552 to the amino acid 1077 was excised from the pEGFP-C1 plasmid with EcoRI; and XhoI, TGN46 was excised from the pEGFP-N1 plasmid with EcoRI and BamHI; PI4KIIα from the pGEX4-T1 plasmid with EcoRI and XhoI; 14-3-3γ from the pET28A plasmid with EcoRI and XhoI; PITPβ from pBluescript plasmid with NcoI and BamHI; FAPP2 from the pTrcHis2 plasmid with BamHI and SalI; ARFGAP1 from the pEGFP-N1 plasmid with EcoRI and AgeI; PKD1 from the modified pME-Py plasmid (Liljedahl *et al.*, 2001; Maeda *et al.*, 2001) with EcoRI –XhoI; PKD2 from the same vector as PKD1 with EcoRI –XhoI; FAPP1 from pEYFP-C1 vector with BglII and SalI, ARL1 from pEGFP-N3 vector with EcoRI and BamHI. Bet3 from pEGFP-C3 with BglI and BamHI, ARL1Q71L from pEGFP-N3 with EcoRI and BamHI. OSBP1 was single digested with BamHI, and the digested plasmid was dephosphorylated with Shrimp alkaline phosphatase (Roche).

When cutting sites were not available, some pairs of PCR primers (listed below) were designed to PCR-amplify the desired ORFs. The PCR primers contained in-frame restriction sites: EcoRI-XhoI for pGAD-T7, and EcoRI-SalI for pGBK-T7.

The ORFs and the primers used to amplify them are listed below, with the restriction sites shown in bold:

Gαi3:

5'-ATA**GAATTC**ATGGGCTGCACGTTGAGC-3' and

5'-ATAGGATCA**CTCGAG**TCAATAAAGTCCACATTCC-3',

FAPP1-PH:

5'-ATA**GAATTC**ATGGAGGGGGTGTTGTACAAG-3' and

5'-ATA**CTCGAG**TGCTTTGGAGCTCCCCAG-3',

FAPP2-PH:

5'-ATA**GAATTC**ATGGAGGGGGTGCTGTACAAG-3' and

5'-ATA**CTCGAG**GCAAGCCTTGGCTGATCCCAG-3',

FAPP2-ΔPH:

5'-ATA**GGATCC**CTGACAGTAGGACCCAGAAGGAG-3' and

5'-ATA**CTCGAG**CATGGACCTCTTATAAAGCGTCCAG-3',

Frequenin:

5'-ATA**CATATG**ATGGGGAAATCCAACAGCAAG-3' and

5'-ATA**CTCGAG**TACCAGCCCGTCGTAGAG-3',

DynaminII: 5'-ATA**GAATTC**ATGGGCAACCGCGGGATG-3' and

5'-ATA**GGATCC**CTAGTCGAGCAGGGACGG-3',

PKD1-catalytic domain:

5'-ATA**GAATTC**GCAAATGTAGTGTATTATGTGGG-3' and

5'-ATA**CTCGAG**ATAGTCCTGTAGCCAAGGGTG-3',

PKD2-catalytic domain:

5'-ATA**GAATTC**AATGTGGACATTGCCACTGTC-3' and

5'-ATA**CTCGAG**GAGAACACTGATGCGCTC-3',

Pak1: 5'-ATA**GAATTC**GTGGTGACAATGTCAAATAACG-3'

and 5'-ATA**CTCGAG**GTGATTGTTCTTTGTTGCCTC-3'.

After their amplification, the PCR products were cut out from the agarose gels with a sterile scalpel, and the DNA was extracted from the agarose using the "QIAEX II extraction kit" (Qiagen, CA, USA), according to the manufacturer instructions. The DNA was eluted in 10 mM Tris-HCl, pH 8.0.

3.1.2 Production of frameshift vectors

The pGAD-T7 and pGBK-T7 vectors (Clontech) are commercially available in one single frame. To obtain frame-shift mutants, I performed single-step mutagenesis that involved amplification of the entire plasmid using high-fidelity PFU-turbo DNA polymerase (Stratagene), inserting 1 or 2 bases (in bold) between the sequences coding for the HA-tag and the multi cloning site, with the aim of producing two alternative frames for both vectors. For this mutagenesis reaction I used the following primers:

5'-GTACCAGATTACGCTA**(A)**CATATGGCCATGGAG-3' and

5'-CTCCATGGCCATATGT**(T)**AGCGTAATCTGGTAC-3' for pGAD-T7

and primers

5'-TCAGAGGAGGACCTGA**(A)**CATATGGCCATGGAG-3' and

5'-CTCCATGGCCATATGT**(T)**CAGGTCCTCCTCTG-3' for pGBK-T7.

The PCR reaction conditions were: 5 µl buffer, 10x PFU-turbo, 20 µg template DNA, 25 µM forward oligo, 25 µM reverse oligo, 8 µl dNTPs (2.5 mM), 2.5 U PFU-turbo DNA polymerase and sterile double distilled water to 50 µl final volume. After denaturation at 95 °C for 5 min, 18 cycles followed with 95 °C for 30 s, 55 °C

(annealing) for 1 min and 68 °C for 9 min. DpnI was added after the PCR reaction, to digest the metylated DNA template, for 1 h at 37 °C. The final products of the two alternative frames were named pGAD-T7-f2 or f3 and pGBK-T7-f2 or f3. In the pGAD-T7 frame-2, a STOP codon appeared due to the frameshift. To make the pGAD-T7 frame-2 usable, the STOP codon was removed with another point mutation reaction using the following oligoes: 5'-ATGGCCATGGAGGCCAGAGAATTCCACCCGGGTG-3' and 5'-CACCCGGGTGGAATTCTCTGGCCTCCATGGCCAT-3'

3.1.3 Ligation

After purification, eluted DNA fragments were used directly for the ligase reaction with pGAD-T7 or pGBK-T7 (Clontech) in their native frames or in their frameshift versions (see above). To ligate the vector and insert, ~100 ng vector and ~3-fold molar amounts of insert were incubated with 1 u T4 DNA ligase in T4-DNA-ligase buffer, for 30 min at room temperature.

3.1.4 Preparation of competent cells

These bacteria were prepared with the help of G. di Tullio (Department of Cell Biology and Oncology, Consorzio Mario Negri Sud). A single colony of XL-1 Blue *Escherichia coli* bacteria was picked up from a Luria-Bertani (LB)-agar plate (10 g/l NaCl, 5 g/l yeast extract, 10 g/l tryptone peptone and 15 g/l agar) and used to inoculate 10 ml of LB broth (10 g/l NaCl, 5 g/l yeast extract, 10 g/l tryptone peptone). The bacteria were grown overnight, then diluted into 190 ml fresh LB broth and incubated at 37 °C until the optical density (OD_{600}) reached 0.5. The bacteria were harvested by centrifugation at 6000x *g* for 10 min at 4 °C. The bacterial pellet was resuspended in 40 ml 30 mM potassium acetate, 100 mM RbCl, 10 mM $CaCl_2$, 50 mM $MnCl_2$, 15%

(v/v) glycerol, pH 5.8, and left on ice for 2 h. After centrifugation and resuspension of the pellet in 4 ml of 10 MOPS, 75 mM $CaCl_2$, 10 mM RbCl, 15% (v/v) glycerol pH 7, cells were stored at –80 °C in 400 µl aliquots.

3.1.5 Transformation of the bacteria by heat shock

The DNA from the ligase reaction (10 µl) was added to 200 µl of competent bacteria previously thawed on ice. After gentle mixing, the sample was placed on ice for 30 min and heat shocked for 90 s at 42 °C, and put again on ice. After addition of 800 µl LB medium, the bacteria were incubated with shaking (200 rpm) at 37 °C for 45 min. The bacteria were then plated on LB-agar plates containing the appropriate selective antibiotic for the correct selection of plasmid-carring bacteria, and incubated overnight at 37 °C. The next day, an isolated bacterial colony was picked and used to inoculate 2 ml LB containing the appropriate antibiotic. The culture was incubated at 37 °C overnight, 300 µl of 50% sterile glycerol was added to 700 µl of the bacterial culture, which was then stored at –80 °C.

3.2 Yeast transformation

The yeast strains used were Y187 for the pGAD-T7 vector, and AH109 for the pGBK-T7 vector. Single colonies of Y187 and AH109 were inoculated in 5ml of YPDA medium (Clontech) at 30 °C overnight under aerobic conditions with vigorous shaking. The next morning, 1 to 2 ml were added to 60 ml of fresh YPDA medium to reach an OD_{600} of 0.1-0.2 O.D., then growth was continued for 4-5 h until OD_{600} is 0.5-0.8. It is very important for the transformation efficiency that OD_{600} does not exceed 0.8, so as to be sure that the yeast cells were still in logarithmic phase of

growth. The cells were collected by centrifugation at 2750x g for 10 min, then washed twice in 20 ml sterile H_2O. Cells were then resuspended in 0.3 ml 0.1 M LiAc. In the meantime, carrier-DNA (sonicated salmon sperm DNA) was boiled for 5 min and then chilled on ice. The following reagents were added, in this order, and they were mixed very gently after each addition (addition of lithium makes the cells extremely fragile): 73 µl cells, 240 µl 50% PEG, 36 µl 1 M LiAc, 5 µl carrier DNA (5mg/ml), 1 µg plasmid DNA, H_2O to a final volume of 360µl. At the end, DMSO was used to a final 10% concentration. After an incubation at 30 °C, without shaking, for 30 min, the cells were incubated at 42 °C for 5 min, then centrifuged in 12x75 mm polypropylene tubes at 200x g for 30 s. The supernatant was removed carefully, and the cells were gently resuspended in H_2O. These cells were plated on SD media (clontech) lacking amino acid Trp or Leu for the pGBK clones in the AH109 strain and the pGAD clones in the Y187 strain respectively.

3.2.1 Protein expression in Yeast

Transformed colonies containing pGAD-T7 and pGBK-T7 were inoculated in 7 ml of SD-Leu and SD-Trp liquid media (Clontech) respectively, under aerobic and vigorous shaking conditions at 30 °C until they reach an OD_{600} between 1.0 and 2.0. The cells were harvested by centrifugation at 4 °C at 2700x *g* for 10 min, washed twice with sterile ddH_2O (centrifuging), and than resuspended in SB with SDS, boiled for 5 min, and frozen, defrozen and sonicated, then boiled again. The samples were loaded onto SDS-page gels and transferred onto nitrocellulose filters for Western blotting. Monoclonal antibodies against the HA tag and the myc tag were used to detect protein expression. In the case of ARL1, FAPP2, PI4KIIα, OSBP1 and TGN38, the antibodies directed against them were used in Western blotting since they were available, and since their expression was undetectable with the above antibodies.

3.3 Two hybrid system

The yeast strains used were Y187 for the pGAD-T7 vector, and AH109 for the pGBK-T7 vector, as described above. The BD-carrying clones from the –80 °C stocks were streacked onto agar plates with DO medium without Trp (Clontech), and the AD-carrying clones from the –80 °C stocks were streacked onto agar plates with DO medium without Leu.

Then the growth was allowed to proceed for 3-5 days at 30 °C, after which the plates were parafilm-sealed and stored at 4 °C. Every three weeks, they were replicated by dispersing some of the cells in sterile water and streacking this onto fresh agar plates. For the mating between yeast clones carrying baits and preys (AH109 and Y187 respectively), the principle was similar to that of (Zhong *et al.*, 2003)), adapted and scaled to this system, as follows.

To provide a pool of preys, an amount (roughly similar to half a colony of 2.5 mm in diameter) of every pGAD clone was taken and dispersed in N x 100µl of 2x YPDA (Clontech), where N is the number of clones. The same criteria was followed to obtain a pool of baits, by collecting every pGBK clone. Greater amounts of empty p-GAD-containing clones and, separately, of empty p-GBK-containing clones were also dispersed in the same volume of YPDA. These amounts were roughly N times greater than the amounts taken in previous step with the pGAD clones. Thus with the aid of a combitip pipettor, 50 ul of the mixes were distributed into U-bottomed 96-well plates: Mix1: pool of X-pGAD; mix2: pool of X-pGBK; mix3: empty pGAD; mix4: empty pGBK. Than every single pGBK clone was dispersed (roughly similar to half a colony of 2.5 mm in diameter) into wells containing the pGAD pool, to look for interactions, and in wells containing the empty pGAD only, as a control for

autoactivation. Similarly, every single pGAD clone was dispersed (roughly similar to half a colony of 2.5mm in diameter) into wells containing the X-pGBK pool, to look for interactions, and in wells containing the empty pGBK only, as a control for autoactivation. These plates were incubated overnight at 30 °C with gentle shaking (50 rpm). The day after two or three wells per plate were chosen randomly to look for diploid mated cells under the optical microscope. Then, using a multichannel pipette, 50 µl of sterile water was added to samples, with 3-4 in and out pipetting used to resuspend the cells, and finally, single drops of cells were spotted onto the DDO/QDO/TDO plates (Matchmaker3 system, Clontech) and finally incubated at 30 °C for seven days.

Single 'submatrix' one-by-one interaction matings of pGAD clones with pGBK clones, and matings of pGAD clones with pGBK empty vector, and of pGBK clones with pGAD empty vector as a control for autoactivation, were performed by dispersing an amount (roughly similar to half a colony of 2.5mm in diameter) in 50µl of 2x YPDA on 96-microwell plates; the plates were keep at 30 °C O/N with 50 rpm shaking. The next morning, the samples were plated as described above for the pooling approach, in the same media and under the same conditions.

To repeat the stronger interaction data and to test several dilutions of the mating product, 20 µl of the samples were diluted 10-, 20-, and 30-fold with sterile water, and each dilution was streaked on 1/6 of a round 100-mm diameter plate with DDO/QDO, in the presence of 2 mg/ml X-αGal (5-bromo-4-chloro-3-indolyl-α-D-galactopyranoside).

3.4 Cell culture

3.4.1 Materials

African green monkey COS7 cells were purchased from American Tissue Type Collection (ATTC, USA). Human fibroblasts (HF) were kindly provided by the Istituto Dermatologico dell'Immacolata (IDI, Italy). HeLa cells were kindly provided by Thierry Dubois (Institute Curie, Paris, France). Dulbecco's modified Eagle's Medium (DMEM) and calf serum (CS) were from Invitrogen (UK). Foetal calf serum (FCS), penicillin, streptomycin, trypsin-EDTA and L-glutamine were from Biochrom KG (Berlin, Germany). All these reagents were purchased as 10x stock solutions. All of the plastic tissue culture materials were from Corning (NY, USA) or Falcon (NJ, USA). The filters with a 0.2 μm cutoff were from Albet (USA)

3.4.2 Growth conditions

COS7 and HeLa cells were grown in DMEM supplemented with 4.5 g/l glucose, 2 mM glutamine, 1 U/ml penicillin and 1 μg/ml streptomycin, and 10% FCS. HFs were grown in DMEM supplemented with 2 mM glutamine, 1 U/ml penicillin and 1 μg/ml streptomycin, and 10% CS. All of the cell lines were grown in a controlled atmosphere in the presence of 5% CO_2 at 37 °C. The cells were grown in flasks until 90% confluence. To detach the cells from the surfaces of the flasks the medium was removed and 0.25% tripsin-EDTA solution was added for 3-6 min. Medium was then added back to block the protease action of the tripsin, and the cells were centrifuged at 450x *g* for 10 min and resuspended in fresh medium, and finally placed in a new plastic flask at the desired dilution.

3.4.3 Cell transfection

Cell transfections with Trans-It (Myrus) (which is the same molecule as Fugene) were performed in 24-well plates at 50% to 70% confluence. A transfection mixture was prepared by diluting the relevant DNA in OptiMEM culture medium and adding Trans-It in a separate test-tube. The mixture was then shaken and incubated at room temperature for 15 min. The transfection mixture (50 µl) was then added to the cells.

Cell transfection with Oligofectamine was used mainly to perform RNA interference (RNAi), according to the manufacturer instructions. HeLa cells (10000-12000) were plated on 24-well plate to have around 20% confluence the day after. A mix containing OptiMEM and the relevant siRNAs was prepared with gentle shaking, and incubated at room temperature for 7 min. At the same time, a mix containing OptiMEM and Oligofectamine was prepared in a second tube, and after gentle shaking it was also incubated at room temperature for 7 min. The two mixes were pooled, and after gentle shaking, they were incubated at room temperature for 15 min, than directly added to the cell media. Of note, the amounts of the siRNAs and oligofectamine varied depending on the gene that was to be silenced, according to manufacturer instructions.

Cell transfection with electroporation was performed on COS7 cells. Five million PBS-washed cells were mixed together with 10 µg of the relevant DNA. The samples were cooled on ice in a sterile electroporation cuvette (0.4 cm) (Biorad, UK). Then the cells were electroporated in a Gene Pulse Electroporator (Biorad, UK) using the following parameters: voltage, 220 V, capacitance, 950 µF . After electroporation,

the cells were immediately plated in warm media, and the day after, the cell culture media was changed.

3.5 Co-immunoprecipitation

The following procedure was used for immunoprecipitation of both endogenous and overexpressed proteins. COS7 cells were transfected with Arfaptin2-FLAG, Sedlin-FLAG and PKD2wt, or a kinase-dead (KD) PKD2. After 24 h of Transfection, the cells were washed five times with PBS and incubated with lysis buffer (50 mM Tris, pH7.5, 150 mM NaCl, 1 mM EDTA, 1% Triton X-100) with the addition of a water-soluble complete protease inhibitor cocktail (Roche), and eventually with the addition of the phosphatase inhibitors 1 mM $NaVO_4$ and 30 mM NaF. The cells were scraped off the plates and lysed by passage (14 times) through a 25-gauge syringe needle. The lysates were collected and centrifuged at 20000x *g* for 10 min at 4 °C. For immunoprecipitation of endogenous proteins, 1 mg lysate was incubated with 3 μg polyclonal antibody, and for the overexpressed proteins, 20 μl of EZview RED anti-FLAG M2 Affinity Gel bed resin (Sigma), was added to immunoprecipitate the FLAG-containing proteins. In the case of the polyclonal antibody, the day after the samples were incubated with 40 μl 50% protein-A Sepharose resin slurry (Amersham) for 1 h at 4 °C on a rotating wheel at 14 rpm. The resin was washed three times with lysis buffer, plus two times with lysis buffer without the Triton X-100, and the proteins were revealed by Western blotting using a polyclonal antibody raised against PKD that recognizes both PKD1 and PKD2 (Santa Cruz). An anti-GST antibody was also used, since the various PKD constructs had a GST-TAG at the N-terminus.

3.6 Immunofluorescence analysis by laser scanning confocal microscopy (LSCM)

Immunofluorescence samples were observed using an Axiophot fluorescence microscope or an Axiophot, LSM5 Pascal (Zeiss) confocal microscope equipped with 40x and 63x objectives (Zeiss, Germany). Optical confocal sections were taken at 1 Airy unit, with a resolution of 512x512 pixels and exported as JPEG files. Table 3.1 lists the dilutions of the primary antibodies used for immunofluorescence.

Table 3.1 Primary antibody dilutions used in immunofluorescence

Specificity	Supplier	Animal Source	Dilution
FLAG M5	Sigma	Mouse	1:500
GST	G. di Tullio	Rabbit	1:150
Arfaptin2	G. di Tullio	Mouse	1:800
VSVG	G. di Tullio	Mouse	1:700
VSVG luminal	G. di Tullio	Rabbit	1:400

3.7 VSVG transport assay

3.7.1 Cell infection with VSVG

The infectious stocks of the temperature sensitive mutant of vesicular stomatitis virus (VSV) were prepared in collaboration with Antonella Di Campli (Department of Cell Biology and Oncology, Consorzio Mario Negri Sud). For each infectious stock, the optimal working concentrations were experimentally defined as the lowest that caused 100% infection of HeLa cells, judged by staining of the viral membrane glycoprotein (VSVG) in immunofluorescence.

Cells were washed 3 times in serum-free culture medium and incubated with the diluted VSV infectious stock for 45 min at 32 °C. The excess virus was removed

by washing three times, and the cells were kept in complete medium at 40 °C for 2.5 h to allow the VSVG to accumulate in the ER.

3.7.2 VSVG transport to the PM

After accumulation of VSVG in the ER, the following steps were carried out in medium with the addition of 100 µg/ml cycloheximide, which prevents neo-synthesis of cellular and viral proteins. The cells were placed at 20 °C for 2 h, to accumulate the VSVG in the Golgi/TGN. Then the temperature was shifted to 32 °C to follow the Golgi-to-PM transport of the viral protein. At each time point after the shift, the cells were fixed in 4% paraformaldehyde to follow the VSVG time-course.

3.8 Glycosaminoglycan (GAG) secretion assay.

3.8.1 Materials

Xyloside and cetylpiridinium were from Sigma, [^{35}S]-sulphate was from Perkin Elmer (USA), Ultima Gold XR scintillation liquid was from Beckman (USA).

3.8.2 Procedure

HeLa cells were plated in 12-well plates for 80% confluence the day of the experiment. These cells were than washed 3 times with 600 µl Tyrode+(Ca^{++}/Mg^{++}) (10 mM HEPES-NaOH, pH 7.2,125 mM NaCl, 5 mM Kcl, 5.6 mM glucose, 1.8 mM $CaCl_2$, 1.8 mM $MgCl_2$). Five hundred µl of 1mM xyloside in Tyrode+(Ca^{++}/Mg^{++}) were added to each well, and the cells were incubated for 15 min at 37 °C.

Subsequently, the cells were pulsed for 15 min at 37 °C with 400 µl 100 µCi/ml [^{35}S]-sulphate in Tyrode+(Ca^{++}/Mg^{++}) plus 1 mM xyloside. Then 500 µl

DMEM, 10 mM HEPES-NaOH, pH 7.2, plus 0.1 mg/ml (w/v) BSA were added to each well, to allow the cells to secrete at 37 °C for the required times.

The cell medium was then collected and centrifuged for 5 min at 16000x *g* to pellet the detached cells and cell debri. GAGs in the supernatant were precipitated for 2 h at 37 °C by adding to the medium: 1 ml H_2O, 50 µl 2 M NaCl, 500 µl 4 mg/ml chondritin sulphate in H_2O, and 2 ml 2% (w/v in H_2O) cetylpiridinium. At the same time, 500 µl 0.1 M NaOH was added to the cell layers for 10 min, to lyse the cells. These cell lysates were collected and the GAGs were precipitated for 2 h at 37 °C by adding to the cell lysate: 750 µl H_2O, 100 µl 2 M NaCl, 500 µl 4mg/ml in H_2O chondritin sulphate, 2 ml 2% (w/v) in H_2O cetylpiridinium, 250 µl 1 M HEPES.

The samples were washed three times with 4 ml 1% (w/v) cetylpiridinium plus 20 mM NaCl in H_2O and resuspended in 500 µl 2M NaCl. They were than transferred into vials for scintillation counting, and 8 ml Ultima Gold XR scintillation reagent was added to each vial.

After counting the samples in a β-counter Beckman LS1701, the percentage GAG release into the medium was calculated according to the formula:

% of release= cpm cell medium/(cpm cell medium+cpm cell lysate)x100.

3.9 Sodium dodecyl sulphate-polyacrylamide gel electrophoresis

3.9.1 Assembling of polyacrylamide gels

Two 16 x 18 cm glass plates were used for assembling standard gels. The plates were assembled to form a chamber by using two 1.5-mm plastic spacers aligned along the

lateral edges of the glass plates. The plates were then fixed using two clamps and mounted in a plastic base, which sealed the bottom. All of the materials were from Hoefer Scientific Instruments (Germany). The 'running' polyacrylammide gel was prepared by mixing H_2O, 40% (w/v) acrylamide-bisacrylamide solution, 1.5 M Tris-HCl, pH 8.8, 10% (w/v) SDS, to have the selected concentration of acrylamide, 375 mM Tris-HCl, 0.1% (w/v) SDS. Then, 0.06% (w/v) ammonium persulfate (APS) and 0.06% (v/v) TEMED were added, and the solution was pipetted and poured into the gap between the plates, leaving ~ 5 cm for the stacking gel. N-butanol or water was percolated to create a layer over the running gel, that was allowed to polymerize for 1 h. After the polymerization, the gel was covered with a layer of 375 mM Tris-HCl, pH 6.8, 10% (w/v) SDS, in order to have 4% (w/v) acrylamide, 125 mM Tris-HCl, 0.1% (w/v) SDS. Then, 0.1% (w/v) APS and 0.07% (v/v) TEMED were added and the solution was pipetted and poured over the running gel. A 15-well comb was immediately inserted between the glass plates and the set up was left 20 min at room temperature for the polimerization of the acrylamide.

3.9.2 Sample preparation and running

The PAGE samples were prepared by adding SDS sample buffer to each experimental sample, followed by an incubation at 100 °C for 5-10 min in a multi-block heater, cooling to room temperature, a brief centrifugation and loading onto the gel. One or two wells were loaded with Full-Range Rainbow Molecular Weight Markers or Low Molecular Weight Markers (Amersham Pharmacia Biotech). The gel was then transferred into the electrophoresis apparatus (Hoefer Scientific Intruments, NJ, USA) and run under a constant current of 8 mA (for overnight runs) or 40 mA (for ~4 h runs).

3.9.3 Coomassie brilliant blue staining

After the removing of the glass plates the gels were incubated in staining solution (50% methanol, 40% H2O, 10% acetic acid, 0.1% Coomassie brilliant blue) for 2 h, washed with water, and then de-stained with 30% methanol, 10% acetic acid for the time required depending on the intensity of the protein bands of interest.

3.10 Western blotting

3.10.1 Protein transfer onto nitrocellulose

The polyacrylamide gels from section 3.9.2 were soaked for 15 min in transfer buffer, placed on a sheet of 3MM paper (Whatman, NJ, USA) and covered with a nitrocellulose filter (Schleicher & Scuell, Germany). The filter was covered with a second sheet of 3MM paper, to form a "sandwich", which was subsequently assembled into the blotting apparatus (Hoefer Scientific Instruments). The protein transfer was at 400 mA for 5 h, or at 120 mA overnight. At the end of the run, the sandwich was disassembled and the nitrocellulose filter was stained with 0.2% Ponceau Red (Sigma-Aldrich), 5% (v/v) acetic acid for 5 min, to visualize the protein bands, and then rinsed with 5% Acetic acid to remove the excess unbound dye.

3.10.2 Probing the nitrocellulose with specific antibodies

The nitrocellulose filters were cut into strips corresponding to the lanes of the polyacrylamide gel with a razor blade. The strips were incubated in blocking solution for 60 min at room temperature, and then incubated with the primary antibodies directed against the protein of interest, which were diluted at the appropriate concentrations in blocking solution. A list of antibodies used in this study and their

working dilutions is provided in Table 3.2. After a 2-3 h incubation at room temperature, or an overnight incubation at 4 °C, the primary antibodies were removed, and the nitrocellulose strips were washed in TTBS twice, for 10 min each.

The nitrocellulose strips were then incubated for 1 h with the appropriate horse radish peroxidase (HRP)-conjugated secondary antibodies (anti-rabbit and anti-mouse: 1:1000) and washed twice in TTBS for 10 min each, and once in TBS for 3 min. After washing, the nitrocellulose strips were incubated with the enhanced chemioluminescence (ECL) reagents, accordingly to the manufacturer instructions for ECL-based detection.

Table 3.2 List of primary antibodies used for Western Blot in this study

Specificity	Supplier	Animal Source	Dilution
PKD1,2	Santa Cruz	Rabbit	1:500
GST	G. di Tullio	Rabbit	1:1500
Bet3	G. di Tullio	Rabbit	1:10000
sedlin	G. di Tullio	Rabbit	1:5000
synbindin	G. di Tullio	Rabbit	1:10000

3.11 Preparation of antibodies

The preparation of the antibodies was performed by G. di Tullio and M.Santoro (Consorzio Mario Negri Sud, Italy) with the procedures described below.

3.11.1 Immunization of the rabbit

One mg of the specific antigen was resuspended in 2 ml PBS (1.5 mM KH_2PO_4, 8 mM Na_2HPO_4, 137 mM NaCl and 2.7 mM KCl, pH 7.4). Two ml of complete Freund's adjuvant were added, and this mixture used to immunize New Zealand rabbits. The

rabbits were boosted after 21 and 42 days with 1 mg antigen containing the same volume of incomplete Freund's adjuvant. The rabbits were bled and the serum prepared as described below.

3.11.2 Serum preparation

After collection, the blood from the immunized rabbit was allowed to clot at 37 °C for 60 min, than kept overnight at 4 °C to allow the clot to contract. The serum was removed from the clot and the insoluble material by centrifugation at 10000x *g* for 10 min at 4 °C, and stored at –80 °C in aliquots.

3.11.3 Protein-A purification of IgGs

Protein-A –Sepharose resin (500 mg) were suspended in 5 ml distilled water and packed into a column, which was then washed with 100 ml distilled water under a constant flow. The packed resin was finally washed with 20 ml PBS, and then 2 ml of serum from chapter 3.11.2 were loaded onto the column at 0.5 ml/min in an FPLC system (Pharmacia Bio-Tec, UK). The resin was then washed with 30 ml PBS, and the retained IgGs were eluted using 15 ml 100 mM glycine, pH 2.5. Fractions of 1 ml were collected and their protein contents measured by spectrometry (as part of the FPLC system).

The six fractions containing the highest concentrations of protein were pooled and the pH neutralised with 1 M Tris, pH 11. The protein concentrations of the pooled fractions were determined using a commercially available protein assay kit (Biorad, UK), according to the manufacturer instructions. Typically, this was 2.5 mg/ml. Different dilutions of the IgGs were tested both in immunofluorescence and Western blotting with the optimal antibody working dilutions as reported in the Table 3.2.

3.11.4 Preparation of antibodies for microinjection

After the affinity purification (see above), the antibodies were dialysed against 70 mM KCl, 10 mM Na_2HPO_4, pH 7.2, for at least 4 h, using dialysis membranes with a molecular weight cut off of 6000/8000 Da (1 ml antibody in 500 ml buffer, twice). The antibodies were quantified again, and then they were ready to be microinjected into the cells.

3.12 Protein purification

3.12.1 His tagged proteins

The His-tagged polypeptides, such as His-BARS, were purified as follows: a transformant colony was inoculated O/N in 4.ml LB with the appropriate antibiotic and the day after this was diluted 1/20 in the same culture media until it reached an OD_{600} of 0.6. Then protein expression was induced with 0.4 mM isopropyl thiogalactoside (IPTG) incubation under shaking (200 rpm) for 2 h at 37 °C.

The culture was cooled on ice for 10 min, than pelleted at 4 °C in JA14 at 9800x *g* for 10 min. The pellet was resuspended in 4 ml lysis buffer (50 mM phosphate buffer, pH 8.0, 300 mM NaCl, 10 mM imidazole, 1 mg/ml lysozyme and water-soluble complete protease inhibitor cocktail (Roche). The resuspended bacteria were fast-frozen in liquid nitrogen (and eventually stored at –80 °C). Then they were defrosted at 4°C in a waterbath, protease inhibitors and 1 mg/ml lysozyme were re-added, and they were incubated for 30 min on a rotating wheel at 14 rpm.

The bacterial samples were then sonicated six times for 10 s. Following the addition of 10 mM MgCl2 and 10 μg/ml DNAse I, they were incubated for 10 min on ice. These samples were then centrifuged at 30000x *g* at 4 °C for 20 min, and in the meantime the Nickel-Select (Sigma) resin was equilibrated with lysis buffer. The supernatant was incubated with 0.5 ml resin for 1 h at 4 °C on a rotating wheel at 14 rpm. The resin was washed five times by centrifugation with lysis buffer, and then eluted in 500 μl elution buffer (50 mM Phosphate buffer pH 8.0, 300 mM NaCl, 250 mM imidazole) several times. The elution fractions, the crude extract, and the lysate supernatant were all run on SDS-PAGE to check for purity and yield.

3.12.2 Glutathione-S-transferase (GST)-fusion proteins

A single colony of *E. coli* transformed by a pGEX vector containing the GST fusion protein of interest was used to inoculate 100 ml LB. The bacterial culture was grown to an OD_{600} of 0.6. Expression was induced with 1 mM IPTG for 3 h at 37 °C. The bacteria were harvested by centrifugation at 6000x *g* for 10 min at 4 °C. The bacterial pellet was resuspended in 25 ml 20 mM TRIS-HCl, pH 8.0, 100 mM NaCl, 1 mM EDTA, 1 mg/ml lysozyme in the presence of water-soluble complete protease inhibitor cocktail (Roche). Triton X-100 (1%) was added, and the suspension agitated continuously for 30 min at 4 °C, and then sonicated for 2 min on ice. The lysed bacteria were centrifuged fo 20 min at 30000x *g* and the pellet was discarded. Meanwhile, 2.5 ml of a glutathione-Sepharose resin were diluted to 40 ml and centrifuged at 2000x *g* for 5 min to remove the preservative. The supernatant was discarded, and the resin was resuspended in 20 ml PBS. This procedure was repeated twice. The cleared bacterial lysate (see above) was then added to this glutathione-Sepharose resin and incubated at 4 °C on a rotating wheel at 14 rpm. The resin was washed three times with 50 ml PBS and poured into a column. The resin was allow to

pack for 10 min, and the protein was eluted with 1 ml elution buffer (100 mM Tris-HCl, 20 mM glutathione, 5 mM DTT). The eluate was collected, and this operation was repeated an additional five times. The protein content of each of the six fractions collected was analysed by SDS-PAGE and the fractions containing the highest protein concentrations were pooled.

3.13 Cell microinjection

The day before microinjection, the cells were plated in glass coverslips or on glass-bottomed Petri dishes, in normal culture medium. For microinjection of cells grown on coverslips, the coverslips were put into small Petri dishes (3 cm diameter) containing normal cultured medium buffered with 20 mM HEPES, pH 7.4. The Petri dishes were then transferred to the thermo-regulated stage of an inverted Zeiss IM 35 microscope, and kept at the temperature required for the experimental transport protocol. Microinjections were performed using a transjector 5246 controlled by a 5171 micromanipulator (Eppendorf, Germany), in the manual mode. The microinjection pressure was varied, depending on the conditions of the microinjection needle and the viscosity of the solution to be injected, in a range from 50 to 500 hPa. The microinjection time was manually defined by the operator as the shortest necessary to observe the propagation through the cytoplasm of a circular wave originating from the tip of the microinjection needle. The microinjections were made in the perinuclear area where the thickness of the cell is greater than that in the periphery. The needles for microinjection were prepared from 1.0-mm-internal-diameter glass capillaries (World precision Instruments, USA), using an automatic capillary puller (Inject-Matic, CH) with the heat controller set to 3. Microinjection needles were then loaded with 3 µl microinjection solution containing the antibody or the protein of interest in the

microinjection buffer (70 mM KCl, 10 mM NaH_2PO_4, pH 7.2). When needed, lysine-fixable fluorescent dextran (Molecular Probes, The Netherlands) was added to the microinjection mixture, to follow efficient microinjections. The microinjected cells were also located by means of a grid on the coverslip (when present), or otherwise by looking directly at the fluorescence using a 10x objective to identify the area of microinjected cells.

3.14 Kinase assay

3.14.1 Preparation of GST-PKD (wt,KD,CA) in Cos7 cells

COS7 cells ($5x10^6$) were electroporated with 10 μg DNA. After 48 h, the cells in Petri dishes were washed five times with cold PBS and preincubated with 1.2 ml RIPA lysis buffer (50 mM Tris-Hcl, pH 7.4, 1% NP-40, 0.25% Na-Deoxycholate, 150 mM NaCl, 1 mM EDTA, 1 mM PMSF (or Pefablock, Fluka), 1 μg/μl Aprotinin, 1 μg/μl Leupeptin, 1 μg/μl Pepstatin, 1 mM Na_3VO_4, 1 mM NaF) at 4 °C for 10 min. The cells were then scraped and passed 3-4 times through a 1-ml syringe. The lysates were centrifuged in 1.5 ml microcentrifuge tubes at 14000 rpm at 4 °C for 10 min in a standard bench-top microcentrifuge. The supernatants were aliquoted (300 μl), quantified, and frozen immediately in liquid nitrogen, and then kept at –80 °C. This protocol usually provided enough kinase for four samples in kinase assay (as follows).

3.14.2 [^{32}P] Kinase assay

Starting from the above cell lysates, every 300 μl aliquot was used for a single sample in the assay. The samples were defrosted in a waterbath at 30 °C and immediately placed at 4°C when they were nearly completely defrosted. Then they were incubated

on a rotating wheel at 14 rpm at 4°C for 1 h with 20 µl GST-Sepharose 4B resin equilibrated with RIPA buffer. The resin was washed twice with RIPA buffer and twice with 20 mM HEPES, then resuspended in 48 µl 100 mM HEPES. The sample was added with 16 µl of GO solution (500 µM ATP, 5 µCi $\gamma[^{32}P]$-ATP, 25 mM $MgCl_2$ and 100 mM HEPES) with the substrates/controls on ice (N.B. the final concentration of ATP was 100 µM). The kinase reaction was started by putting the samples at 30 °C and after 10 min the reaction was stopped with sample buffer and boiled for 5 min.

4 Results

4.1 The thematic interactome: known interactions

I started to collect interactions relevant to TGN-to-PM trafficking for several reasons. First of all, I considered the elements present in Figure 7 for which a defined participation in this pathway is clear. Then, I added other elements that are significantly related, together with their interactors. I selected them from literature mainly, and from interaction databases, such as STRING (http://string.embl.de//). In the interaction map shown in Figure 8 it is possible to appreciate the complexity of the resulting interaction network. What is immediately evident is the importance of some specific elements, such as CtBP1-S/BARS, PKD and PI4KIIIβ, which have nodal positions in the network. Many other elements are connected in this network (Fig. 8), which considers only the positive, direct, and physical interactions among them. Also, this network comprises only mammalian proteins for the sake of clarity.

There are many interesting interactions also in yeast, as shown in Figure 9. The choice here was to keep the yeast and mammals interaction networks separate, with the focus of the study on mammals.

4.2 The two-hybrid interaction matrix: the search for new interactions

To provide new interactions among the interesting players that can participate in post-Golgi trafficking from the TGN to the PM, I choose the elements present in Tables 4.1, 4.2 and 4.3 for two-hybrid screening, based on their potential relevance in TGN-to-PM

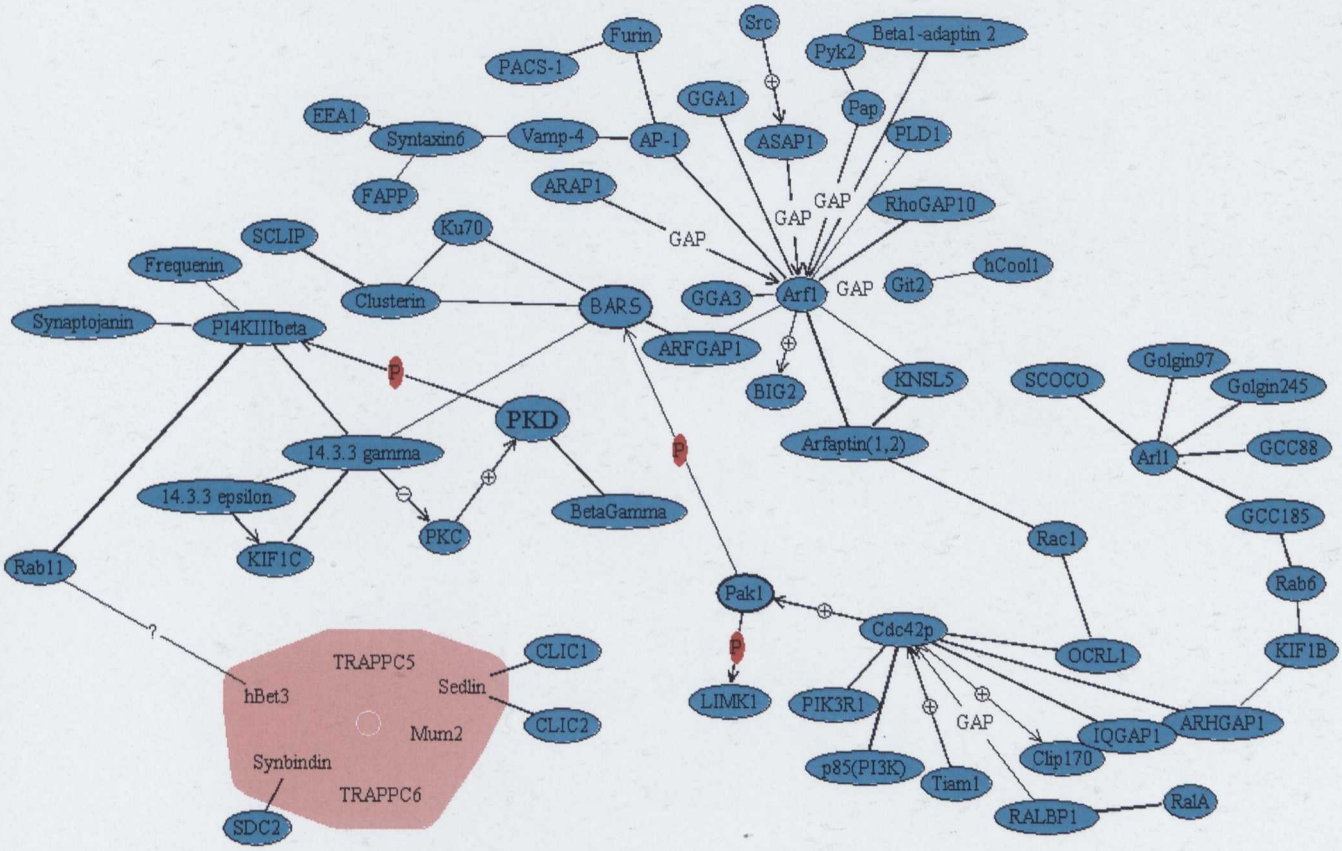

Figure 8. The mammalian thematic interactome

This interaction map was created with our home-made software, to graphically collect and display only direct and mammalian interactors. The lines represent two-hybrid direct interactions, bold lines represent interactions confirmed by our laboratory or present in the literature. Lines marked with + or – or (P) represent functional interactions i.e. activation, inactivation and phosphorylation, respectively. The question mark labels the interaction between the TRAPP complex (represented as the pink area) and the Rab family protein Rab11; this interaction is not proven but is strongly suspected, due to the high level of yeast-mammalian homology in both counterparts. Compare also with yeast proteins in the yeast interaction map (Figure 9)

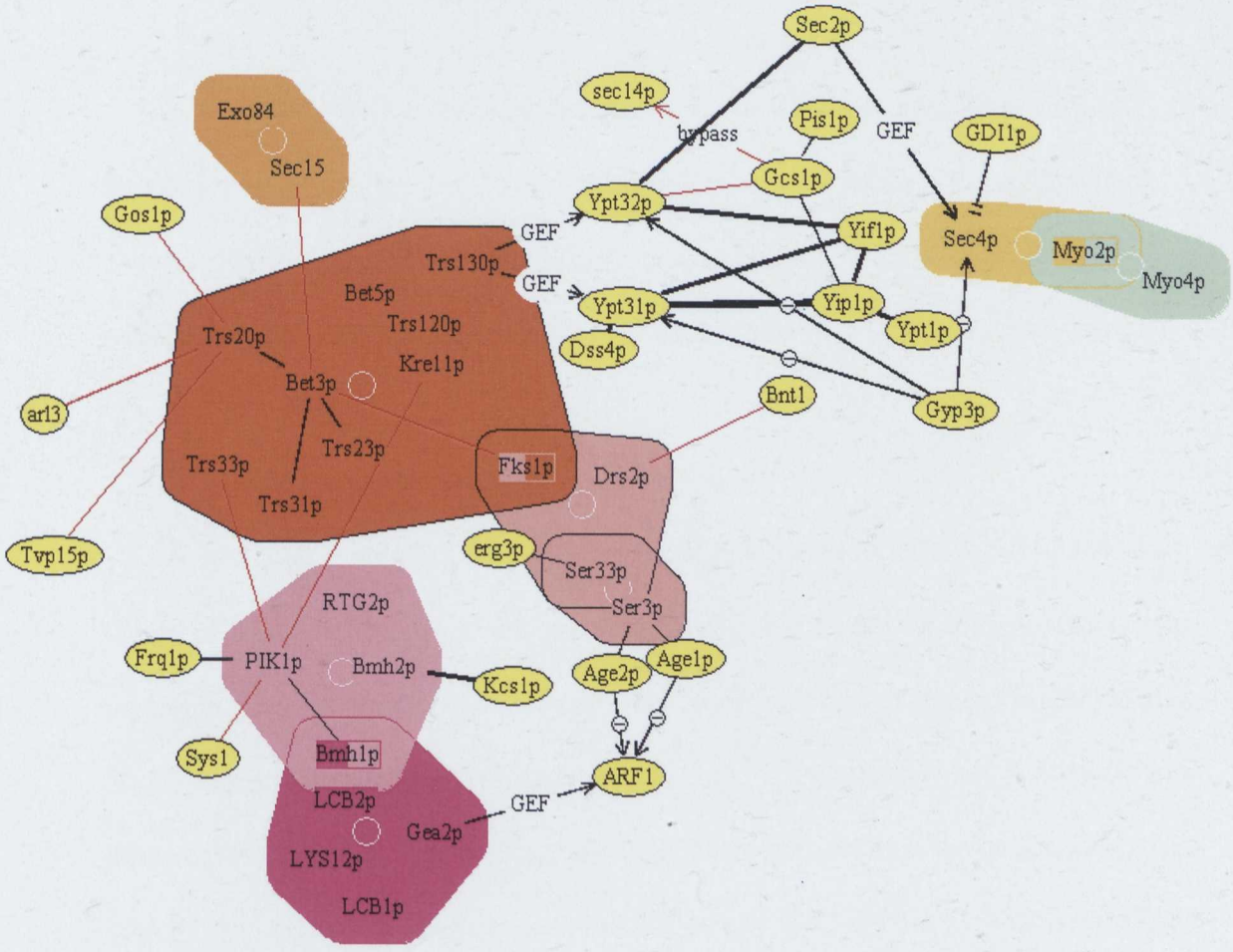

Figure 9. The yeast interaction network

This network presents direct physical interactions (lines) and complexes (coloured areas) in yeast. The red lines represent genetic interactions. In this network, the important interactions between well known elements of yeast post-Golgi trafficking are shown, such as Ypt31/32, ARF1, PIK1 (PI4K homologue). Ser3 is what we consider as the putative homologue of BARS, and it has interesting interactions with some ARF1 GAPs. Moreover, it is complexed with Drs2p, which is a 'flippase' that is involved in post-Golgi transport. Bmh1p (14-3-3 homologue) interacts with PI4K, as in mammals. The TRAPP complex, presented as the dark-orange area, clearly gives interesting links with post-Golgi trafficking elements such as Ypt31, Pik1, Fks1p. Compare also with mammalian proteins in the yeast interaction map (Figure 8)

trafficking. To decide the candidates for the two-hybrid study, the interaction network in Figure 8 was particularly helpful.

The two-hybrid system has the advantage of showing only direct phisical interactions between proteins, and the possibility to work on high-throughput basis. In contrast, it also gives false positives, and consequently there is the need to further confirm the positive interactions using different methods (e.g. IP, co-localization).

4.2.1 Preparation of candidates

As a first technical step for the two-hybrid analysis, I prepared the DNA constructs (listed in Tables 4.1, 4.2, 4.3) that are compatible with the two-hybrid system, thus I performed the subcloning of the coding sequences into vectors that are suitable for the Matchmaker3 (Clontech) two-hybrid system (see Figure 10). The two-hybrid system allows proteins to be expressed in yeast cells fused with the activation domain (AD), which activates the reporter gene expression on one side, and fused with the binding domain (BD) that binds the DNA in the proximity of the promoter on the other side (Fig. 10). Every interaction is revealed by the proximity between the BD and AD domains, a condition that occurs if the two partners interact. The original purpose was to subclone each gene of interest into both the AD and BD domain, and this was done for the majority, but not for all, of the players listed in Tables 4.1-4.3 (for technical reasons). Some of them are in only one of the two forms, as shown in Table 4.4 which illustrates the matrix of the interactions tested in this study.

Table 4.1 The proteins chosen for the two-hybrid screening in this study are listed, along with their synonyms, Swiss-Prot accession numbers, aminoacidic length and function. The clones marked with * were kindly provided in pGBK vectors by the Sallese laboratory of the DCBO.

NAME	Synonyms	SwissProt code	Length (AA)	Function
Gαi3		P08754	354	Signalling
Src		P41239/P00523	533	Signalling
Gβ/γ*				Signalling
Cdc42	G25K	P60953	191	Signalling
PKD1*	PKCμ	Q62101	916	Signalling/Golgi-to-PM transport
PKD2		Q9BZL6	878	Signalling/Golgi-to-PM transport
Pak1	P65-PAK	Q13153	545	Signalling
ARF1*		P32889	180	Golgi maintenance and trafficking
ARL1		P40616	181	Arf-related protein that interact with GRIP-domain of golgins
ARFGAP1	ARG1	Q62848	415	ARF1 GTPase activating protein
ARAP1a	CentaurinD2	Q96L71	1205	ARF1 GTPase activating protein
Arfaptin2*	POR1	P53365	341	ARF1 and Arl1 interacting protein
Arfaptin1*		Q2M2X4	341	ARF1 and Arl1 interacting protein
PI4KIIIβ*	PI4K92	Q9UBF8	816	Phospholipid metabolism
PI4KIIα			479	Phospholipid metabolism
FAPP1	PLEKHA3	Q9HB20	300	Golgi-to-PM transport
FAPP2	PLEKHA8	Q96JA3	507	Glycolipid transfer activity/Golgi-to-PM transport
OSBP1		P22059	807	Oxysterol binding protein
PLD1*				Phospholipid metabolism
PITPβ		P53811	271	Phospholipid metabolism
14-3-3γ		P61983	247	Scaffold protein
GAPDH*		P00354	334	Energy metabolism/BFA-ribosylated substrate
BARS*	CtBP1-S, BARS50	Q9Z2F5	430	BFA-ribosylated substrate/membrane fission activity
VSVG		P04884	511	Viral capsid protein (cargo used as a trafficking probe)
OCRL-1*		Q01968	901	Inositol polyphosphate 5-phosphatase
Dynamin II		P39052	870	Membrane fission activity
Sedlin*	TRAPPC2	O14582	140	Component of the TRAPP complex
Bet3	TRAPPC3	O43617	181	Component of the TRAPP complex
Synbindin	TRAPPC4	Q9Y296	219	Component of the TRAPP complex
TGN46		O43493	480	TGN-specific matrix protein
TGN38*		P19814	357	TGN-specific matrix protein
Frequenin	NCS-1	P62168	190	Regulator of PI4-kinase

I also subcloned into the above vectors some selected domains present into the following proteins: PKD, BARS, ARAP, FAPP1 and FAPP2, as listed in Table 4.2.

Table 4.2 Deletion fragments

The names of these deletion fragments are as used into the main text. The parental proteins from which fragments were extracted are also listed here, along with the formal name of the domain they comprise, and its position, length, and function. The clones marked with * were kindly provided in pGBK vectors by the Sallese laboratory of the DCBO. PKD 1CD comprises the region 589-845 previously used in a two-hybrid experiment (Haworth *et al.*, 2004).

NAME	NAME of Full-length protein	domain	position	Length (AA)	function
FAPP1-PH	FAPP1	PH	1-93	93	PIP2 binding/Golgi-to-PM trafficking
FAPP2-PH	FAPP2	PH	1-93	93	PIP2 binding/Golgi-to-PM trafficking
diFAPP1-PH*	FAPP1	PH dimer	(1-93)LLCSLL(1-93)	192	PIP2 binding/Golgi-to-PM trafficking
FAPP2 w/o PH	FAPP2	GLTP	97-507	410	Glycolipid transfer activity
ARAP(552-1077)	ARAP1a	PH domain plus RhoGAP	552-1077	525	Stimulation of GTPase activity of ARF1
BARS-NBD*	BARS	NBD	111-306	195	Nucleotide-binding domain
BARS-SBD*	BARS	SBD	1-111/308-430	233	Binding of PXDLS motif present in transcriptional regulators
PKD1-CD	PKD1	Catalytic	501-901	400	Substrate phosphorylation
PKD2-CD	PKD2	Catalytic	542-878	336	Substrate phosphorylation
Src-SH2*	Src	SH2	82-156	74	P-Tyr binding

I also subcloned the small G-protein mutants in their active (GTP-bound) forms, since it is well established that they preferentially interact with their partners/effectors when they are bound to GTP instead of GDP. These are listed in Table 4.3

Table 4.3 The active form mutants of GTPases used in the two hybrid assay, together with the name of their mutant forms, effectors and functions.

Name	Mutant form	Effectors in GTP form	Specific Function
ARF1-GTP	Q71L	Arfaptin1,2, COPI, adaptor proteins (APs), FAPP	Retrograde trafficking Golgi-ER, Chlatrin-mediated transport from the TGN, TGN-to-PM
ARL1-GTP	Q71L	Arfaptin2, Golgin97, Golgin245	Recruitment of GRIP-domain matrix proteins to the TGN
Cdc42-GTP	V12	Wasp, Pak1, COPI	Actin regulation, enhancer of polarization state, basolateral transport

Finally, 34 candidates as 'bait' vectors and 29 candidates as 'prey' vectors were prepared in the Matchmaker3 System (BD Clontech) for the two-hybrid assay (Table 4.4). These were made, where possible, with the classical cut and paste procedures using restriction enzymes. When this was not possible, I designed oligonucleotides plus restriction sequences to PCR-amplify the ORFs. After ligase reactions and transformation of the *E. coli,* several clones from every single candidate were checked on agarose gels, to assess the presence of the correct-weight digested fragments. I then sequenced their ORFs in the 5' direction, starting from the T7

promoter upstream of the multi-cloning site, to check for their correct orientation and frame.

Subsequently I transformed the Y187 and AH109 yeast strains (provided with the Matchmaker3 System) with the Gal4 activation domain (AD)-fused proteins and with the DNA binding domain (BD)-fused proteins, respectively (see Methods, section 3.2). Both the AD and BD were fused at the N-terminus of the subcloned ORFs.

4.2.2 Protein expression testing

I used Western blotting to check the protein expression of the yeast clones grown to stationary phase, using antibodies against the HA and Myc tags, which were present at the N-terminus of the subcloned ORFs (Fig. 10). In some cases, protein expression was not detectable due to several factors, such as proteolytic degradation or toxicity. In these cases, I checked the DNA sequence of the ORFs also in the 3' direction, and in parallel I performed a second round of at least three different yeast-transformed clones, with both anti-tag and protein-specific antibodies when available, such as in the case of ARL1, FAPP2, PI4KIIα, OSBP1 and TGN38. Table 4.4 shows the yeast clones that were finally available for the two-hybrid assay, and thus the interactions tested among them included up to 986 possible combinations. Proteins for which the expression in yeast was not detected were also considered (grey area of Table 4.4).

4.2.3 Advantages of the two-hybrid matrix strategy

The use of the full-length proteins crossed in a two-hybrid interaction matrix, as used here, is much more advantageous compared to a classical two-hybrid library screening for four main reasons: (i) first and most important reason is the need for the correct folding of the protein, which is much more likely to occur when the polypeptide chain

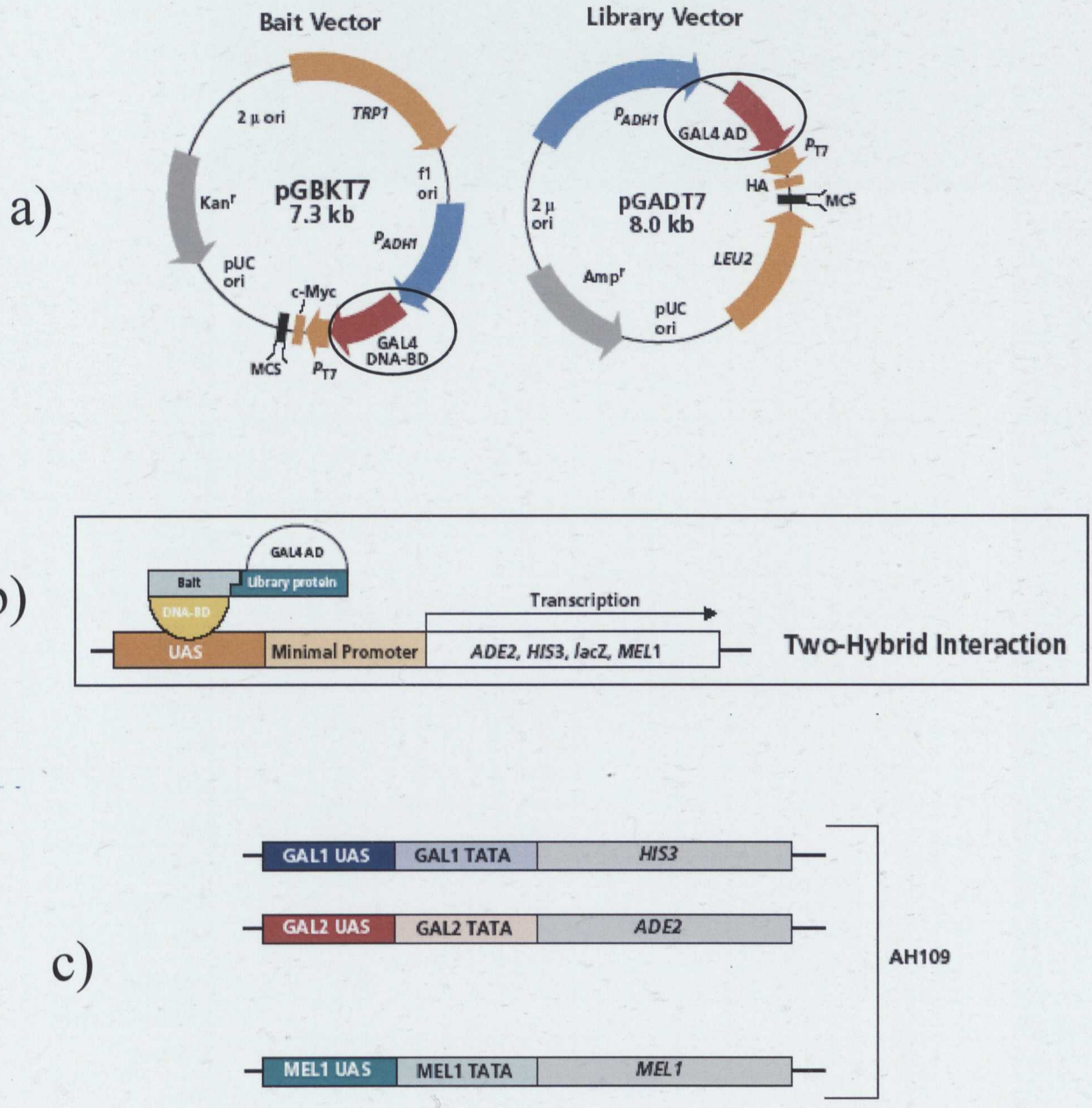

Figure 10. The two-hybrid principle

As shown in the Materials and Methods, the first step for every two-hybrid system is the subcloning of the genes of interest into vectors that allow their expression in yeast (a). When the two vectors are in the same yeast diploid cell after the mating of the two strains (one with pGAD, the other with pGBK) the two fusion proteins (b) enter the nucleus and (after a positive interaction) the activation domain (AD) and the binding domain (BD) activate reporter gene expression (c), here shown as His3, Ade2, Mel1. For further details, see Materials and Methods in section 3.3

Table 4.4 The two-hybrid matrix

This Table collects all of the prepared and sequence-checked preys and baits that are available for the two hybrid, and gives the possibility to appreciate all the interactions (986) that can be tested between the 29 preys and the 34 baits with their AD and BD domain respectively. This is thus the so-called two-hybrid interaction matrix. The grey area represents proteins with expression levels that were not detectable by Western blotting. ARFGAP1 gave a good expression level, but its MW was 10 kDa lower than expected. All of the present clones were used for the two-hybrid anyway, but caution should be used when interpreting negative results regarding these. Asterisks indicate clones that were kindly provided by Sallese laboratory in our Department (DCBO)

pGAD (Prey) 29 34 / pGBK (Bait)	ARF1	Arfaptin2	FAPP1-PH (dimero)	ARF-GTP	14.3.3γ	Synbindin	ARL1-GTP	PKD2-CD	Pak1	Bet3	OSBP1	FAPP1	PITPβ	ARAP1 (552-1077)	TGN46	BARS	PKD2	FAPP2*	FAPP1-PH	Gαi3	Cdc42-GTP	Frequenin	FAPP2 w/o PH	FAPP2-PH	PI4KIIα	PKD1-CD	ARL1	Dynamin II	ARFGAP1
Src-SH2*																													
Gβγ*																													
FAPP2*																													
ARF1*																													
Arfaptin1*																													
Arfaptin2*																													
PI4KIIIβ*																													
PLD1*																													
GAPDH*																													
BARS*																													
BARS-NBD*																													
BARS-SBD*																													
OCRL-1*																													
Sedlin*																													
TGN38*																													
diFAPP1-PH																													
ARF1-GTP*																													
PI4KIIα																													
14-3-3γ																													
Synbindin																													
Cdc42																													
ARL1																													
PITPβ																													
PKD2																													
OSBP1																													
ARL1-GTP																													
Dynamin II																													
FAPP1-PH																													
FAPP2-PH																													
TGN46																													
Bet3																													
PKD1*																													
Cdc42-GTP																													
Gαi3																													

is complete and not in a truncated form; (ii) the second reason is the significant decrease in false-positive results that are due to interactions with 'sticky' misfolded portions of truncated domains; (iii) the third reason is the reduction of false-negative results due to the presence of several interacting motifs spread along several positions that fall into sometimes very distant domains, which makes mandatory to have a full-length polypeptide in this case; and (iv) the last reason is that in a library screening, not all of the clones present in the library are expressed to the same level, thus resulting in the exclusion of some (potentially interesting) interactions that are undetected or below a threshold that is overcome by many other clones. This arises because in a library screening the selection is based on quantitative activation of reporter genes, which often depends on the amount of the expressed interacting peptides.

Considering a two-hybrid interaction matrix, which is, as in this case, a collection of prey and bait full-length clones that here provide a high number (986) of testable interactions (Table 4.4), there is a way to reduce this time-consuming, high-throughput laboratory work. I set up for our purpose a two-hybrid strategy that was originally developed for the construction of large protein interaction maps (Zhong *et al.*, 2003), which allowed the discovery of new interactions in a more rapid way when compared to the single, one-by-one crossing of the whole clone collection, which has also been applied by M. Vidal to a huge human-clones collection (Rual *et al.*, 2005).

This strategy consists of the pooling of yeast clones that contain the AD-fused proteins (on the one side) and in the pooling of the yeast clones containing the DNA-binding BD-fused proteins (on the other). Subsequently, individual AD-clones were mated with the BD pool, and *vice-versa*, individual BD-clones were mated with the

AD pool. As a first step, I obtained single AD and BD clones that showed positive interactions (with any other counterparts in the respective pool) that had not been identified yet.

To determine which interacted with which, these 'incomplete' results were used to design a 'submatrix', which consisted of the single protein-protein crossings between the AD- and BD- positive clones from the above screening. This 'submatrix' contained 154 possible interactions, all of which were tested one by one in 96-well plates, to determine who interacts with whom. A schematic view of the strategy is shown in Figure 11. This approach was useful, since I tested six-fold fewer single interactions, compared to the full matrix in Table 4.4 that comprises 986 possible crossings.

4.2.4 Confirmation of results

All of the binary interactions resulting from this two-hybrid approach were tested again with serial dilutions (not shown), and Table 4.5 reports only the positive, confirmed results. The positive clones were plated in QDO plates (see Materials and Methods, section 3.3) for the control of the expression of three reporter genes, and in parallel they were plated also in TDO plates, for the assessment of only two reporter genes, in order to also reveal any weaker interactions.

The interaction strengths in Table 4.5 depended mainly on this difference, and also on the growth levels. The interactions that activate all three of the reporter genes present in the Matchmaker3 (Clontech) two-hybrid system (see Materials and Methods, section 3.3) are likely to be stronger, and are less likely to be false negatives.

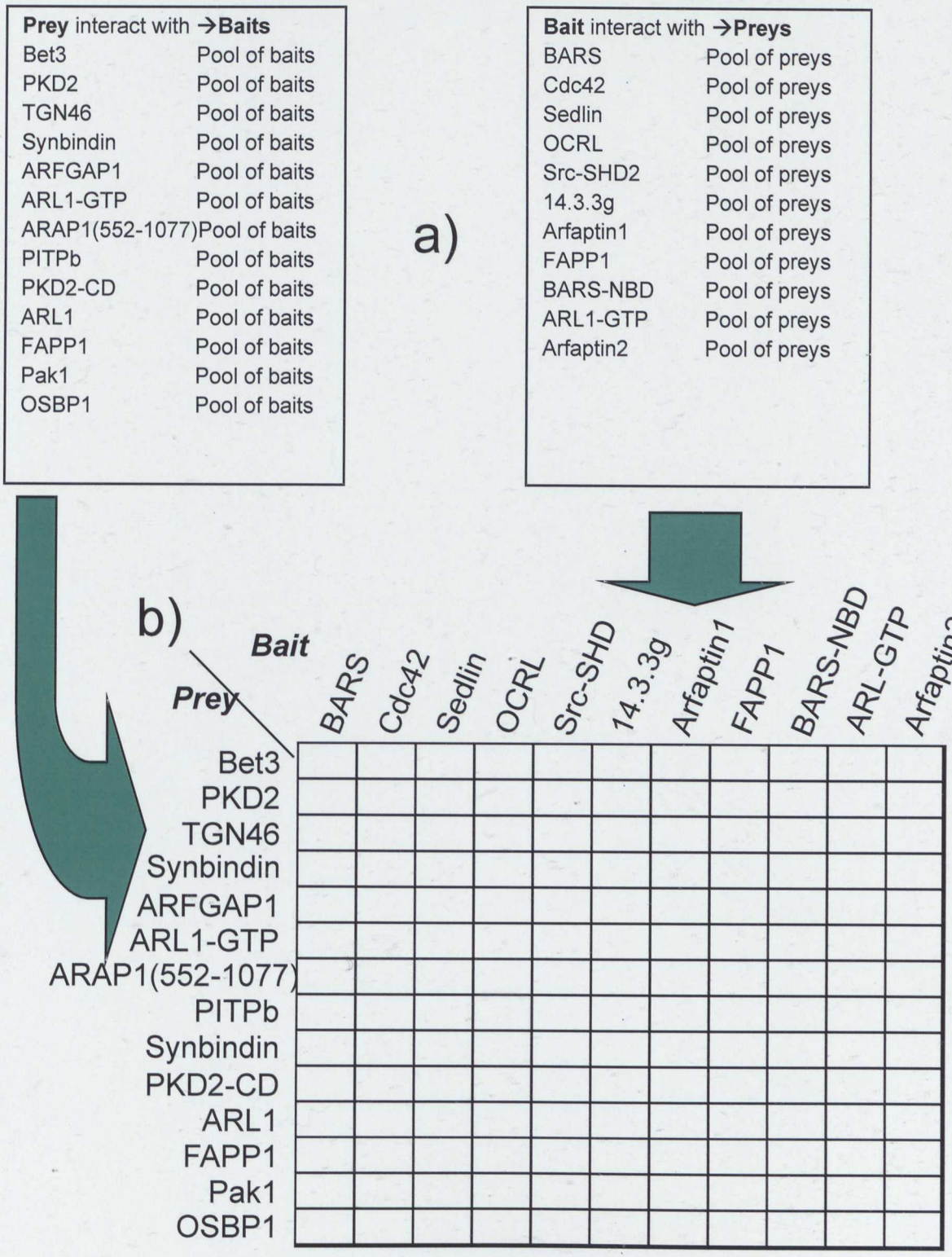

Figure 11. The two hybrid strategy

This scheme summarizes the approach used to discover new interactions using a two-hybrid system. (a) Single clones with the activation domain (AD) are each crossed with the binding domain BD pool, and *vice-versa* for all of the BD clones *versus* the AD pool. The proteins (out of the total) that give positive results by interacting with at least one of their counterparts in the pool are shown. (b) To identify which

preys	baits	I S	reporter genes	QDO	TDO	CTRL AD	CTRL BD
Bet3	Sedlin	++++	3		/		
ARL1-GTP	Arfaptin2	++++	3		/		
PKD2-CD	Sedlin	++++	3		/		
Arfaptin2	Arfaptin1	+++	3		/		
Arfaptin2	Arfaptin2	+++	3		/		
PKD2	Arfaptin2	+++	3		/		
PKD2	BARS-NBD	+++	3		/		
ARL1-GTP	BARS	++	3		/		
ARAP1(552-1077)	14-3-3γ	+	2	/			
Synbindin	14-3-3γ	+	2	/			
PITPβ	Arfaptin2	+	2	/			
Cdc42-GTP	14-3-3γ	+	2	/			
Cdc42-GTP	Arfaptin2	+	2	/			

Table 4.5 two-hybrid interactions

The newly discovered interactions between the activation (AD)- and binding domains (BD)-fused proteins. These came from the high-throughput strategy described in the text, after their confirmation in single experiments in which they were crossed again and tested again for growth, with all of the autoactivation controls (righthand columns). The results are ordered following the strengths of the interactions (IS= interaction strenght). Thus, the interactions between baits and preys, namely the AD- and BD-tagged clones, that allow the growth on plates with QDO media came first, since the QDO plates allow for the growth of the clones that activate all of the three reporter genes (see Methods, section 3.3). At the bottom part of the Table, there are the interactions that allow for the growth on TDO media plates, because they activate two of the reporter genes (see Methods, section 3.3).

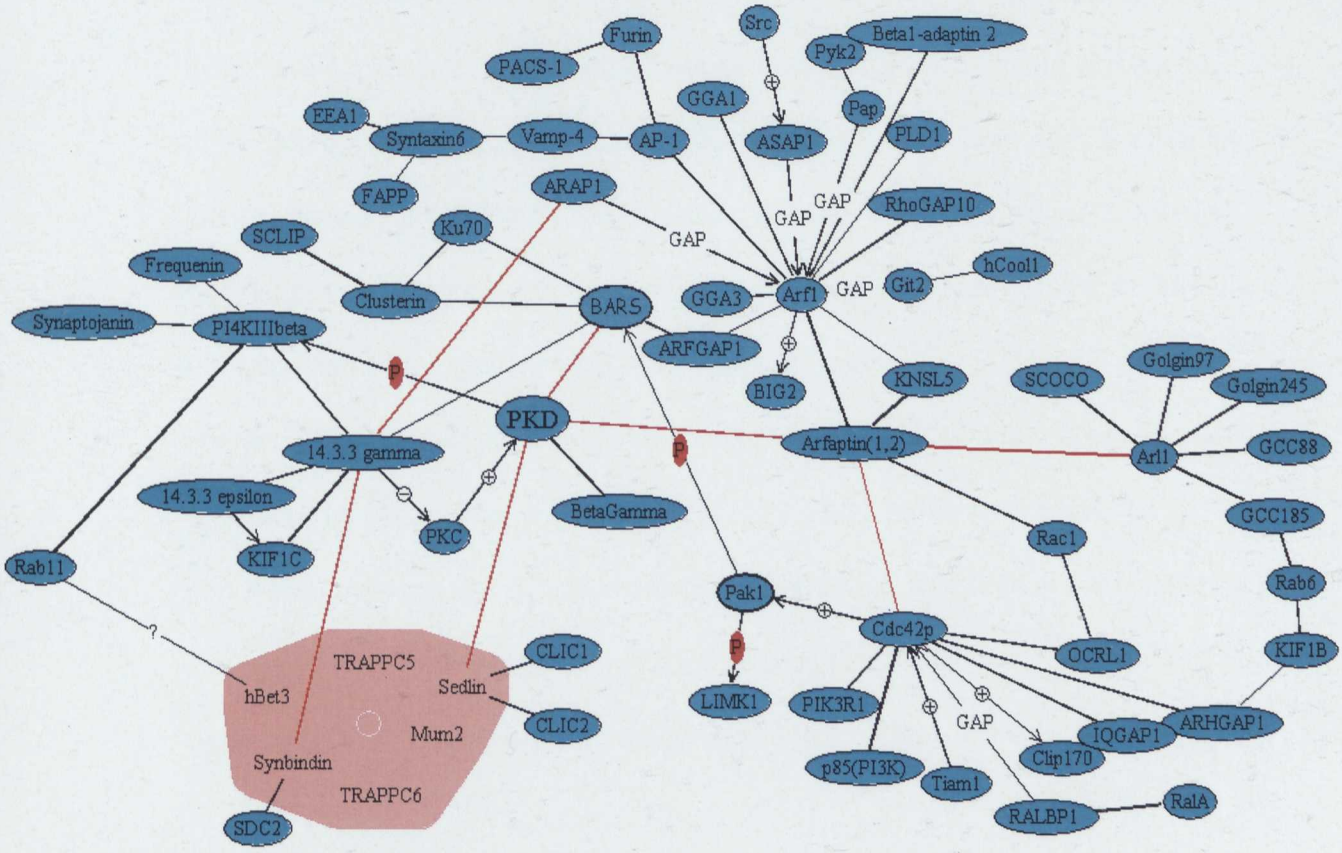

Figure 12. Adding in the novel mammalian interactions

The novel two-hybrid interactions from Table 4.5 are shown in red. PKD appears to be an important hub towards which many pathways converge. Arfaptins 1 and 2 also occupy a central position in the network, even if their functional roles are not fully clarified yet. TRAPP is also well connected in the network via its components Sedlin and Synbindin.

What also should be noted is that a quantitative difference cannot be directly related to the strength of the interactions themselves, since the detectability of the two-hybrid system can vary according to several factors: first, the protein expression levels of the two interacting partners can vary from one case to another; then, the topology of the interaction partners on the DNA molecule at the level of the promoter can vary. This latter is responsible for the activation of the reporter genes. Also responsible for the activation of the reporter genes is the level of entry of the AD or BD domain chimera into the yeast nucleus, and the Km of the individual interactions themselves, which can be very stable or very transient, depending on the case. Thus, the correlation between strength of interaction and level of activation of the reporter genes can be masked by the variables indicated here and thus the growth strength seen in a two-hybrid system cannot be directly related to the biology of the interaction.

4.3 Enriching the TGN-to-PM interaction network

As a first use of the newly discovered interactions, I inserted them into the interaction network shown in Figure 8. As is clearly seen, the nodal proteins PKD, Arfaptin, and 14-3-3γ dramatically become "more nodal" than before when these novel interactions are considered (Fig 12). The TRAPP complex, which was suspected to be linked to post-Golgi routes in yeast, appears to be even more strongly linked to the post-Golgi stages, due to the new PKD-Sedlin interaction, as shown in the hybrid map that combines the yeast and mammal interactions together (Fig. 13), Moreover, the TRAPP complex subunit Synbindin interact with 14-3-3γ, and this interaction also contributes to this direction. The fact that this map is hybrid (yeast and mammals) is also very helpful, and it is justified since the TRAPP complex is particularly conserved between species (Table 4.6).

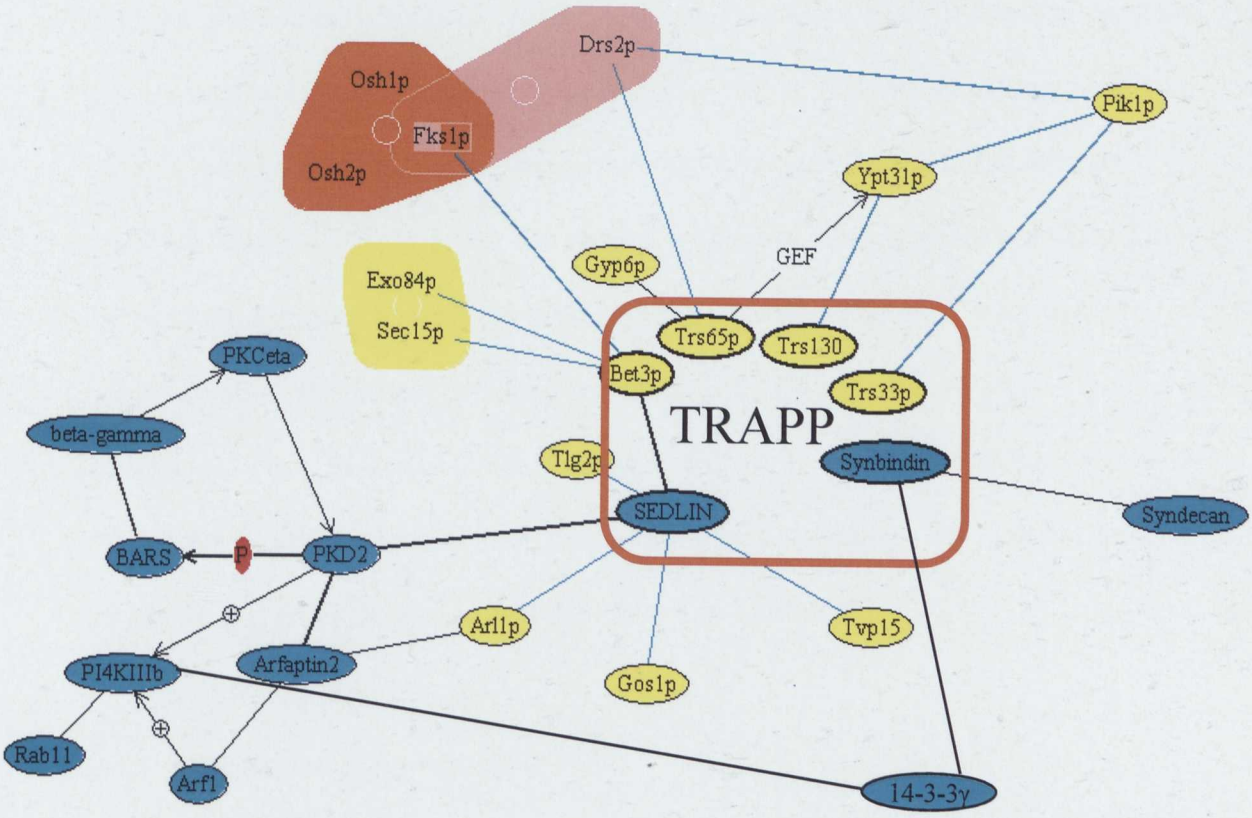

Figure 13. The TRAPP interactions in yeast and mammals

The interactions around the TRAPP complex (within the orange border) are collected together in this interaction map, for both yeast (yellow) and mammals (cyan). The novel interactions (PKD2-Sedlin, 14-3-3γ-Synbindin) contribute to the concept of TRAPP as a post-Golgi player. Black lines represent direct interactions, cyan lines represent genetic interactions in yeast and coloured areas represent complexes.

4.4 Going deeply into some binary interactions

The two-hybrid system provides information on binary interactions, even if, as widely accepted, there is the possibility of false positives. However, the Matchmaker3 system (Clontech) that I used is designed to dramatically reduce the number of false positives, and this is especially true for the interactions that activate all three of the reporter genes (see Table 4.5). Moreover, the promoters of these reporter genes are located in different independent areas of the yeast genome. Nevertheless, there is always the need to confirm the protein-protein interactions with different experimental approaches. Thus, I decided to confirm some of them. In the present section I describe the functional implications of these interactions, thus providing a rationale for their choice among all of the two-hybrid data shown in Table 4.5.

4.4.1 Arfaptin interacts with Arl1

The direct interaction between the small G-protein Arf-like protein 1 (Arl1)-GTP and Arfaptin2 turns out to be a positive control into our two-hybrid data set because it was already known (Van Valkenburgh *et al.*, 2001). Thus this particular interaction is already confirmed by previous studies. Arl1 is highly similar to the well characterized small G-protein Arf1 (Beraud-Dufour and Balch, 2001; Donaldson *et al.*, 2005); however, its precise functional role is still not known. Arl1 has an exclusive localization at the TGN, as has been shown by immunofluorescence and EM (Burd *et al.*, 2004). The Q71L mutant of Arl1 is not able to hydrolyze GTP, and thus it remains in its active/membrane-bound form. At present, nothing is known about the function of this Arl1(Q71L)-Arfaptin2 interaction.

The Arfaptins (1 and 2) have a BAR domain that has been structurally determined (at least for Arfaptin2) as a membrane-curvature-promoting and/or sensor

domain (Peter *et al.*, 2004). This feature is interesting, because as it might have a role in the process of membrane bending and the subsequent budding, it can be hypothesized that Arl1 is an anchor for the TGN localization of Arfaptin, which would favour the activity of Arfaptin on carrier formation, which is the first step in TGN to PM transport (see Introduction, section 1.2).

4.4.2 Arfaptin interacts with PKD

Another interesting interaction that comes from the two-hybrid assay occurs between Arfaptin2 and PKD2. The three PKD isoforms PKD 1, 2 and 3, are Ser-Thr kinases that are involved in trafficking at the level of TGN to PM trafficking, and their kinase activities are necessary for membrane fission, (Liljedahl *et al.*, 2001; Yeaman *et al.*, 2004).

With the use of confocal microscopy, we have seen that Arfaptin2 co-localizes with the TGN compartment marker TGN46 (Figure 21), and we know using immuno-EM that it is mainly TGN-associated (De Matteis laboratory, unpublished observations). Arfaptin1 is strongly similar to Arfaptin2, and it was discovered later, despite its name. The overexpression of Arfaptin1 is inhibitory for the secretion of metalloproteinase 9 (MP9), a constitutive cargo that is directed to the PM (Ho *et al.*, 2003). The transport of MP9 is known to be mediated by the phorbol 12,13-dibutyrate (PDB)-activated form of PLD, and PLD is known to be inactivated by Arfaptin1 overexpression (Williger *et al.*, 1999). PDB is one of the family of phorbol esters, which are known to mimic diacylglycerol (DAG) activity and to recruit and activate PKD on the TGN.

Moreover, Arfaptin 1 and 2 can heterodimerize, as also demonstrated with our two-hybrid system (see Table 4.5). Considering that PKD is activated by PDB as well, and that an active pool of PKD is important for membrane fission, a parallel mechanism can be hypothesised for a role for the Arfaptin2-PKD interaction, where Arfaptin2 can have a regulatory role on the activity that PKD exerts on transport. This fits with the idea that Arfaptin via its BAR domain, can be important for the first step (membrane deformation/budding) of the process, maybe by blocking the activity of PKD on membrane fission which has to occur only when a completely mature carrier is formed.

To confirm the two-hybrid interaction between Arfaptin2 and PKD2, my first attempt was to co-immunoprecipitate overexpressed Arfaptin2-FLAG together with the wild-type or kinase dead (KD) PKD2 (Fig. 14). The co-overexpression of Arfaptin2-FLAG and GST-PKD2 clearly showed co-immunoprecipitate *in vivo*, as revealed by the antibody for the GST tag in Western blotting of the anti-FLAG immunoprecipitate. In parallel, the immunofluorescence analysis showed co-localization between Arfaptin2 overexpressed with a FLAG tag and GST-PKD2 in the perinuclear area of HeLa cells (Fig. 14 C).

Encouraged by the above result, I subsequently attempted to co-immunoprecipitate the endogenous proteins in HeLa and COS7 cells using specific antibodies. Thus, I performed immunoprecipitation of Arfaptin2 in the cell lysate with 1% Triton with anti-Arfaptin polyclonal antibody. Western blotting with a PKD specific polyclonal antibody (Santa Cruz) showed a band of 100 kDa were Arfaptin2 immunoprecipitate was present, corresponding to the molecular weight expected for PKD (Fig. 15). This antibody does not allow a distinction between PKD1 and 2 (that

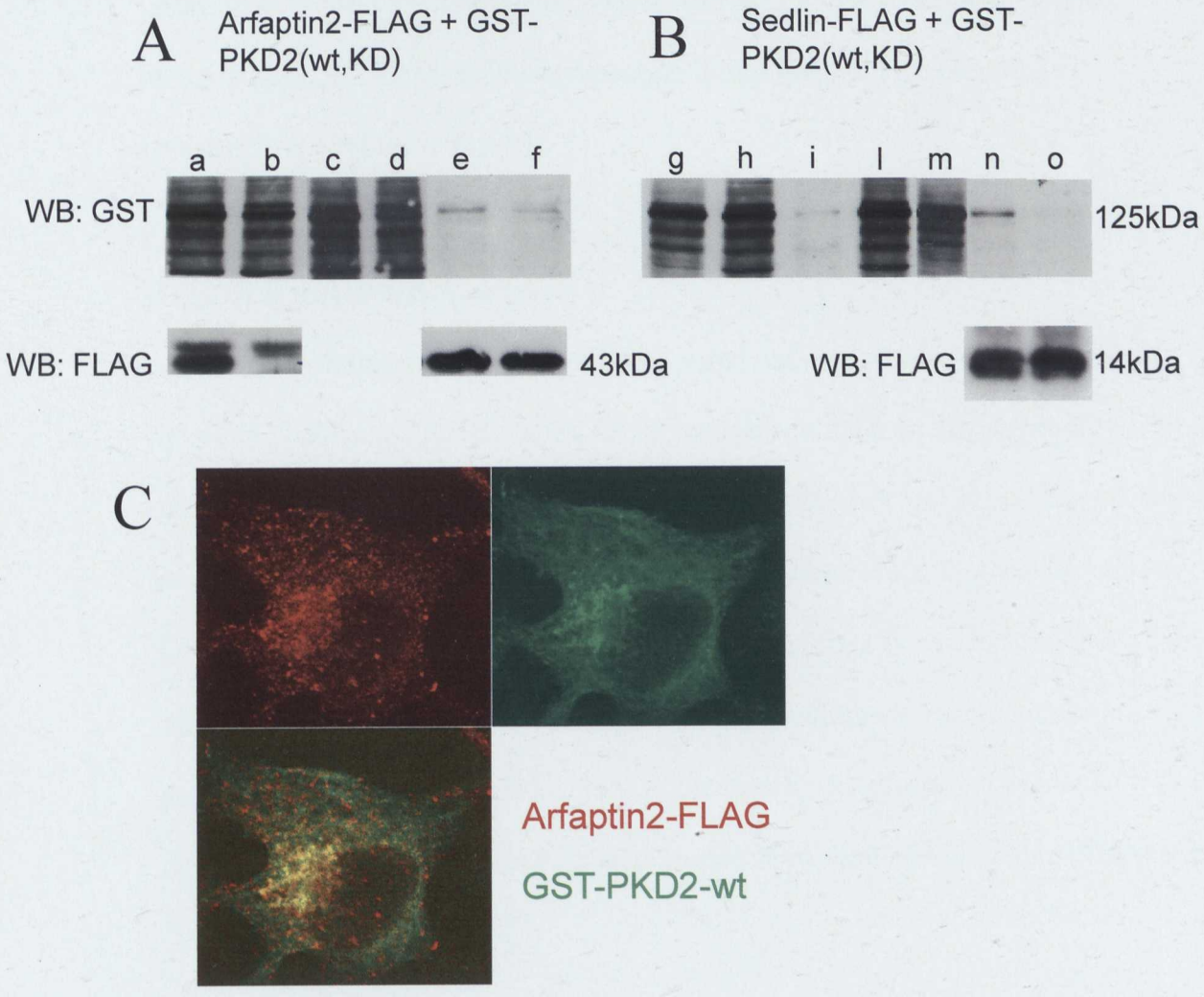

Figure 14. Arfaptin and Sedlin co-immunoprecipitate PKD mainly in its functional, wild-type form

COS7 cells were co-transfected with Arfaptin2-FLAG and GST-PKD2 in the wild-type or in the kinase dead (KD) form, than the cell lysates were immunoprecipitated with the EZ view RED Anti-FLAG (SIGMA) antibody on affinity resin (see Methods, section 3.5). (A) Western blotting showing the GST signal in the input lysate and in the flow-through of the GST-PKD2-wt cooverexpressed with Arfaptin2-FLAG (a input, b flow-through), and of the GST-PKD2-KD cooverexpressed with Arfaptin2-FLAG (c input, and d flow-through), and the GST signal in the immunoprecipitate in the presence of GST-PKD2-wt or GST-PKD2-KD (e and f, respectively). Western blotting with the anti-FLAG antibody shows the presence of the Arfaptin2-FLAG in the corresponding lanes. (B) COS7 cells were co-trasfected with Sedlin-FLAG and GST-PKD2 in the wild-type or in the KD form, than the cell lysates were immunoprecipitated with the EZ view RED Anti-FLAG (SIGMA) antibody on affinity resin (see Methods, section 3.5). A pull down with anti-FLAG in cells overexpressing only GST-PKD provided a negative control for both A and B: western blotting shows the GST signal in the input lysate and in the flow-through (g and h, respectively) and in the immunoprecipitate (i). Western blotting of the GST signal in the input in presence of Sedlin-FLAG plus GST-PKD2-wt (l) or GST-PKD2-KD (m). Western blotting of the GST signal in the anti-FLAG immunoprecipiate in the presence of Sedlin-FLAG plus GST-PKD2wt (n) or GST-PKD2-KD (o). Western blotting with the anti-FLAG antibody shows (below) the presence of the Sedlin-FLAG in the corresponding lanes. (C) In confocal sections, Hela cells co-transfected with Arfaptin2-FLAG and GST-PKD2-wt shows co-localization in the perinuclear area.

have a high homology, especially in their catalytic/substrate recognition domains), since it was raised by immunizing a rabbit with a common N-terminal peptide. Interestingly, the Arfaptin-PKD interaction is dependent on the presence of phosphatase inhibitors (Fig. 15).

4.4.3 Sedlin interacts with PKD

Another interesting interaction that I discovered with the two-hybrid assay occurs between Sedlin and PKD2, via the PKD2 catalytic domain. Sedlin is part of the trafficking protein particle (TRAPP) complex, both in yeast and in mammals (Gavin *et al.*, 2002), and the TRAPP complex is characterized as a tethering factor for ER-to-Golgi trafficking (Sacher *et al.*, 1998); (Loh *et al.*, 2005);(Yu *et al.*, 2006). Interestingly, from the medical point of view, the Sedlin gene is mutated in spondiloephiphiseal displasia late (SEDL), a chondro-dysplasia that involves condrogenesis impairment (short stature, barrel chest, spine deformation) (Shaw *et al.*, 2003).

Interestingly, in yeast Sedlin is part of both the TRAPPI and TRAPPII complexes, which are different complexes that contain particular elements: basically TRAPPII is TRAPPI (seven components: Bet5p, Trs20p, Bet3p, Trs23p, Trs31p, Trs33p, Trs85p) plus three other components (Trs65p, Trs120p, Trs130p) (Sacher *et al.*, 2000), as shown in Table 4.6. There is a lot of evidence implying that TRAPPII is relevant in the late-Golgi pathways in yeast: first, its GEF activity on ypt31/32, which is important for constitutive exocytosis (Liang *et al.*, 2007); then also relevant, synthetic lethality is seen for both the TRAPPII-specific component Trs65p and the shared component Trs33p, with phosphoinositide 4-Kinase Pik1p (Sciorra *et al.*, 2005); moreover the TRAPPII-specific component Trs130p co-fractionates with

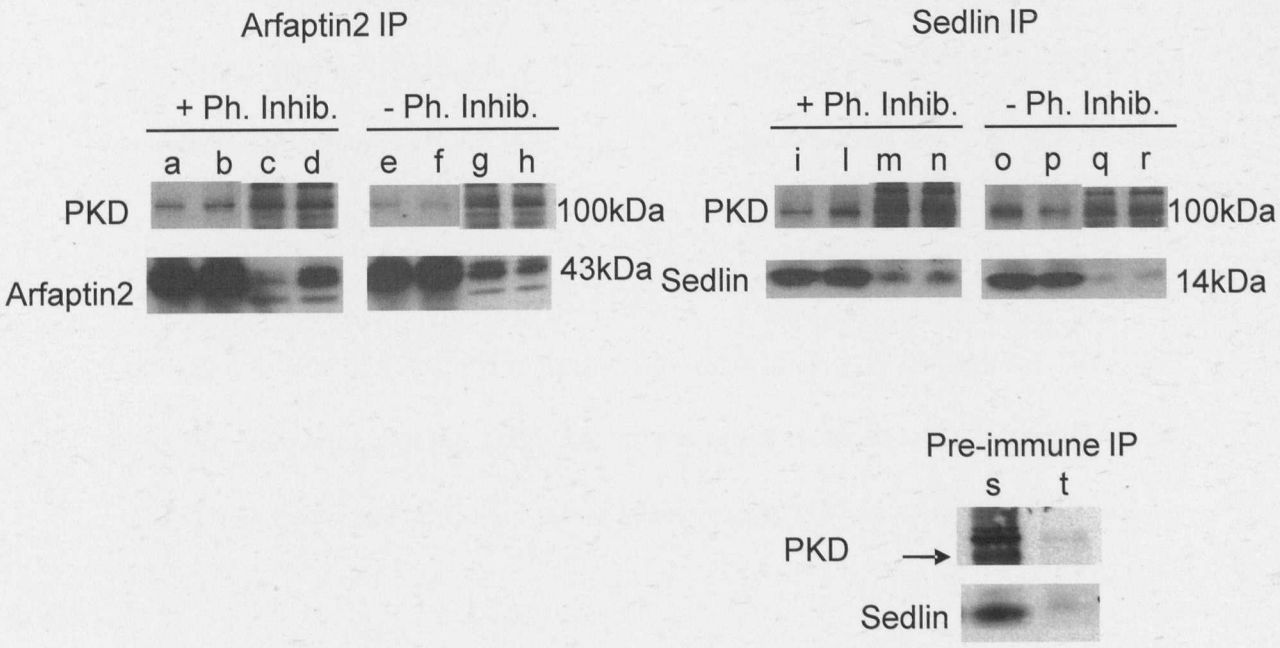

Figure 15. Endogenous Arfaptin and Sedlin co-immunoprecipitate with PKD

Immunoprecipitations of the endogenous Arfaptin2 and Sedlin proteins (left and right, respectively) were performed with the respective rabbit polyclonal antibodies in Hela cell lysates with 1% Triton X-100, using Protein A Sepharose. The immunoprecipitation was carried out with or without phosphatase inhibitors (sodium fluoride and activated sodium orthovanadate) as indicated (-/+ Ph inhib). Lanes a and b, e and f, i and l and o and p are duplicates of the immunoprecipitates. Lanes c,g,m,q are the flow-throughs after immunoprecipiation and d,h,n,r are the input lysates. The polyclonal antibody (Santa Cruz) against PKD (1 and 2 without distinction) shows a band corresponding to the molecular weight of PKD, indicating co-immunoprecipitation of the PKD, which is decreased with Arfaptin2 immunoprecipitate in the presence of the phosphatase inhibitors. Immunoprecipitation of the same cell lysate with Pre-immune IgG, s input, t immunoprecipitate.

Chs3p, which is a late Golgi and early endosome marker, and when Trs130p is knocked-out invertase accumulates inside the Golgi complex (Cai *et al.*, 2005). Moreover, the functional data on the TRAPPII-specific component Trs120p is also relevant: Cai and co workers (Cai *et al.*, 2005) characterized Trs120p as a factor that is required for the recycling of Snc1p and Chs1p from early endosomes to the late Golgi. In the light of these considerations, it will be interesting to investigate a possible role of Sedlin as part of TRAPPII in post-Golgi trafficking, even though the TRAPPII-specific components in mammals are only putative on an *in-silico* basis (Cox *et al.*, 2007), and this is not sufficient to definitely establish its existence in mammals.

However, between mammals and yeast, the TRAPPI components share a high level of homology, as shown in Table 4.6. Thus considering that basically TRAPPII in yeast is TRAPPI plus three additional components, it cannot be excluded that TRAPPI in mammals acts as TRAPPII, but via different adaptors/machinery, such as PKD.

To confirm the two-hybrid interaction between Sedlin and PKD2, first of all I co-immunoprecipitated Sedlin-FLAG overexpressed together with the wild-type or KD forms of PKD2 (Fig. 14). The co-overexpressed Sedlin-FLAG and GST-PKD2 clearly co-immunoprecipitated *in vivo*, as shown by the antibody for the GST tag in the Western blotting of the anti-FLAG immunoprecipitate.

Subsequently, encouraged by the above result, I tried to co-immunoprecipitate the endogenous proteins in HeLa and COS7 cells using specific antibodies. Thus, I performed the immunoprecipitation of Sedlin in cell lysates with 1% Triton with an anti-Sedlin polyclonal antibody. The Western blotting with the PKD-specific polyclonal antibody showed a band of 100 kDa in the Sedlin immunoprecipitate,

Subunit	Yeast (# of AA)	Human (# of AA)	AA identity	TRAPP I	TRAPP II
Bet5	159	145	30%	+	+
Trs20	175	140(SEDL)	40%	+	+
Bet3	193	180	53%	+	+
Trs23	219	219(Synbindin)	30%	+	+
Trs31	283	188	27%	+	+
Trs33	268	160(Trs33A) 158(Trs33B)	24% 33%	+	+
Trs65	560(Kre11p)	-	-	-	+
Trs85	698(Gsg1p)	-	-	+	+
Trs120	1289	-	-	-	+
Trs130	1102	1259(EHOC-1/GT334)	12%(28%)	-	+

Table 4.6
Homologies between the yeast and human TRAPP complex subunits

which corresponds to the molecular weight expected for PKD (Fig. 15). This antibody did not allow a distinction between PKD1 and 2, as described above. Interestingly, and as shown in Figure 15, the interaction was not dependent on the presence of phosphatase inhibitors, as was the case for the Arfaptin2-PKD2 interaction.

In our two-hybrid assay, another direct interaction occurred between two mammalian subunits of the TRAPP complex: Bet3 and Sedlin, as it happens in yeast, as revealed by a two-hybrid analysis (Ito *et al.*, 2001). This interaction is not surprising, since both Bet3 and Sedlin share more than 40% identity with their yeast counterparts, and since they are the most conserved among all of the TRAPP subunits (see Table 4.6). After our discovery, this direct interaction was also seen between mammalian Sedlin and Bet3 via a gel-filtration approach (Menon *et al.*, 2006), and thus it can be considered as a well confirmed direct interaction between two components within the same protein complex, and this provides important information concerning the internal organization of the complex itself.

4.4.4 CtBP1-S/BARS interacts with PKD

In the case of the PKD-BARS interaction, I tested the kinase activity of PKD on His-BARS as substrate. Since I had the recombinant protein, it was technically possible in this case, while in the case of His-Sedlin instead, it was not possible due to the absence of enough of the pure recombinant protein. I expressed GST-PKD1 in COS7 cells and I then purified it directly from the cell lysate (see Material and Methods section 3.14.1), since it is not at present possible to obtain a recombinant PKD from bacteria. I performed a classical kinase assay with the use of radio-labelled $\gamma[^{32}P]$-ATP, testing BARS and some of its deletion mutants together with PKD in its wild-type and KD forms as controls. As shown in Figure 16, the results here are interesting,

since BARS is phosphorylated *in vitro* and the nucleotide-binding domain of BARS (BARS-NBD) is the most phosphorylated domain among all of the other domains tested: A, E, C, NBD and SBD (see in Figure 16 for details). However, the E fragment that contains the NBD plus an additional 122 amino acids at the C-terminus is not phosphorylated. This may be explained as a structural problem of the additional 122 amino acids that can cover the phosphorylation site, possibly due to incorrect dimerization since it is known that BARS homodimerizes. NBD is also the domain that interacts with PKD2 in our two-hybrid system. Unfortunately, the kinase used for the phosphorylation assay was PKD1, because it was the only one available in a functional form, although it is of note that PKD 1 and 2 are very similar, and especially in their C-terminal catalytic domains (>80% identity).

I observed PKD autophosphorylation as the positive control of the catalytic activity, and I observed a clear phosphorylation signal on BARS, calculated to be 0.1% of the total protein.

To check the specificity of this phosphorylation, I tested several randomly chosen proteins as other potential PKD substrates, testing them with BARS and GST in the same set of experiments. I thus tested purified G-βγ, phosphorylase B, albumin, ovalbumin, carbonic anhydrase, trypsin inhibitor and α-lactalbumin. None of these was phosphorylated by PKD (Fig. 17).

Of note, in these experiments, I tested purified G-βγ also in the presence of BARS, and I observed a clear 5-fold decrease in the phosphorylation signal of BARS in the same experiments. This thus indicates G-βγ interference in PKD-mediated BARS phosphorylation (Fig. 16).

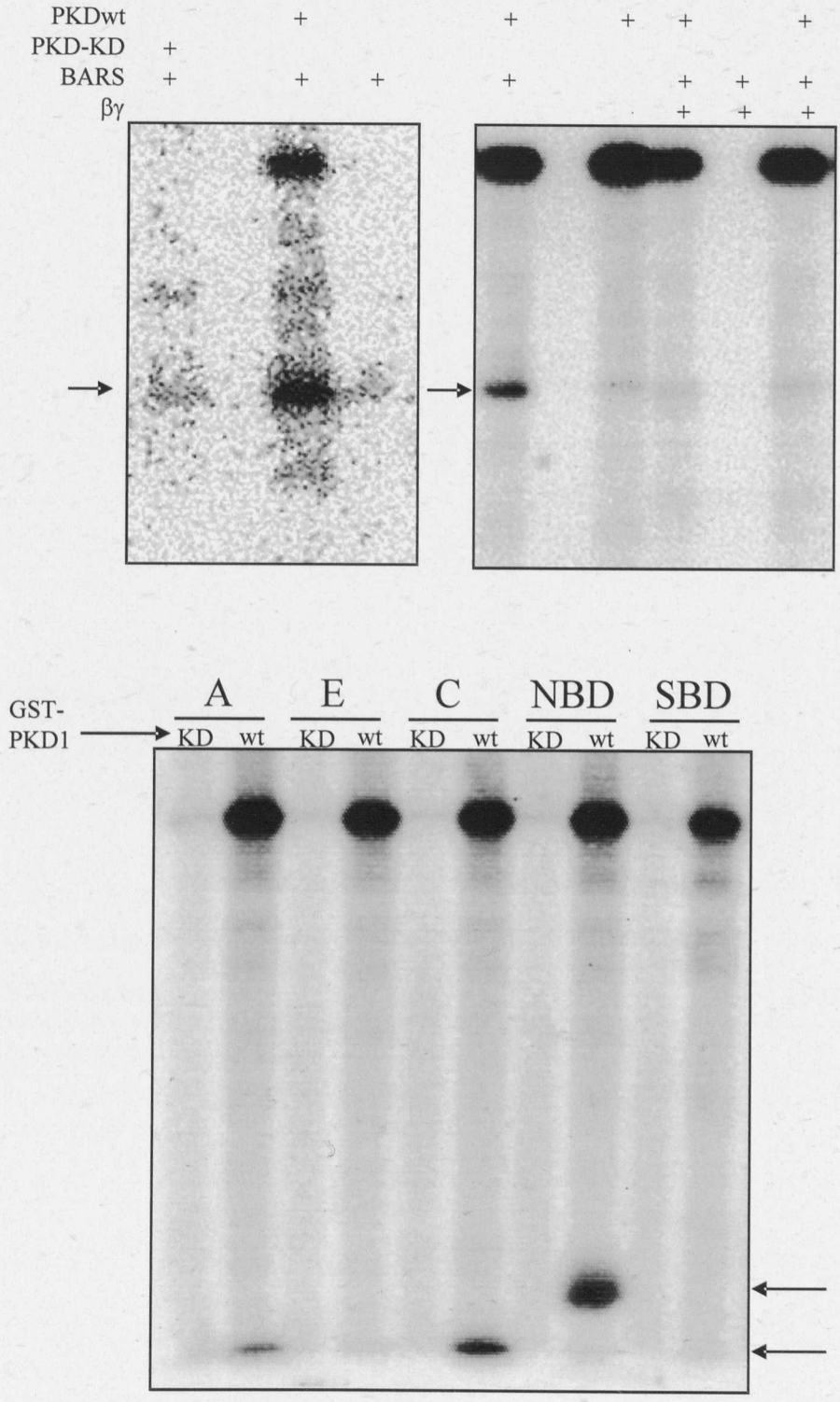

Figure 16. PKD phosphorylate BARS *in vitro*

BARS is phosphorylated by PKD, as revealed by $\gamma[^{32}P]$-ATP phosphorylation assays (see Methods, section 3.14). The βγ dimer of heterotrimeric G proteins (purified from bovine brain) inhibits this BARS phosphorylation mediated by PKD without affecting the activity of PKD, as shown by the PKD autophosphorylation signal. Autoradiograms showing the phosphorylation signal on BARS (arrow) in the upper panels, and on several BARS-deletion mutants in the lower panel: A = 1-111, E = 112-430, C = 306-430, NBD = 112-308, SBD = 1-112/307-430. BARS and BARS fragments are indicated by arrows, PKD autophosphorylation signals are on the top, KD is kinase dead form of PKD.

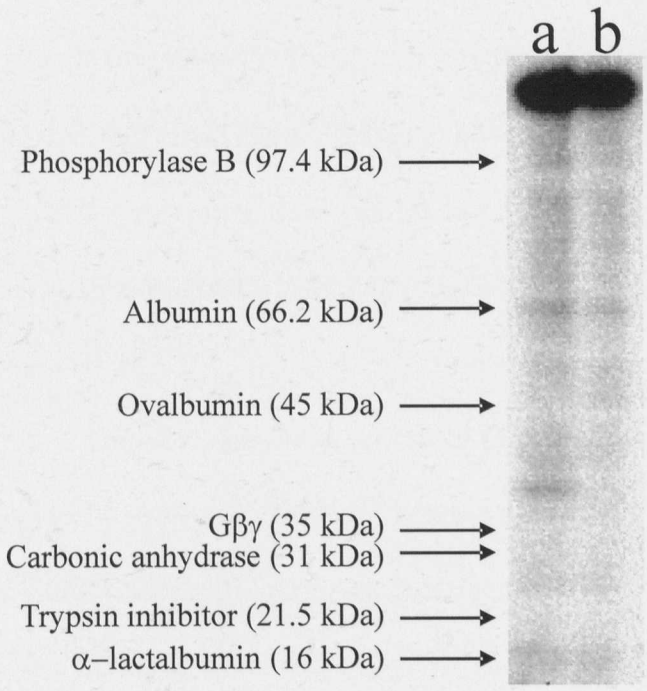

Figure 17. PKD does not phosphorylates a mix of 7 proteins

(a) Purified G-βγ, phosphorylase B, albumin, ovalbumin, carbonic anhydrase, trypsin inhibitor and α-lactalbumin were all tested in the same reaction with PKD in the same conditions as in Figure 17 (see Methods, section 3.14). Their position is indicated by arrows. (b) PKD alone

PKD is known to exert its activity on Golgi fragmentation through regulation mediated by G-βγ. Indeed, G-βγ alone can fragment Golgi membranes in permeabilized cells, and PKD inhibitors can reverse this effect (Jamora C. et al. 1999). At present, an open question is: why does G-βγ inhibit BARS phosphorylation by PKD? In the presence of G-βγ, the autophosphorylation signal of PKD is not affected, and thus this effect is more likely to be due to an interaction between G-βγ and BARS; indeed, we assume that they do interact from the observation that the ADP-ribosylation of BARS is inhibited by G-βγ (Di Girolamo M. et al. 1995).

The phosphorylation of BARS is very interesting, since BARS exerts its effects on TGN-to-PM trafficking of the cargo molecule VSVG at the fission step (Bonazzi *et al.*, 2005), and this is the same phenomena that was seen by Malhotra and colleagues with PKD using dominant-negative PKD-KD which decorates the TGN-originated tubules that are impaired in fission (Liljedahl *et al.*, 2001; Yeaman *et al.*, 2004).

Later, the interaction between BARS and PKD was further confirmed with co-immunoprecipitation by a colleague (Carmen Valente, Corda laboratory, unpublished).

4.5 PKD as a key protein

PKD thus appears to have many interesting interactors, and this is the reason why we believe it is an important hub into the interaction map in Figure 12: it interacts with PI4KIIIβ, PKC, and the βγ subunit of heterotrimeric G-proteins. From our recent work, it is now clear that it also interacts with Sedlin, BARS and Arfaptin2. Every one

of these PKD interactors is important in our research focus because PKD acts as a fissioning player at the level of GPCs. The most interesting interaction here is the phosphorylation of BARS, since Arfaptin and Sedlin have not yet been characterized from the trafficking point of view. BARS, instead, is known to be relevant in the specific step of fission of VSVG-containing carriers when they originate from the TGN (Bonazzi *et al.*, 2005). In the following sections, I will describe in detail the roles in transport also of Arfaptin and Sedlin, and thus I have started to discover new interesting functions of these proteins; functions that were previously unknown from the trafficking point of view.

4.6 Arfaptin

4.6.1 Arfaptin possesses a BAR domain

The controlled bending of membranes is crucial for many fundamental cellular processes including membrane trafficking. The transfer of material between organelles depends on physical changes in the membranes that are mediated, in part, by vesicle-coat proteins, such as COPI, COPII and clathrin. Coat proteins bind to a donor membrane and then polymerize. Coincident with their polymerization, the membrane deforms into a bud, which then separates from the parent membrane, thus forming a transport intermediate. The possible protein-based mechanisms involved include curvature-inducing proteins, such as the BAR family members. Among these, the γ–BAR protein is known to associate with the TGN (Neubrand *et al.*, 2005), as is Arfaptin2 (Peter *et al.*, 2004), and possibly endophilin B (Farsad *et al.*, 2001). Moreover, the aforementioned GRIP domain-containing proteins (section 1.2.2) have also been proposed to be involved in membrane tubulation (Gleeson *et al.*, 2004), although their mechanisms of action have yet to be established.

The effectors of Arl1 at the TGN include the Arfaptins and the GRIP-golgins p97 and p230. The three-dimensional structure of the BAR domain of Arfaptin senses and/or induces positive membrane curvature (Tarricone *et al.*, 2001). Moreover Arfaptin is present in the tubular compartment but not in the stacks (De Matteis laboratory DCBO, unpublished) suggesting that the peculiar curved and tubulated structure of the TGN is where Arfaptin functions. Arfaptin can interact with several small G-proteins: Arf1 and Arl1, and also Rac1 (Tarricone *et al.*, 2001). The interaction with the small G-protein occurs, at least with Rac1, through the concave side of the BAR domain, and thus it is likely to regulate the function of the BAR-domain itself, preventing its association with membranes. In other words, Arfaptin is not active when it is not at the TGN, and needs to be recruited to the TGN by small G proteins such as Arl1. The interaction with Arl1 is clear, and it was also reproduced by the two hybrid-system here.

The BAR domain of Arfaptin is located at the C-terminus of this protein. From structural comparisons and from the high level of conservation between the C-terminus of Arfaptin2 and Arfaptin1 (Figure 18) it appears likely that the heterodimerization of the Arfaptins 1 + 2 is compatible with the formation of an active BAR domain conformation (Figure 19). Here in the two-hybrid interaction between Arfaptin1 and Arfaptin2, the same growth pattern as for the homodimer Arfaptin2-Arfaptin2 was seen (Table 4.5), indicating the same interaction strength. It has been shown that the effects on artificial membranes were clearly due to membrane-bending effects that produce highly tubulated membranes starting from artificial large unilamellar vesicles (LUVs) (Peter *et al.*, 2004) (Figure 20). Once overexpressed, Arfaptin localizes to many tubules from the perinuclear area as I have seen in vivo at

Figure 18. Arfaptins 1 and 2 have a conserved BAR domain

The two Arfaptin sequences are overall conserved, expecially from position 118 along all the C-terminus, from were they are nearly identical. The region boxed in pink indicates the BAR domain.

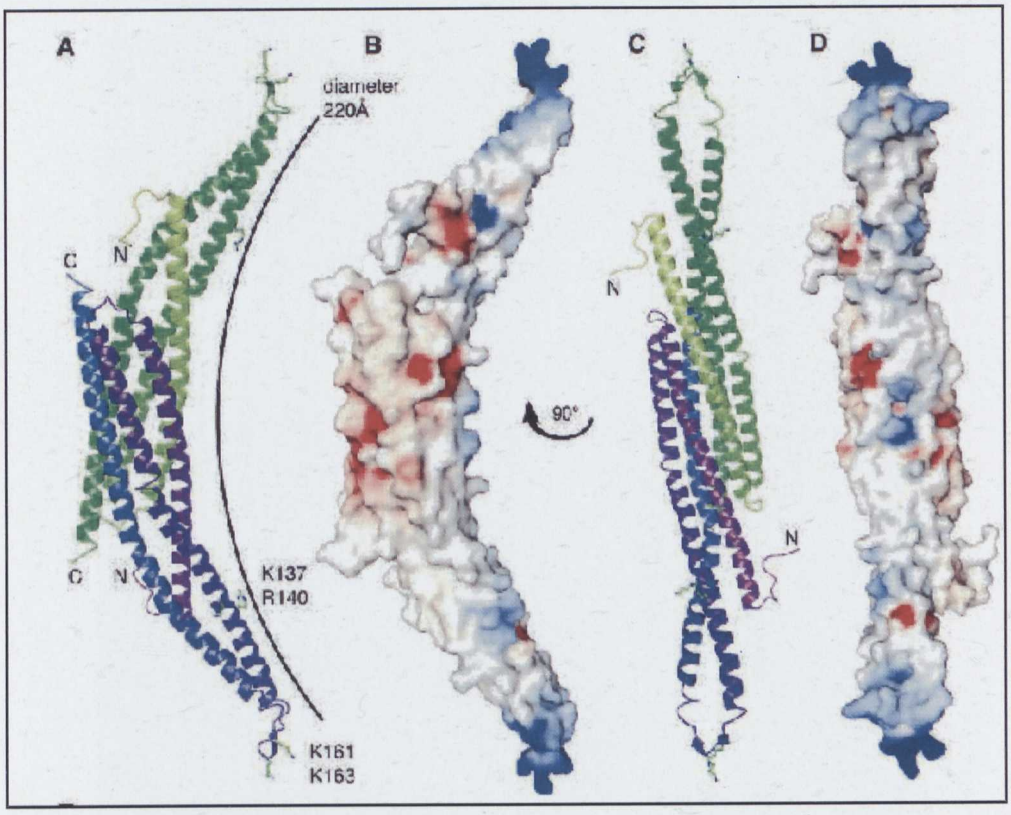

Figure 19. The BAR domain is an elongated 'banana-shaped' dimer
The BAR domain is an elongated banana-shaped dimer. Each BAR domain monomer has a coiled-coil structure of three long kinked α helices, which form a six-helix bundle (A and C). The curvature of the dimer is partly due to the way the monomers intersect, and partly due to the kinks in helices 2 and 3. The Kd for dimer formation is 6 μM, which may mean that the protein is in a monomer:dimer equilibrium *in vivo*. The positively charged loop between helices 2 and 3 at the extreme ends of the dimer is flexible and poorly ordered; the concave surface of the dimer also has several positively charged patches (B and D), which suggests that this is the surface that interacts with the phospholipid membranes. This structure of the BAR domain would fit a curved membrane with a diameter of 220 Å.

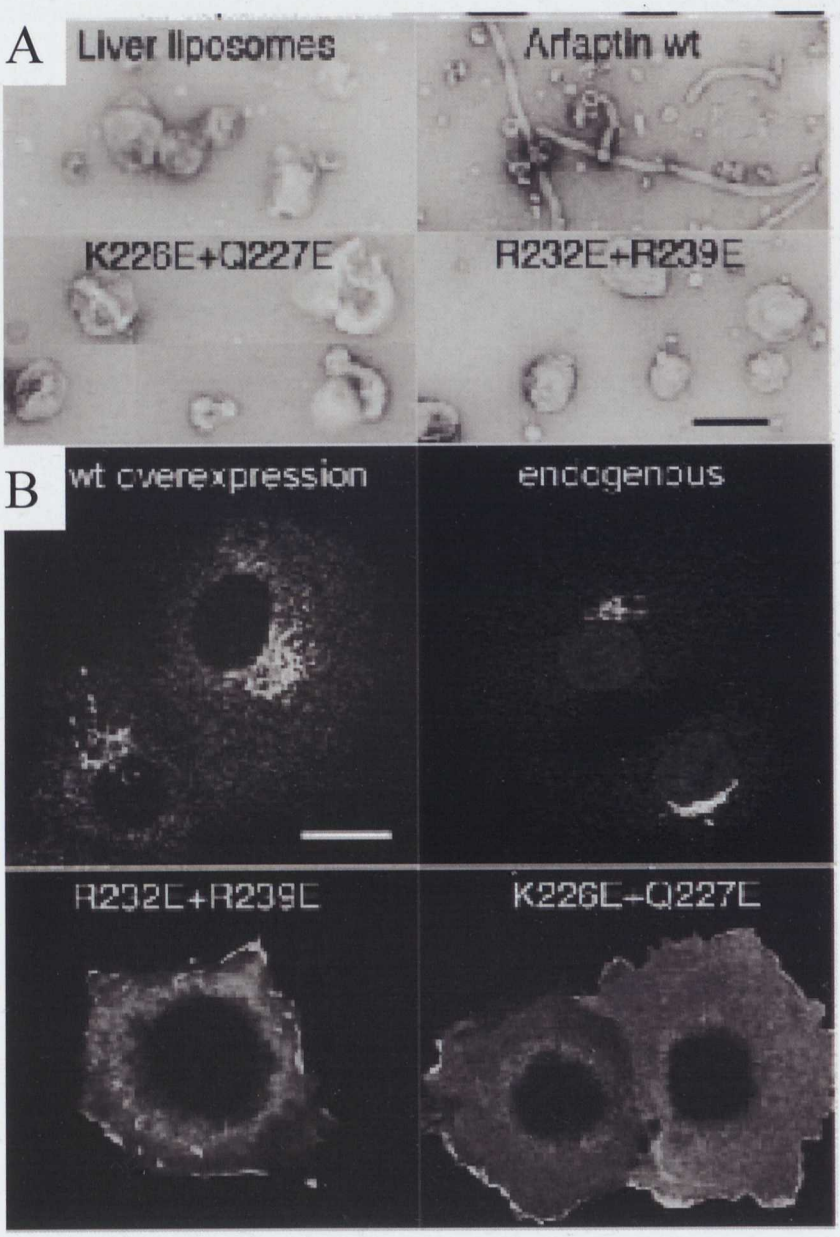

Peter et al 2004

Figure 20. Arfaptin can tubulate membranes *in vitro*

(A) Electron micrographs of liver liposomes incubated with wild-type Arfaptin and the indicated mutants, that were designed to change the critical positive residues that are considered to be important for phospholipid binding. Scale bar, 300 nm. (B) COS7 cells expressing wild-type and mutant Arfaptins, showing a lack of localization due to an altered ability to localize on membranes. Scale bar, 20 μm. Picture taken from *Peter et al Science 04*

the immunofluorescence level (Fig. 22), even if it is not yet possible to relate these tubules to *in-vitro* tubulation, which is much more clear under EM analysis.

4.6.2 Arfaptin at the TGN

Nothing is at present known about Arfaptin from the transport point of view, nor is its localization in the cell known. Here I looked first of all to the localization of Arfaptin compared to the TGN marker TGN46, and the staining showed a high level of co-localization, even after nocodazole treatment (Figure 21) since is known that the absence of microtubules provoke the scission of the Golgi complex in 'ministacks' that maintain the *cis*-to-*trans* orientation, and this gives a better separation between the *cis*- and the *trans* elements (by a still unclarified mechanism). As a negative control I also performed double-staining of Arfaptin with ER exit sites (ERES) using Sec31 marker, and I observed no colocalization of Arfaptin with these structures (not shown). The significant data are the TGN localization of Arfaptin with EM microscopy (Unpublished, De Matteis laboratory DCBO) Another EM experiment identified Arfaptin on a tubular compartment and not in the stack (Unpublished, De Matteis laboratory DCBO).

According to my data, Arfaptin is a TGN-resident protein, and thus it may well act on Golgi exit sites and/or influence the Golgi-to-PM trafficking of a viral protein such as VSVG. To verify this hypothesis, I overexpressed GFP-Arfaptin2 and I looked at the transport of VSVG from the Golgi to the PM (Fig 23 - 24). This overexpression of Arfaptin2 strongly delayed the exit from the Golgi complex of VSVG, even after long times (120 min at 32 °C; Fig. 24). These data support a regulatory role for Arfaptin in carrier formation at the TGN.

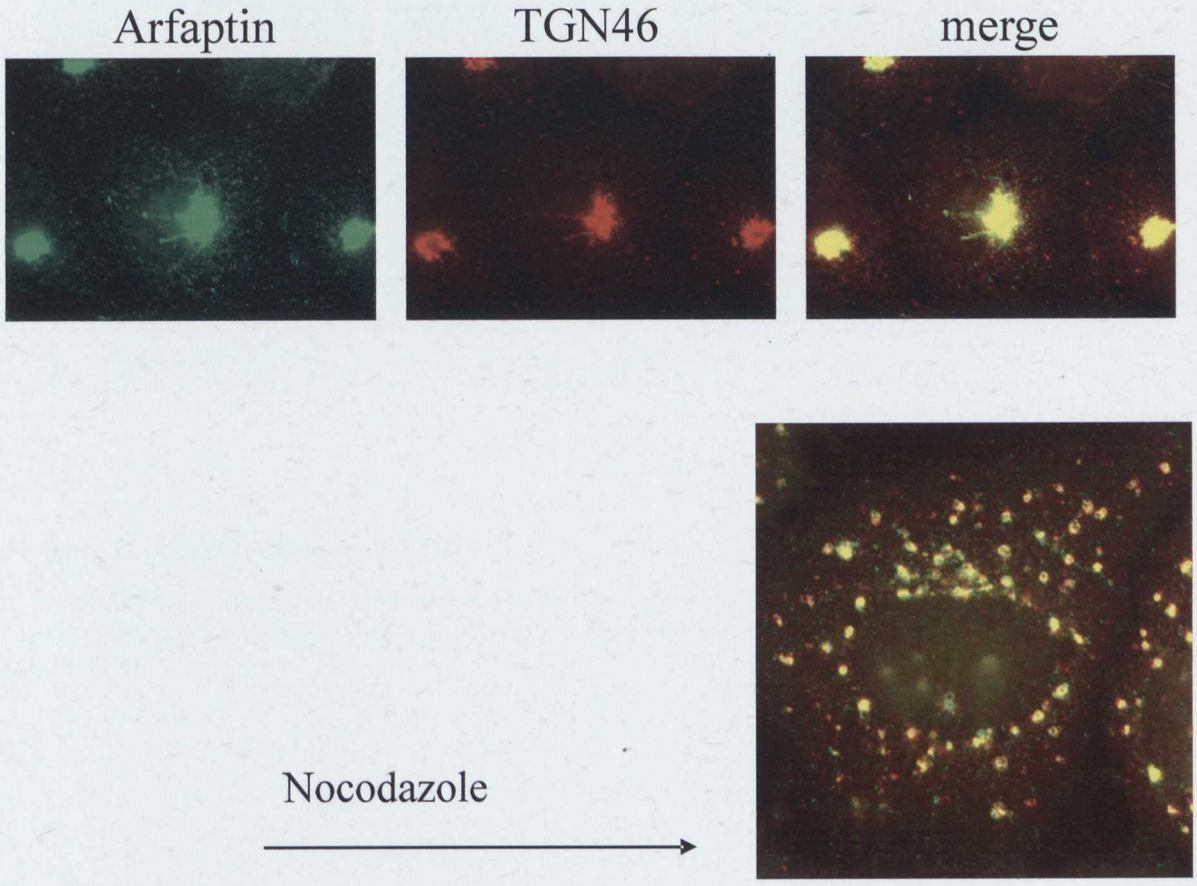

Figure 21. Arfaptin2 co-localizes with a TGN marker

Immunofluorescence confocal images in Hela cells showing the co-localization of endogenous Arfaptin and TGN46 at steady-state, and also in the presence of nocodazole (as indicated) which fragments the Golgi complex into ministacks that generally maintain their *cis-trans* orientation.

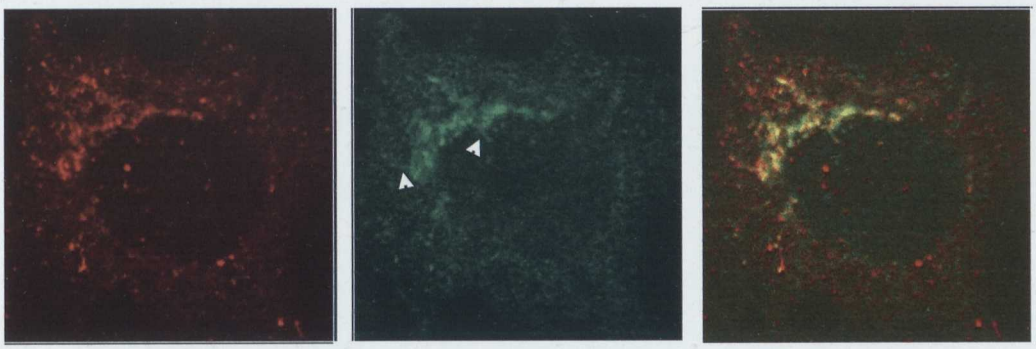

GST-PKD Arfaptin2-FLAG merge

Figure 22. Arfaptin-decorated tubules

Arfaptin2-FLAG localizes on tubules as shown by white arrows into these confocal sections in HeLa cells co-transfected with GST-PKD. The Arfaptin2-FLAG decorated tubules do not co-localize with GST-PKD.

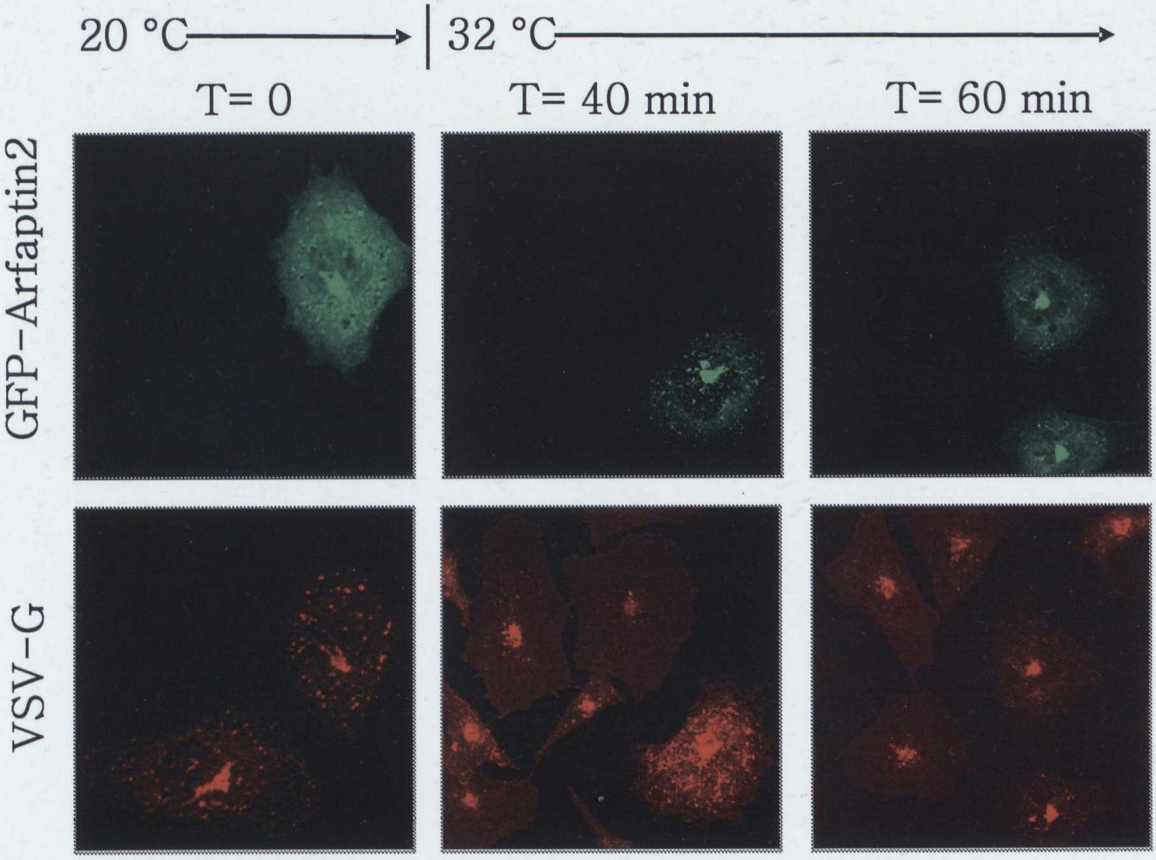

Figure 23. Arfaptin overexpression blocks VSVG transport to the plasma membrane

Hela cells were transfected with GFP-Arfaptin2 and infected with the VSV virus. A temperature block protocol was used (see Methods, section 3.7) to follow the transport of VSVG out of the Golgi complex. The 20 °C block was performed for 2 h and then several time points were followed during the release at 32 °C. At 40 and at 60 min, the VSVG appears clearly confined inside the cells, while the control cells (untransfected) present VSVG on PM.

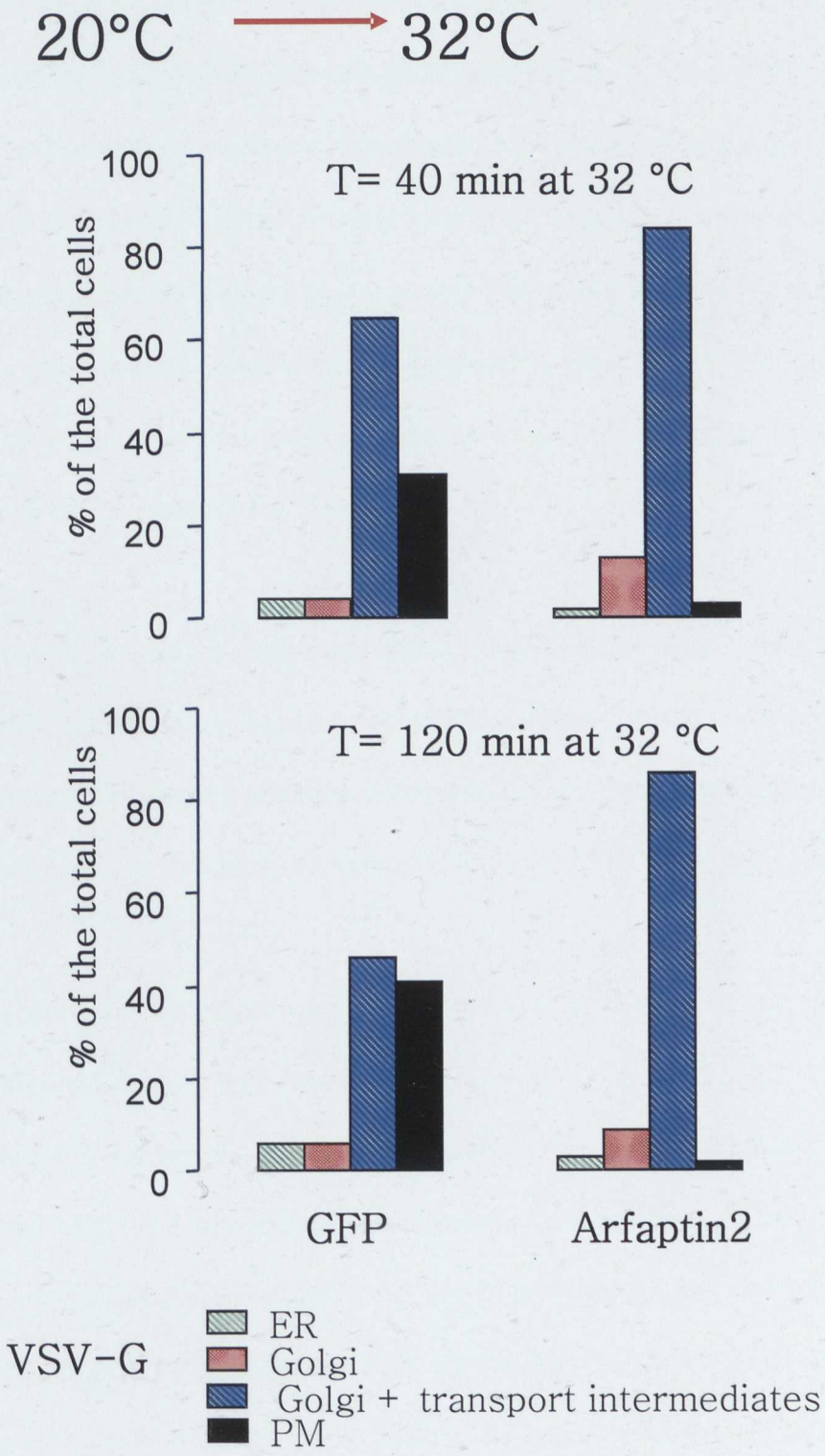

Figure 24. Arfaptin blocks Golgi-to-PM transport

Arfaptin has an inhibitory role on transport to the PM. Histograms of the qualitative classification of VSVG patterns inside Hela cells overexpressing Arfaptin2, compared to cells overexpressing GFP alone as the control. The same 20 °C – 32 °C protocol was used as for Figure 21; see Materials and Methods, section 3.7.2.

4.6.3 PKD regulates Arfaptin2

The interaction with PKD appears to be affected by phosphatase inhibitors, although this would not help to distinguish between PKD and Arfaptin, in terms of which one of the these two interactors is affected. I performed a phosphorylation assay with the $\gamma[^{32}P]$- ATP to examine the effects of kinase activity on Arfaptin. *In vitro*, Arfaptin appears to be phosphorylated by PKD, suggesting a regulation mediated by the kinase activity (Fig. 26). Since it has not been possible to verify this kinase activity *in vivo* yet, I investigated whether there is a correlation between PKD and Arfaptin, because they may work on the same trafficking pathway.

First of all, we tried to understand if the Arfaptin pattern on the Golgi complex can be affected by PKD. Here, I transfected a PKD construct in HeLa cells and I observed a clear redistribution of endogenous Arfaptin into the cytosol. This effect was increased when the constitutively active (CA) form of PKD was used (Fig. 27).

This result was not surprising considering that these two players may work in different temporal steps in a pathway that starts with Arl1: once Arl1 is active, it recruits Arfaptin to the Golgi complex to initiate tubulation, with the fissioning protein PKD involved later, (as demonstrated) by displacing Arfaptin (Fig. 27), making it free for another cycle of tubulation. Arfaptin can also be recruited by Arf1, but since Arfaptin is localized specifically at the TGN, we consider that for the TGN-specific localization the element that has a role might be an element specifically localized at TGN, such as Arl1.

I next investigated whether GST-PKD-decorated tubules were co-localized with endogenous Arfaptin-decorated tubules, or Arfaptin-FLAG decorated tubules.

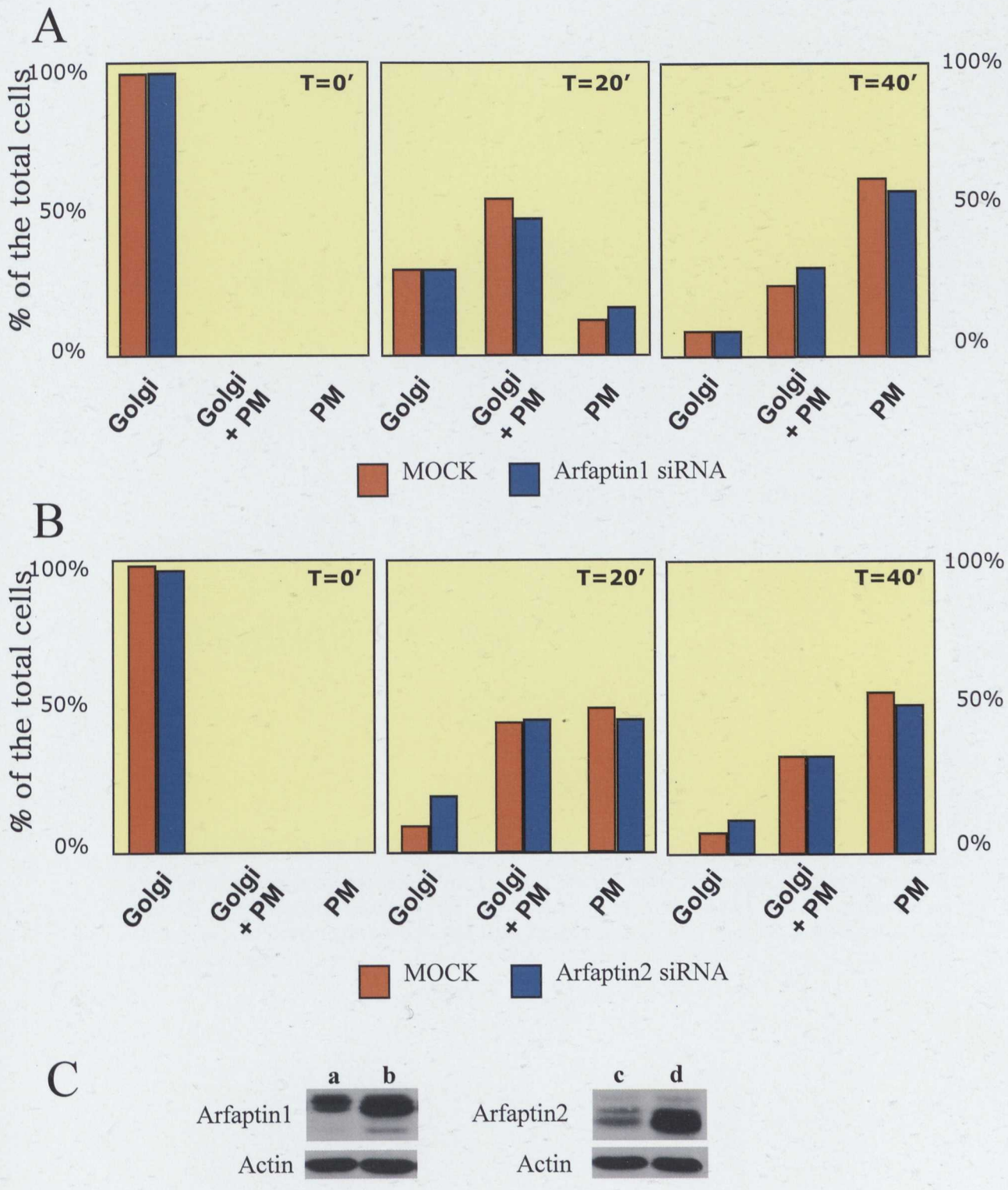

Figure 25. Arfaptin 1 and 2 removal does not affect VSVG exit in Hela cells

The pattern of VSVG localization after the release from the 20 °C block are represented here for PM only, Golgi only or both Golgi plus PM localization, as indicated during 20 and 40 minutes of release at 32°C. (A) Arfaptin1 knocked down by siRNAs and (B) Arfaptin2 knocked down by siRNAs. The same effect is observed in Arfaptin 1 plus Arfaptin2 siRNAi (not shown). (C) Western blotting of Arfaptin1 in (a) siRNA or (b) mock-treted cells and Western blotting of Arfaptin2 in (c) siRNA or (d) mock-treated cells. Actin is used as a reference.

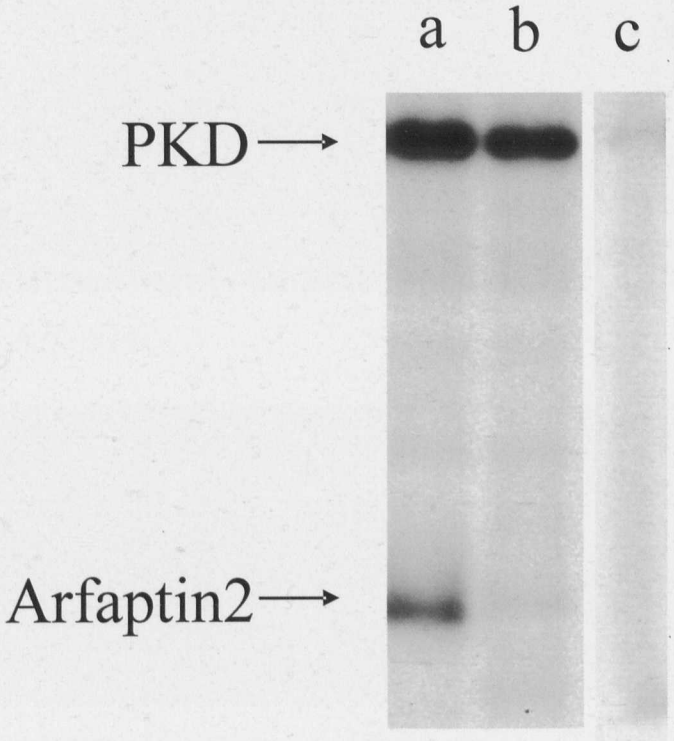

Figure 26. PKD phosphorylates Arfaptin2 *in vitro*

Autoradiogram showing Arfaptin2 (lane a) with a [^{32}P]-phosphorylaton signal following incubation with PKD (see Methods, section 3.14.2). (b) Incubation only with the PKD and (C) incubation only in the presence of Arfaptin, as control. The same conditions were used when PKD was incubated with BARS (see Figure 17)

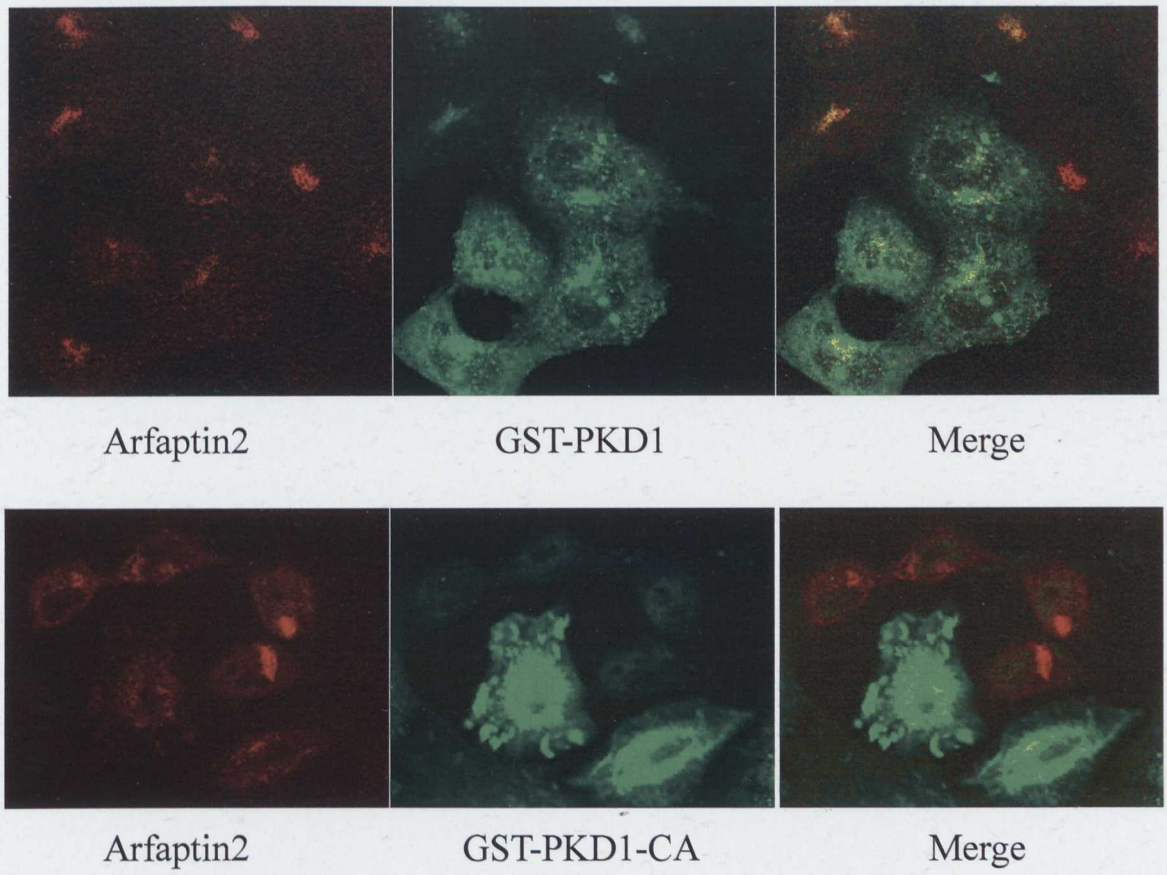

Figure 27. PKD displaces endogenous Arfaptin from the Golgi complex

Hela cells were transfected with wild-type and constitutively active (CA) GST-PKD1. The cells were fixed after 24 h and stained with an anti-Arfaptin2 antibody and with anti-GST antibody.

However, the result was negative here, looking at least at three focal planes per cell of HeLa and Cos7 cells (Fig. 22). This is in line with our model of temporal regulation, in which Arfaptin and PKD cannot be on the same structure at the same time.

4.7 The TRAPP complex

The TRAPP complex (Yu *et al.*, 2006) component Sedlin interacts with PKD, and another component, Synbindin, interacts with 14-3-3γ. It is also interesting to note the many genetic interactions that, at least in yeast, link TRAPP to late Golgi trafficking steps (Fig. 13). Thus a study of the role of TRAPP in post-Golgi trafficking is of absolute importance. The interaction between Bet3 and Sedlin was expected since it is known to occur in yeast, and Bet3 and Sedlin are the two most conserved among the TRAPP subunits (Table 4.6). This interaction was also confirmed in mammals in the literature a short time after our two-hybrid result (Menon *et al.*, 2006). However Sedlin is (at least in yeast) sub-stoichiometric in the complex, and after a series of attempts to study its role in transport, it appeared not to be relevant in trafficking of VSVG (data not shown). Bet3 instead, once it was knocked-down by siRNA or acutely depleted after microinjection of its Bet3-specific antibody, blocked the VSVG travelling from the TGN to the PM. As shown in Figure 29, using a 20 °C - 32 °C transport protocol (see Methods, section 3.7), the VSVG protein reached the Golgi complex but did not proceed to exocytosis, at least not efficiently. Using the transport protocol on cells with siRNA interference for Bet3, with a mock as control, I revealed a strong delay at 30 min, 60 min and also at 90 min after the release at 32 °C. This indicates the important participation of Bet3, which was here knocked down >80% (Western blotting), and it also indicates participation of the whole TRAPP complex, because with the knocking down of Bet3, Sedlin and Synbindin also underwent

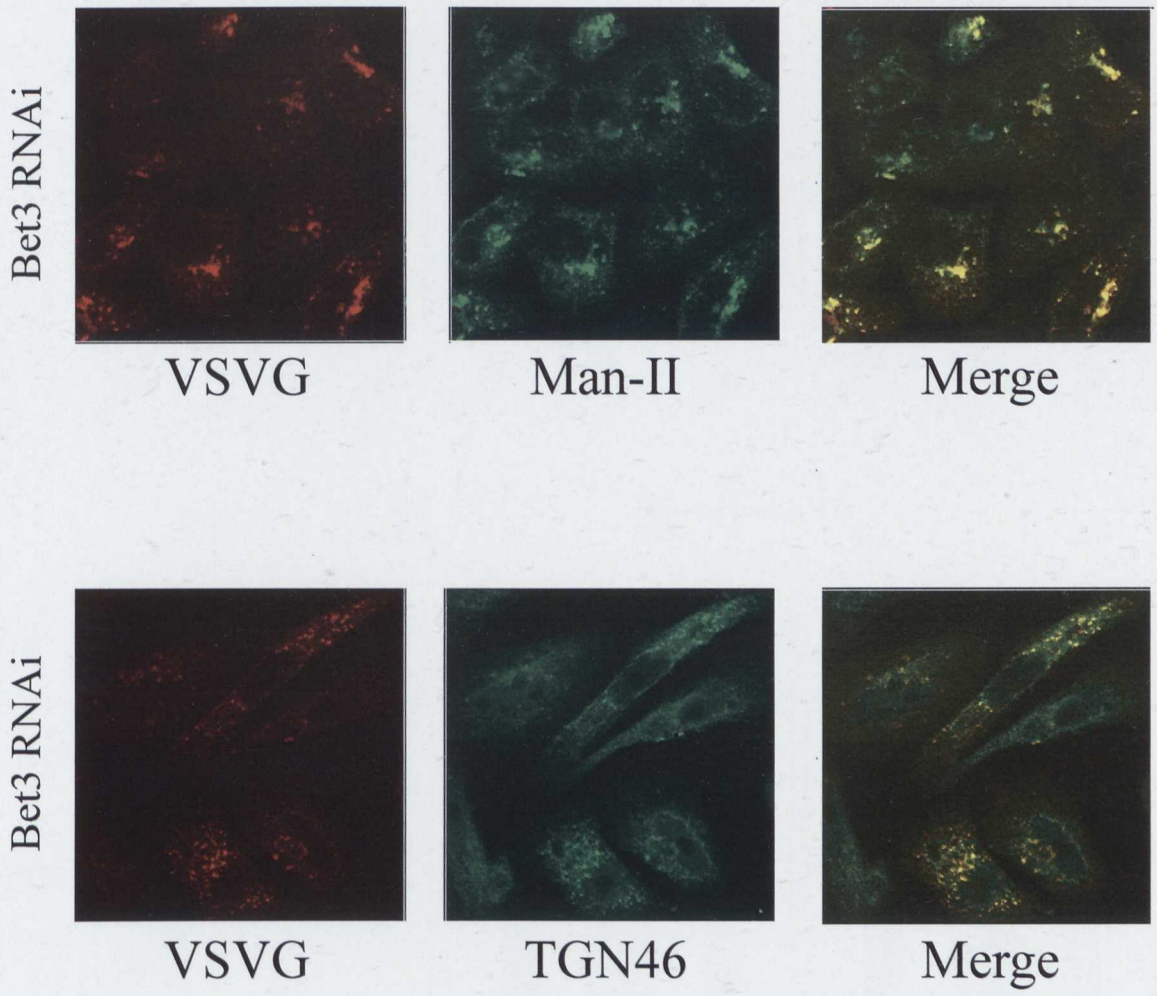

Figure 28. VSVG reaches Golgi complex and TGN in Bet3 knocked-down cells

VSVG at the end of the 20 °C block reaches the MannosidaseII (Man-II) compartment and the TGN (TGN46) compartment as shown in confocal sections of HeLa cells interfered for Bet3. This is the same experiment in which cells were counted for VSVG pattern of transport in Figure 28 A.

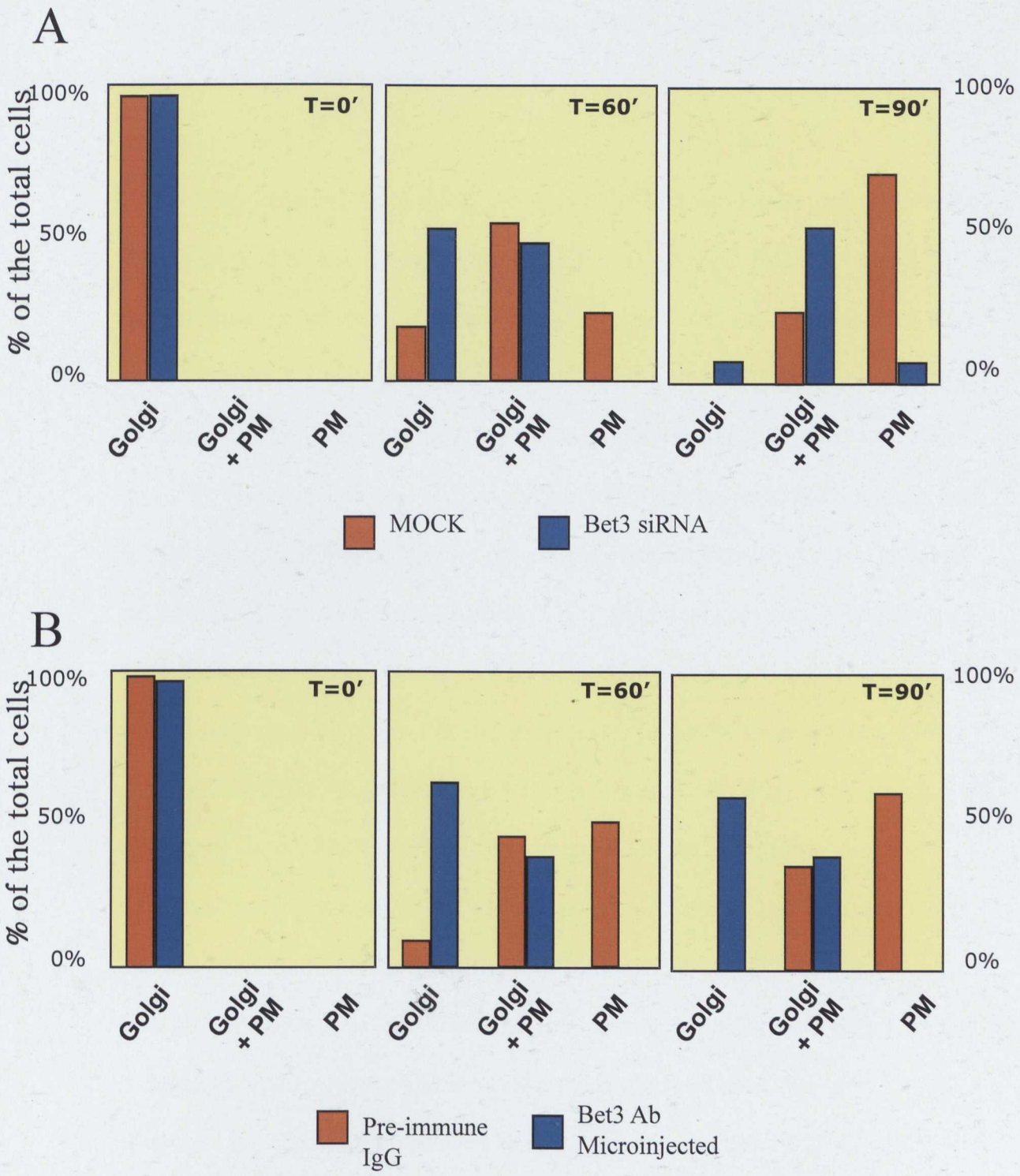

Figure 29. Bet3 removal blocks VSVG exit in Hela cells

The pattern of VSVG localization after the release from the 20 °C block are represented here for PM only, Golgi only or both Golgi plus PM localization, as indicated during 60 and 90 minutes of release at 32°C. (A) Bet3 knocked down by RNAi (up to 85% by Western blotting as shown in Figure 31) and (B) a Bet3 antibody was microinjected into the cells during the last 30 min of the 2 h block at 20 °C. A pre-immune IgG was microinjected as a control. A total of 200 cells from three different experiments were counted for (A) and a total of 150 cells from three different experiments were counted for (B).

reductions at the protein level (Western blotting; Fig. 30). This would indicate that Sedlin and Synbindin are probably more exposed to proteolytic degradation in the absence of the functional TRAPP complex.

I also observed the same effects on acutely blocking Bet3 by microinjecting a Bet3-specific antibody just before the end of the 20 °C block. This defines and confirms that the defects in transport seen here are not due to an impairment in ER-to-Golgi transport or to any intra-Golgi step, since under steady state conditions VSVG proceeded to reach the Golgi/TGN before the microinjection of the Bet3 antibody (Fig. 29). Ferro-Novick and colleagues (Yu *et al.*, 2006) have claimed a role for Bet3 in ER-to-Golgi trafficking, but they did not use a synchronization protocol to define the trafficking step they were looking at in their Bet3-depleted cells. Blocking antibodies are particularly useful, since we can choose the exact step of transport we wish to study, as the TGN-to-PM step in this case. Co-localization between VSV-G and ManII and TGN46 was seen in Bet3 siRNA-treated cells (Fig. 28), since in chronically depleted cells is not possible to do the temporal restriction made for microinjection of antibodies, thus it is necessary to observe if the VSV-G can reach the compartments that came before the TGN and the TGN itself. Then we observed a clear colocalization between VSVG and TGN46 at time = 0 (Fig. 28), indicating that previous transport steps are apparently not significantly affected. VSVG is a viral protein, so its reliability can be questioned for many reasons, and thus we decided to also follow endogenous cargoes; for this reason, we performed GAG transport assays. GAGs are constituents of the extracellular matrix and they are sulphated specifically at the TGN. Thus, by following their [^{35}S] incorporation, we can measure their transport specifically from the TGN to the PM (see Methods, section 3.8).

The results showed a clear delay in GAG transport out of the Golgi in HeLa cells siRNA-interfered for Bet3 and also for Sedlin, even if this delay was not so strong (Fig. 31). Of note, the GAGs are a bulk-flow marker, and can use many pathways to bypass transport defects and to reach the external surface of the PM (Buccione *et al.*, 1996; Vuong *et al.*, 2006), and thus it is quite common not to have a strong delay in any case (Fig. 31).

Thus, looking at VSVG blocked following Bet3 removal in acute and chronic ways and at GAG sulphation under Bet3 and Sedlin knock-down in a chronic way, we have demonstrated for the first time that TRAPP is necessary for TGN-to-PM transport in mammalian cells.

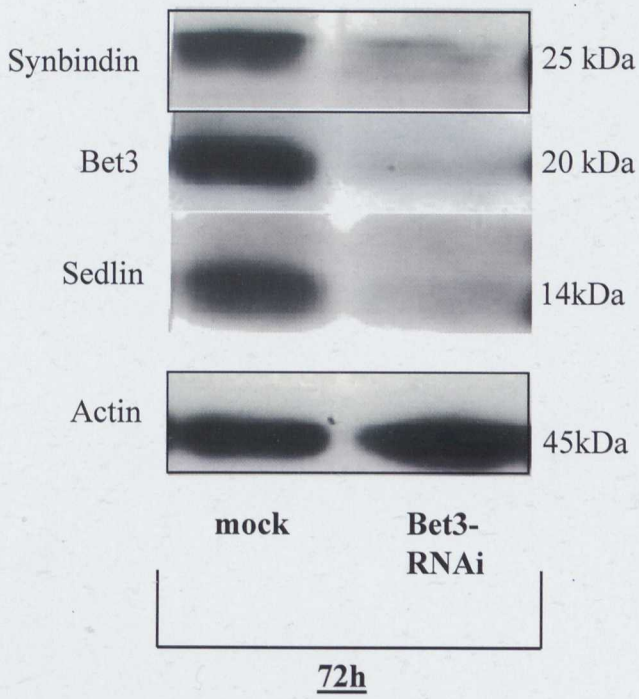

Figure 30. The knock-down of Bet3 decreases the protein levels of other TRAPP components

Western blotting showing how the levels of Sedlin and Synbindin are also knocked down after Bet3 RNAi for 72 h. The destruction of Bet3 destabilizes the complex and the other TRAPP components are more prone to proteolitic degradation

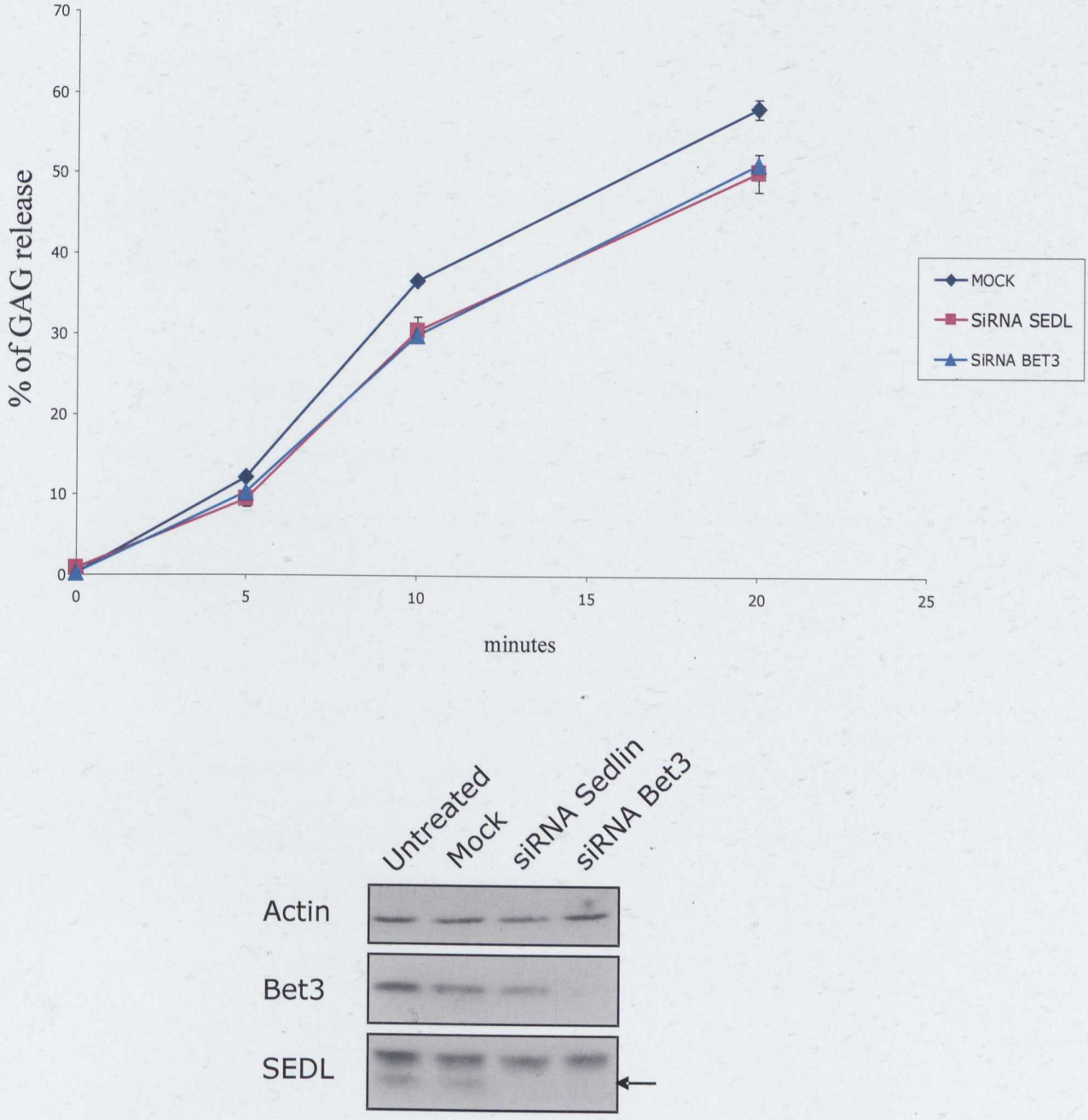

Figure 31. GAG release in Bet3 and Sedlin knock-downs

Individually knocking-down the two subunits of the TRAPP complex, Bet3 and Sedlin in Hela cells, shows a weak delay in the transport of the GAGs, as compared to the mock control. The experiment was carried out in triplicate (upper part). The percentage GAG release represents the ratio between the GAG levels outside of the cells and the total GAG (outside plus inside) (see Methods, section 3.8.2). Western blotting (below) shows knock-down efficiencies for Sedlin and Bet3. Actin is used as a reference.

5 Discussion

5.1 Overview

What has emerged from every overview of TGN function is the complexity of this organelle, which is arguably the most complex organelle among the eukaryotic trafficking stations (De Matteis and Luini, 2008).

Over the past few decades, we have gained some degree of understanding of the morpho-dynamics of this organelle, and also an awareness that our knowledge of the underlying molecular machineries is still incomplete and fragmentary. A number of pieces of a large mosaic have been revealed, but a coherent picture still escapes us.

The ability of cells to export proteins in a constitutive fashion is basically used in all cell types (Fig. 5). The membranous carriers involved in the trafficking step from the TGN directly to the PM are much larger than 'standard' vesicles, and are pleiomorphic rather than vesicular; they also do not have a proteinaceus coat, as is the case for many other transport steps (e.g. clathrin, COPI and COPII vesicles) (Polishchuk *et al.*, 2003).

The first approach of my PhD project was to compile an interaction map of interesting interactions between the elements known to be part of the (not yet clearly defined) machineries that work in the TGN-to-PM pathway at different levels. I collected the protein-protein interactions from databases such as STRING (http://string.embl.de/) and from the literature (Fig. 8)

I specifically considered tubulating agents such as Arfaptin, lipid-metabolizing enzymes such as the PI4Ks, and fission proteins such as PKD and BARS. All of these proteins appear to act in the steps shown in Figure 7, but their roles can be overlapping between the boundaries of these steps, and our state-of-the-art knowledge about the boundaries between these machineries is very poor.

For this reason, one of the most important aspects here is the study of the protein-protein interactions that help to better define the molecular machineries. For this reason, I set up two-hybrid assays between the chosen proteins, thus allowing me to enrich the network, as shown in Figure 12. This can also help in our understanding of which proteins of not yet clear function are a part of the process, thus identifying new players in TGN-to-PM trafficking, e.g. Arfaptin and the TRAPP complex.

The use of full-length proteins crossed in a two-hybrid interaction matrix, as carried out in the present work, is much more advantageous, compared to classical two-hybrid library screening, since the correct folding of proteins is much more likely to occur when their polypeptide chains are complete, and not in a randomly truncated form, as in the case of libraries. However, full-length proteins can have regulatory domains that can mask interaction sites.

Out of 13 newly discovered two-hybrid interactions (Table 4.5) I chose to specifically confirm three of them: Arfaptin-PKD, Sedlin-PKD and BARS-PKD, with different approaches, as co-immunoprecipitation for Sedlin-PKD, co-immunoprecipitation, co-localization and kinase assays for Arfaptin-PKD, and kinase assays for BARS-PKD.

Highly connected protein modules are mostly found to be protein complexes that often perform specific biological functions. The concept of protein interaction modules as fundamental functional units was outlined many years ago (Hartwell *et al.*, 1999). Protein interaction modules are composed of a variable number of proteins, with discrete functions that arise from their individual constituents and their synergistic interactions. A multi-protein complex, such as the ribosome, is one common form of interaction module; other examples of protein functional modules include proteins working collectively in a pathway, such as signal transduction proteins, which do not necessarily form tightly associated, stable protein complexes.

From my analysis, PKD turns out to be an important 'hub' that connects many elements of post-Golgi trafficking (Fig. 12). PKD may act not only in fissioning steps, as widely described in literature, but also in the regulation of other machineries that have been implicated in different transport steps, such as Sedlin and Arfaptin, defining their temporal role in GPC formation.

5.2 BARS is a PKD substrate

PKD and BARS have previously been characterized separately into TGN-to-PM trafficking, and the new discovered phosphorylation of BARS *in vitro* opens new possibility relating to our understanding of the actions and regulation of BARS via PKD.

BARS acts in dynamin-independent fission events (Bonazzi *et al.*, 2005), and its better clarified role is in the fission of VSVG-containing carriers involved in TGN-to-PM transport. PKD acts on this pathway by specifically blocking basolateral VSVG transport in MDCK cells when a kinase-dead (KD) mutant is used, and also in COS7

and HeLa cells (Hausser *et al.*, 2005; Bossard *et al.*, 2007). The PKD-KD mutant is effective in blocking the fission of VSVG-containing structures, and acts as a dominant-negative mutant. This phenotype is very similar to what is observed in BARS knock-down, or with its nucleotide binding domain (NBD), which is a dominant-negative domain.

PKD acts on BARS by phosphorylating its NBD domain, which is a dominant-negative domain in transport from the TGN to the PM, once it is microinjected into cells (Bonazzi *et al.*, 2005). This indicates that NBD is relevant for fission, and thus we believe it is not by chance that NBD is the domain of BARS that interacts with PKD in the two-hybrid system, and that it is the most phosphorylated domain *in vitro* compared to other deletion fragments of BARS (Fig. 16). Our hypothesis considers BARS as a substrate of PKD that drives membrane fission. In the future, the identification of specific Ser or Thr residues in BARS that can be phosphorylated by PKD would better clarify the functionality of this interaction.

5.3 PKD regulates Arfaptin activity

Arfaptin is a BAR-domain-containing protein (Peter *et al.*, 2004), and thus it can tubulate TGN membranes and is an interactor of both Arf1 and Arl1. Arl1 is specifically localized at the TGN (Lu and Hong, 2003; Lu *et al.*, 2006), and Arf1 is known to recruit PI4K to the TGN and to activate it (De Matteis and Godi, 2004).

Even if many elements show that Arfaptin is linked to TGN processes, until now the Arfaptin role has remained completely obscure; thus we wanted to investigate its role in transport. We have seen here that its overexpression blocks the exit of VSVG to the PM, even 120 minutes after the release of the 20 °C block (Fig. 24). This

suggests a regulatory role for Arfaptin (Fig. 23 - 24). Separate siRNA silencing of Arfaptins 1 and 2, and of Arfaptins 1 and 2 together did not produce any relevant phenotype in transport (Fig. 25), thus indicating that Arfaptin is not strictly necessary for trafficking and it might be an inhibitory-regulatory component, at least for VSVG trafficking. We cannot exclude other roles of Arfaptin for other cargoes. The absence of effect of siRNA on Arfaptin 1,2 could be also due to an incomplete KD, since a small amount of Arfaptin protein can be sufficient for its function.

Arfaptin localization is TGN-specific, as shown by immunofluorescence (Fig. 21), even in the presence of nocodazole, which forms mini-stacks from the Golgi complex that maintain their *cis* to *trans* orientation.

Even if the formal proof of a role in tubulating of the TGN is missing for Arfaptin, starting from the tubulation activity *in vitro* (Peter *et al.*, 2004), we hypothesize that Arfaptin acts in the first step of GPC formation, which is a step that requires membrane-deformation activity.

The action of Arfaptin on TGN tubules should occur prior to the action of PKD, and thus we conclude that they do not work together at the Golgi complex, but that PKD regulates Arfaptin by 'switching off' its activity, and hence releasing it from TGN membranes, to enter into the system and play its fission role via PI4KIIIβ□□ (Hausser *et al.*, 2005) and BARS, cutting off the mature GPCs. Arfaptin thus may act on the forming GPCs in their initial stages of formation.

Looking at the interaction maps in Figure 12, we can conclude that PKD is a central player that can link this fissioning activity to other functions, such as

membrane bending (Arfaptin). Membrane bending precedes the fission events, and fission can occur in 'hot spots' where the forming GPC is narrow (Polishchuk *et al.*, 2003). At this step, Arfaptin must be removed to let PKD work on those hot spots, possibly phosphorylating BARS exactly at this fissioning site (Fig. 32). According to this model, I have demonstrated that endogenous Arfaptin is displaced from the Golgi complex due to PKD overexpression (Fig. 27), and this makes sense in this context, considering also that Arfaptin is phosphorylated by PKD (Fig. 26). Arfaptin tubulates and prepares the forming GPC for its removal from the parental membranes, through its membrane-bending activity, and it is in turn regulated by PKD, which needs to displace Arfaptin in order to attach to the DAG present at the forming GPC, and to exert its fissioning activity via BARS (Fig. 32). Arfaptin thus has to be removed to allow a GPC to mature, and this can explain the block of VSVG transport to the plasma membrane under Arfaptin overexpression (Figs. 23, 24).

Arfaptin in turn can regulate PKD, allowing its fissioning activity to occur only with well formed intermediates. An unregulated activity of PKD, such as in the case of a constitutively active form of PKD (PKD-CA), promotes vesiculation of the TGN in an uncontrolled way (Bossard *et al.*, 2007). Both Arfaptins 1 and 2 can have tubulating activities, since their BAR domains are conserved (Fig. 18) and they can heterodimerize, as demonstrated by the two-hybrid interactions between Arfaptins 1 and 2 (Table 4.5).

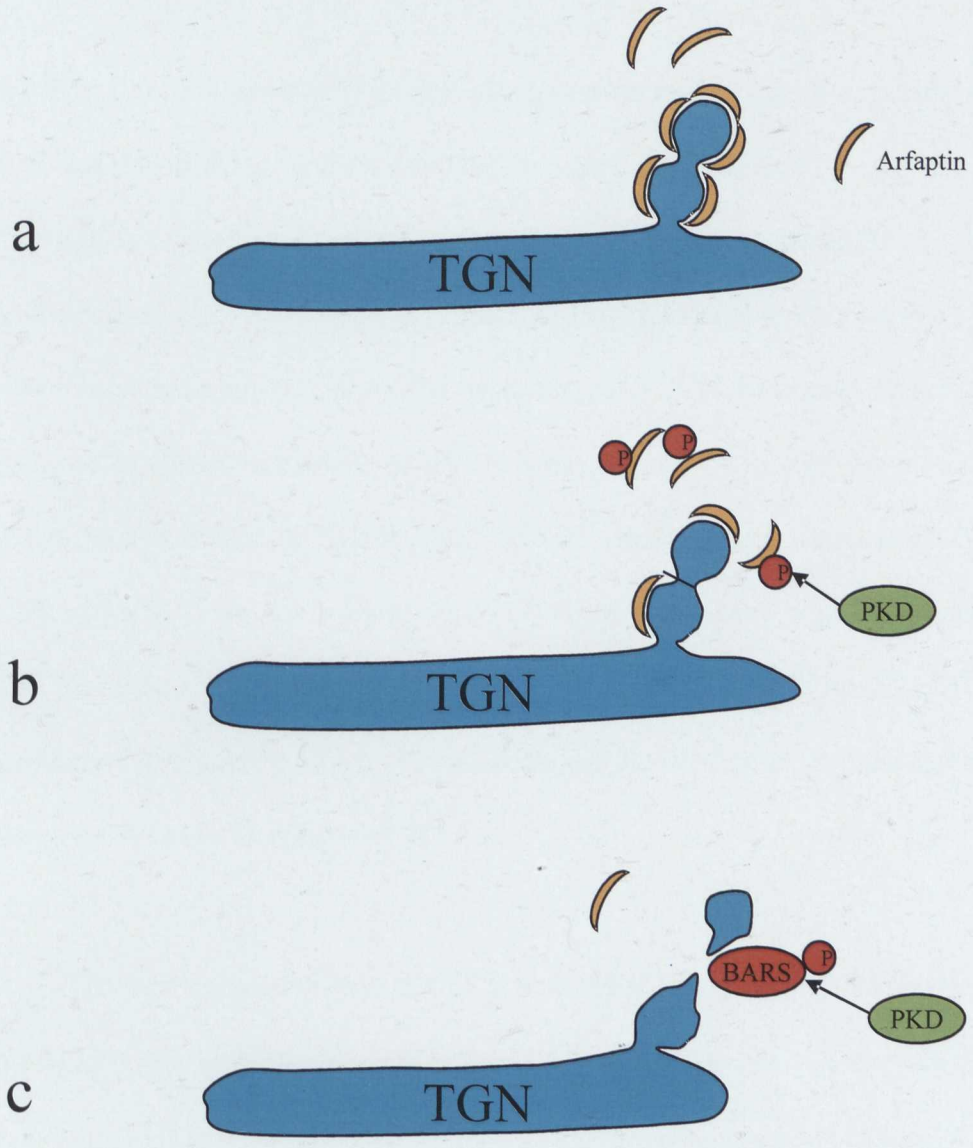

Figure 32. A working model

Into this model, Arfaptin promotes the formation of GPCs (a), while PKD acts later (b), when the GPCs are mature, by phosphorylating Arfaptin, which is thus released from its site of action. BARS, that is phosphorylated by PKD can then freely fission the transport intermediate (c) at the sites previously occupied by Arfaptin. PKD thus has a double role, since it first removes Arfaptin, and then it activate BARS for the fission.

5.4 TRAPP is involved in the TGN-to-PM trafficking of VSVG

TRAPP has been characterized as a tethering protein complex with a specific role in ER-to-Golgi trafficking, both in yeast and in mammals. This now appears not to be the only function of the TRAPP complex since I have here demonstrated for the first time that it is relevant in VSVG transport from the Golgi complex to the PM, since the KD of Bet3 strongly impairs TGN-to-PM trafficking of VSVG. Moreover I have shown that the ER-to-Golgi trafficking of VSVG is not affected by interference of TRAPP, since at the end of a 20 °C block in Bet3 KD cells there was no staining of VSVG in the ER and VSVG arrives in ManII and TGN46 compartments (Fig. 28). Also, the entire TRAPP complex is impaired by knocking-down Bet3, because after siRNA treatment of Bet3, the protein levels of Sedlin and Synbindin are also decreased, as I showed by Western blotting (Fig 30).

The new interaction between PKD and Sedlin, together with the new Synbindin -14-3-3γ □interaction (see Table 4.5) led me to investigate a role for TRAPP in TGN-to-PM transport, which was previously suspected because of the role that TRAPP has in the recycling of Snc1p from early endosomes to the Golgi complex and in the transport of invertase out of the Golgi complex in *S. cerevisiae* (Cai *et al.*, 2005).

At present, nothing is known about the function of the Sedlin-PKD interaction, leaving this to future work for further investigation. Moreover, there are many genetic interactions between the TRAPP components and Pik1p and Ypt31/32, upon which TRAPPII also has GEF activity (Fig. 12). In mammals, TRAPP is involved in TGN-to-PM trafficking as I observed here looking at VSVG transport (Fig. 29). This is true

in chronic Bet3 depletion, and also in acute depletion using Bet3-specific antibodies. The use of Bet3 antibodies was temporally restricted to the end of 20 °C block, to be sure that the VSVG was accumulated inside the Golgi complex.

Sedlin is part of the TRAPP complex and its interaction with PKD is intriguing because it provides additional clues to TRAPP participation in post-Golgi events. Unfortunately, the localization of Sedlin could not be visualized here, and when Sedlin was overexpressed or knocked-down via siRNA, this did not affect VSVG trafficking (data not shown) supporting the concept that Sedlin is an accessory/regulatory factor that might function under an as yet unexplored condition. However, if we want to study the role of the TRAPP complex, it makes more sense to affect the functioning of Bet3, since Bet3 is the physical anchor for TRAPP on the membranes (Turnbull *et al.*, 2005).

In the light of these considerations, it would be interesting to investigate a possible role of PKD as part of TRAPPII in post-Golgi trafficking, even though TRAPPII-specific components in mammals are only putative, on an in-silico basis and with a low homology-score (Cox et al., 2007), and this is not sufficient to definitely establish its existence in mammals.

Considering this possibility, I would postulate that a role for TRAPP in post-Golgi transport is provided by additional specific factor(s) that restrict the field of action of TRAPP to TGN-to-PM transport. This is precisely the case for the yeast TRAPP complex, when the addition of three subunits (Trs65p, Trs120p, Trs130p) switches the specificity of GEF activity from Ypt1p to Ypt31p, and the mutant of one of these (Trs130p) blocks invertase inside the Golgi; one of these factors could be

PKD. PKD is not present in yeast, and this might represent an example of the evolution of TRAPP functions into higher organisms.

Regulation of TRAPP can be mediated by Sedlin, one of its components. Sedlin removal has no effect in transport of VSVG, and its structure is similar to the longin domain, which is the regulatory N-terminus of some SNAREs e.g. Ykt6 (Jang *et al.*, 2002).

The sulphated GAG secretion assay allowed the possibility of looking at an endogenous soluble cargo. Both Sedlin- and Bet3-siRNA-interfered cells showed a slight delay in GAG secretion (Fig. 31), indicating a role in TGN-to-PM for an endogenous cargo that is different from VSVG. GAG molecules are soluble, VSVG is a membrane protein instead. The small effect of the Bet3 KD in GAG secretion contrasts with the large inhibition observed for VSVG. This probably indicates a selective effect on VSVG-containing carriers. The effect of the Sedlin KD that delays GAG secretion at the same rate as Bet3 KD, contrasts with the absence of effects observed on the exit of VSVG (data not shown) during Sedlin KD. This may indicates a selective effect on GAG-containing carriers.

5.5 Concluding remarks for the future

The aim of my project was the identification of new protein-protein interactions between proteins that are implicated in TGN-to-PM transport. Moreover, my PhD project was also focused on the possible discovery of a role in TGN-to-PM for some proteins that have never been characterized as working in this pathway before, such as Arfaptin and the TRAPP complex. Arfaptin probably has a regulatory role, since when

it was overexpressed, it blocked VSVG exit, but since siRNA experiments gave no relevant phenotype, we are not completely sure about its involvement in TGN-to-PM trafficking, which could be dependent on other factors; for this reason, Arfaptin might not be directly involved in TGN-to-PM transport.

The TRAPP complex is necessary for the exit of VSVG from the Golgi complex, since siRNA against Bet3 and anti-Bet3 antibodies blocked the exit of VSVG to the PM. The importance of the Sedlin-PKD interaction is linked to the whole of the TRAPP complex, because from the 'interactome' point of view (see Figure 12), the TRAPP complex can be related to late-Golgi trafficking steps, and in yeast, also functionally (see section 4.4.3). The Bet3 component of the TRAPP complex is a key element (both in mammals and in yeast), since its depletion destabilizes the complex, and the other components are then proteolitically degraded (Fig. 30). From the crystal structure, it is also clear that this central role for Bet3 is important for both membrane anchoring and catalytic activity as a GEF for Ypt1p (Kim *et al.*, 2006; Cai *et al.*, 2008).

PKD is a part of the same pathway in which BARS works; thus the identification of BARS as a PKD substrate, at least *in vitro,* is an important finding. The phosphorylation of BARS needs to be further confirmed *in vivo,* to clearly confirm its role downstream of PKD; moreover, the identification of phosphorylated residues is necessary, to go deeper into the functionality of this PKD-BARS interaction.

Considering the many interesting interactions of the several important players involved in TGN-to-PM transport, another major challenge will be the understanding

of how the sorting and trafficking processes at the TGN are regulated. For future work, the study of modular elements, such as PKD, will help experimental design for the perturbation of more than one element at time, with systematic double siRNA interference assays looking at transport or at Golgi morphology on a high-throughput basis. This is what is routinely carried out in yeast for genetic interactions, looking at the viability of double mutants.

Ang, A.L., Folsch, H., Koivisto, U.M., Pypaert, M., and Mellman, I. (2003). The Rab8 GTPase selectively regulates AP-1B-dependent basolateral transport in polarized Madin-Darby canine kidney cells. J Cell Biol *163*, 339-350.

Au, J.S., Puri, C., Ihrke, G., Kendrick-Jones, J., and Buss, F. (2007). Myosin VI is required for sorting of AP-1B-dependent cargo to the basolateral domain in polarized MDCK cells. J Cell Biol *177*, 103-114.

Barlowe, C., d'Enfert, C., and Schekman, R. (1993). Purification and characterization of SAR1p, a small GTP-binding protein required for transport vesicle formation from the endoplasmic reticulum. J Biol Chem *268*, 873-879.

Beraud-Dufour, S., and Balch, W.E. (2001). Structural and functional organization of ADP-ribosylation factor (ARF) proteins. Methods Enzymol *329*, 245-247.

Bonazzi, M., Spano, S., Turacchio, G., Cericola, C., Valente, C., Colanzi, A., Kweon, H.S., Hsu, V.W., Polishchuck, E.V., Polishchuck, R.S., Sallese, M., Pulvirenti, T., Corda, D., and Luini, A. (2005). CtBP3/BARS drives membrane fission in dynamin-independent transport pathways. Nat Cell Biol *7*, 570-580.

Bonifacino, J.S., and Lippincott-Schwartz, J. (2003). Coat proteins: shaping membrane transport. Nat Rev Mol Cell Biol *4*, 409-414.

Bonifacino, J.S., and Rojas, R. (2006). Retrograde transport from endosomes to the trans-Golgi network. Nat Rev Mol Cell Biol *7*, 568-579.

Bossard, C., Bresson, D., Polishchuk, R.S., and Malhotra, V. (2007). Dimeric PKD regulates membrane fission to form transport carriers at the TGN. J Cell Biol *179*, 1123-1131.

Buccione, R., Bannykh, S., Santone, I., Baldassarre, M., Facchiano, F., Bozzi, Y., Di Tullio, G., Mironov, A., Luini, A., and De Matteis, M.A. (1996). Regulation of constitutive exocytic transport by membrane receptors. A biochemical and morphometric study. J Biol Chem *271*, 3523-3533.

Burd, C.G., Strochlic, T.I., and Gangi Setty, S.R. (2004). Arf-like GTPases: not so Arf-like after all. Trends Cell Biol *14*, 687-694.

Burguete, A.S., Fenn, T.D., Brunger, A.T., and Pfeffer, S.R. (2008). Rab and Arl GTPase family members cooperate in the localization of the golgin GCC185. Cell *132*, 286-298.

Cai, H., Zhang, Y., Pypaert, M., Walker, L., and Ferro-Novick, S. (2005). Mutants in trs120 disrupt traffic from the early endosome to the late Golgi. J Cell Biol *171*, 823-833.

Cai, Y., Chin, H.F., Lazarova, D., Menon, S., Fu, C., Cai, H., Sclafani, A., Rodgers, D.W., De La Cruz, E.M., Ferro-Novick, S., and Reinisch, K.M. (2008). The structural basis for activation of the Rab Ypt1p by the TRAPP membrane-tethering complexes. Cell *133*, 1202-1213.

Chen, W., Feng, Y., Chen, D., and Wandinger-Ness, A. (1998). Rab11 is required for trans-golgi network-to-plasma membrane transport and a preferential target for GDP dissociation inhibitor. Mol Biol Cell *9*, 3241-3257.

Chinnadurai, G. (2002). CtBP, an unconventional transcriptional corepressor in development and oncogenesis. Mol Cell *9*, 213-224.

Cohen, D., Musch, A., and Rodriguez-Boulan, E. (2001). Selective control of basolateral membrane protein polarity by cdc42. Traffic *2*, 556-564.

Cox, R., Chen, S.H., Yoo, E., and Segev, N. (2007). Conservation of the TRAPPII-specific subunits of a Ypt/Rab exchanger complex. BMC Evol Biol *7*, 12.

D'Angelo, G., Polishchuk, E., Di Tullio, G., Santoro, M., Di Campli, A., Godi, A., West, G., Bielawski, J., Chuang, C.C., van der Spoel, A.C., Platt, F.M., Hannun, Y.A., Polishchuk, R., Mattjus, P., and De Matteis, M.A. (2007). Glycosphingolipid synthesis requires FAPP2 transfer of glucosylceramide. Nature *449*, 62-67.

De Matteis, M.A., and Godi, A. (2004). PI-loting membrane traffic. Nat Cell Biol *6*, 487-492.

De Matteis, M.A., and Luini, A. (2008). Exiting the Golgi complex. Nat Rev Mol Cell Biol *9*, 273-284.

Deborde, S., Perret, E., Gravotta, D., Deora, A., Salvarezza, S., Schreiner, R., and Rodriguez-Boulan, E. (2008). Clathrin is a key regulator of basolateral polarity. Nature *452*, 719-723.

Diaz Anel, A.M., and Malhotra, V. (2005). PKCeta is required for beta1gamma2/beta3gamma2- and PKD-mediated transport to the cell surface and the organization of the Golgi apparatus. J Cell Biol *169*, 83-91.

Donaldson, J.G., Honda, A., and Weigert, R. (2005). Multiple activities for Arf1 at the Golgi complex. Biochim Biophys Acta *1744*, 364-373.

Doolittle, W.F. (2000). Uprooting the tree of life. Sci Am *282*, 90-95.

Egea, G., Lazaro-Dieguez, F., and Vilella, M. (2006). Actin dynamics at the Golgi complex in mammalian cells. Curr Opin Cell Biol *18*, 168-178.

Ellgaard, L., and Helenius, A. (2003). Quality control in the endoplasmic reticulum. Nat Rev Mol Cell Biol *4*, 181-191.

Erickson, J.W., Zhang, C., Kahn, R.A., Evans, T., and Cerione, R.A. (1996). Mammalian Cdc42 is a brefeldin A-sensitive component of the Golgi apparatus. J Biol Chem *271*, 26850-26854.

Farsad, K., Ringstad, N., Takei, K., Floyd, S.R., Rose, K., and De Camilli, P. (2001). Generation of high curvature membranes mediated by direct endophilin bilayer interactions. J Cell Biol *155*, 193-200.

Fugmann, T., Hausser, A., Schoffler, P., Schmid, S., Pfizenmaier, K., and Olayioye, M.A. (2007). Regulation of secretory transport by protein kinase D-mediated phosphorylation of the ceramide transfer protein. J Cell Biol *178*, 15-22.

Gavin, A.C., Bosche, M., Krause, R., Grandi, P., Marzioch, M., Bauer, A., Schultz, J., Rick, J.M., Michon, A.M., Cruciat, C.M., Remor, M., Hofert, C., Schelder, M., Brajenovic, M., Ruffner, H., Merino, A., Klein, K., Hudak, M., Dickson, D., Rudi, T.,

Gnau, V., Bauch, A., Bastuck, S., Huhse, B., Leutwein, C., Heurtier, M.A., Copley, R.R., Edelmann, A., Querfurth, E., Rybin, V., Drewes, G., Raida, M., Bouwmeester, T., Bork, P., Seraphin, B., Kuster, B., Neubauer, G., and Superti-Furga, G. (2002). Functional organization of the yeast proteome by systematic analysis of protein complexes. Nature *415*, 141-147.

Gillingham, A.K., and Munro, S. (2007). The small G proteins of the Arf family and their regulators. Annu Rev Cell Dev Biol *23*, 579-611.

Gleeson, P.A., Lock, J.G., Luke, M.R., and Stow, J.L. (2004). Domains of the TGN: coats, tethers and G proteins. Traffic *5*, 315-326.

Godi, A., Di Campli, A., Konstantakopoulos, A., Di Tullio, G., Alessi, D.R., Kular, G.S., Daniele, T., Marra, P., Lucocq, J.M., and De Matteis, M.A. (2004). FAPPs control Golgi-to-cell-surface membrane traffic by binding to ARF and PtdIns(4)P. Nat Cell Biol *6*, 393-404.

Goldenring, J.R., Smith, J., Vaughan, H.D., Cameron, P., Hawkins, W., and Navarre, J. (1996). Rab11 is an apically located small GTP-binding protein in epithelial tissues. Am J Physiol *270*, G515-525.

Griffiths, G., Ericsson, M., Krijnse-Locker, J., Nilsson, T., Goud, B., Soling, H.D., Tang, B.L., Wong, S.H., and Hong, W. (1994). Localization of the Lys, Asp, Glu, Leu tetrapeptide receptor to the Golgi complex and the intermediate compartment in mammalian cells. J Cell Biol *127*, 1557-1574.

Griffiths, G., Fuller, S.D., Back, R., Hollinshead, M., Pfeiffer, S., and Simons, K. (1989). The dynamic nature of the Golgi complex. J Cell Biol *108*, 277-297.

Griffiths, G., and Simons, K. (1986). The trans Golgi network: sorting at the exit site of the Golgi complex. Science *234*, 438-443.

Grigoriev, I., Splinter, D., Keijzer, N., Wulf, P.S., Demmers, J., Ohtsuka, T., Modesti, M., Maly, I.V., Grosveld, F., Hoogenraad, C.C., and Akhmanova, A. (2007). Rab6 regulates transport and targeting of exocytotic carriers. Dev Cell *13*, 305-314.

Hartwell, L.H., Hopfield, J.J., Leibler, S., and Murray, A.W. (1999). From molecular to modular cell biology. Nature *402*, C47-52.

Hattula, K., and Peranen, J. (2000). FIP-2, a coiled-coil protein, links Huntingtin to Rab8 and modulates cellular morphogenesis. Curr Biol *10*, 1603-1606.

Hausser, A., Link, G., Hoene, M., Russo, C., Selchow, O., and Pfizenmaier, K. (2006). Phospho-specific binding of 14-3-3 proteins to phosphatidylinositol 4-kinase III beta protects from dephosphorylation and stabilizes lipid kinase activity. J Cell Sci *119*, 3613-3621.

Hausser, A., Storz, P., Martens, S., Link, G., Toker, A., and Pfizenmaier, K. (2005). Protein kinase D regulates vesicular transport by phosphorylating and activating phosphatidylinositol-4 kinase IIIbeta at the Golgi complex. Nat Cell Biol *7*, 880-886.

Haworth, R.S., Cuello, F., Herron, T.J., Franzen, G., Kentish, J.C., Gautel, M., and Avkiran, M. (2004). Protein kinase D is a novel mediator of cardiac troponin I phosphorylation and regulates myofilament function. Circ Res *95*, 1091-1099.

Haynes, L.P., Thomas, G.M., and Burgoyne, R.D. (2005). Interaction of neuronal calcium sensor-1 and ADP-ribosylation factor 1 allows bidirectional control of phosphatidylinositol 4-kinase beta and trans-Golgi network-plasma membrane traffic. J Biol Chem *280*, 6047-6054.

Ho, W.T., Exton, J.H., and Williger, B.T. (2003). Arfaptin 1 inhibits ADP-ribosylation factor-dependent matrix metalloproteinase-9 secretion induced by phorbol ester in HT 1080 fibrosarcoma cells. FEBS Lett *537*, 91-95.

Holthuis, J.C., and Levine, T.P. (2005). Lipid traffic: floppy drives and a superhighway. Nat Rev Mol Cell Biol *6*, 209-220.

Ito, T., Chiba, T., Ozawa, R., Yoshida, M., Hattori, M., and Sakaki, Y. (2001). A comprehensive two-hybrid analysis to explore the yeast protein interactome. Proc Natl Acad Sci U S A *98*, 4569-4574.

Jang, S.B., Kim, Y.G., Cho, Y.S., Suh, P.G., Kim, K.H., and Oh, B.H. (2002). Crystal structure of SEDL and its implications for a genetic disease spondyloepiphyseal dysplasia tarda. J Biol Chem *277*, 49863-49869.

Jaulin, F., Xue, X., Rodriguez-Boulan, E., and Kreitzer, G. (2007). Polarization-dependent selective transport to the apical membrane by KIF5B in MDCK cells. Dev Cell *13*, 511-522.

Kaiser, C.A., and Schekman, R. (1990). Distinct sets of SEC genes govern transport vesicle formation and fusion early in the secretory pathway. Cell *61*, 723-733.

Keller, P., and Simons, K. (1997). Post-Golgi biosynthetic trafficking. J Cell Sci *110 (Pt 24)*, 3001-3009.

Kim, Y.G., Raunser, S., Munger, C., Wagner, J., Song, Y.L., Cygler, M., Walz, T., Oh, B.H., and Sacher, M. (2006). The architecture of the multisubunit TRAPP I complex suggests a model for vesicle tethering. Cell *127*, 817-830.

Kreitzer, G., Marmorstein, A., Okamoto, P., Vallee, R., and Rodriguez-Boulan, E. (2000). Kinesin and dynamin are required for post-Golgi transport of a plasma-membrane protein. Nat Cell Biol *2*, 125-127.

Kroschewski, R., Hall, A., and Mellman, I. (1999). Cdc42 controls secretory and endocytic transport to the basolateral plasma membrane of MDCK cells. Nat Cell Biol *1*, 8-13.

Ktistakis, N.T., Delon, C., Manifava, M., Wood, E., Ganley, I., and Sugars, J.M. (2003). Phospholipase D1 and potential targets of its hydrolysis product, phosphatidic acid. Biochem Soc Trans *31*, 94-97.

Ladinsky, M.S., Wu, C.C., McIntosh, S., McIntosh, J.R., and Howell, K.E. (2002). Structure of the Golgi and distribution of reporter molecules at 20 degrees C reveals the complexity of the exit compartments. Mol Biol Cell *13*, 2810-2825.

Letourneur, F., Gaynor, E.C., Hennecke, S., Demolliere, C., Duden, R., Emr, S.D., Riezman, H., and Cosson, P. (1994). Coatomer is essential for retrieval of dilysine-tagged proteins to the endoplasmic reticulum. Cell *79*, 1199-1207.

Levine, T., and Loewen, C. (2006). Inter-organelle membrane contact sites: through a glass, darkly. Curr Opin Cell Biol *18*, 371-378.

Liang, Y., Morozova, N., Tokarev, A.A., Mulholland, J.W., and Segev, N. (2007). The role of Trs65 in the Ypt/Rab guanine nucleotide exchange factor function of the TRAPP II complex. Mol Biol Cell *18*, 2533-2541.

Liljedahl, M., Maeda, Y., Colanzi, A., Ayala, I., Van Lint, J., and Malhotra, V. (2001). Protein kinase D regulates the fission of cell surface destined transport carriers from the trans-Golgi network. Cell *104*, 409-420.

Litvak, V., Dahan, N., Ramachandran, S., Sabanay, H., and Lev, S. (2005). Maintenance of the diacylglycerol level in the Golgi apparatus by the Nir2 protein is critical for Golgi secretory function. Nat Cell Biol *7*, 225-234.

Lock, J.G., and Stow, J.L. (2005). Rab11 in recycling endosomes regulates the sorting and basolateral transport of E-cadherin. Mol Biol Cell *16*, 1744-1755.

Loh, E., Peter, F., Subramaniam, V.N., and Hong, W. (2005). Mammalian Bet3 functions as a cytosolic factor participating in transport from the ER to the Golgi apparatus. J Cell Sci *118*, 1209-1222.

Lu, L., and Hong, W. (2003). Interaction of Arl1-GTP with GRIP domains recruits autoantigens Golgin-97 and Golgin-245/p230 onto the Golgi. Mol Biol Cell *14*, 3767-3781.

Lu, L., Tai, G., Wu, M., Song, H., and Hong, W. (2006). Multilayer interactions determine the Golgi localization of GRIP golgins. Traffic *7*, 1399-1407.

Luini, A., Mironov, A.A., Polishchuk, E.V., and Polishchuk, R.S. (2008). Morphogenesis of post-Golgi transport carriers. Histochem Cell Biol *129*, 153-161.

Luini, A., Ragnini-Wilson, A., Polishchuck, R.S., and De Matteis, M.A. (2005). Large pleiomorphic traffic intermediates in the secretory pathway. Curr Opin Cell Biol *17*, 353-361.

Maeda, Y., Beznoussenko, G.V., Van Lint, J., Mironov, A.A., and Malhotra, V. (2001). Recruitment of protein kinase D to the trans-Golgi network via the first cysteine-rich domain. Embo J *20*, 5982-5990.

Manifava, M., Thuring, J.W., Lim, Z.Y., Packman, L., Holmes, A.B., and Ktistakis, N.T. (2001). Differential binding of traffic-related proteins to phosphatidic acid- or phosphatidylinositol (4,5)- bisphosphate-coupled affinity reagents. J Biol Chem *276*, 8987-8994.

McNiven, M.A., Cao, H., Pitts, K.R., and Yoon, Y. (2000). The dynamin family of mechanoenzymes: pinching in new places. Trends Biochem Sci *25*, 115-120.

Menon, S., Cai, H., Lu, H., Dong, G., Cai, Y., Reinisch, K., and Ferro-Novick, S. (2006). mBET3 is required for the organization of the TRAPP complexes. Biochem Biophys Res Commun *350*, 669-677.

Mironov, A.A., Mironov, A.A., Jr., Beznoussenko, G.V., Trucco, A., Lupetti, P., Smith, J.D., Geerts, W.J., Koster, A.J., Burger, K.N., Martone, M.E., Deerinck, T.J.,

Ellisman, M.H., and Luini, A. (2003). ER-to-Golgi carriers arise through direct en bloc protrusion and multistage maturation of specialized ER exit domains. Dev Cell *5*, 583-594.

Mogelsvang, S., Marsh, B.J., Ladinsky, M.S., and Howell, K.E. (2004). Predicting function from structure: 3D structure studies of the mammalian Golgi complex. Traffic *5*, 338-345.

Munro, S. (2005). The Arf-like GTPase Arl1 and its role in membrane traffic. Biochem Soc Trans *33*, 601-605.

Musch, A., Cohen, D., Kreitzer, G., and Rodriguez-Boulan, E. (2001). cdc42 regulates the exit of apical and basolateral proteins from the trans-Golgi network. Embo J *20*, 2171-2179.

Nakata, T., and Hirokawa, N. (2003). Microtubules provide directional cues for polarized axonal transport through interaction with kinesin motor head. J Cell Biol *162*, 1045-1055.

Neubrand, V.E., Will, R.D., Mobius, W., Poustka, A., Wiemann, S., Schu, P., Dotti, C.G., Pepperkok, R., and Simpson, J.C. (2005). Gamma-BAR, a novel AP-1-interacting protein involved in post-Golgi trafficking. Embo J *24*, 1122-1133.

Novikoff, A.B., and Novikoff, P.M. (1977). Cytochemical contributions to differentiating GERL from the Golgi apparatus. Histochem J *9*, 525-551.

Orth, J.D., and McNiven, M.A. (2003). Dynamin at the actin-membrane interface. Curr Opin Cell Biol *15*, 31-39.

Pelham, H.R. (1994). About turn for the COPs? Cell *79*, 1125-1127.

Pepperkok, R., Scheel, J., Horstmann, H., Hauri, H.P., Griffiths, G., and Kreis, T.E. (1993). Beta-COP is essential for biosynthetic membrane transport from the endoplasmic reticulum to the Golgi complex in vivo. Cell *74*, 71-82.

Perry, R.J., and Ridgway, N.D. (2005). Molecular mechanisms and regulation of ceramide transport. Biochim Biophys Acta *1734*, 220-234.

Peter, B.J., Kent, H.M., Mills, I.G., Vallis, Y., Butler, P.J., Evans, P.R., and McMahon, H.T. (2004). BAR domains as sensors of membrane curvature: the amphiphysin BAR structure. Science *303*, 495-499.

Polishchuk, E.V., Di Pentima, A., Luini, A., and Polishchuk, R.S. (2003). Mechanism of constitutive export from the golgi: bulk flow via the formation, protrusion, and en bloc cleavage of large trans-golgi network tubular domains. Mol Biol Cell *14*, 4470-4485.

Pulvirenti, T., Giannotta, M., Capestrano, M., Capitani, M., Pisanu, A., Polishchuk, R.S., San Pietro, E., Beznoussenko, G.V., Mironov, A.A., Turacchio, G., Hsu, V.W., Sallese, M., and Luini, A. (2008). A traffic-activated Golgi-based signalling circuit coordinates the secretory pathway. Nat Cell Biol *10*, 912-922.

Robinson, M.S. (2004). Adaptable adaptors for coated vesicles. Trends Cell Biol *14*, 167-174.

Rosso, S., Bollati, F., Bisbal, M., Peretti, D., Sumi, T., Nakamura, T., Quiroga, S., Ferreira, A., and Caceres, A. (2004). LIMK1 regulates Golgi dynamics, traffic of Golgi-derived vesicles, and process extension in primary cultured neurons. Mol Biol Cell *15*, 3433-3449.

Roth, M.G., Bi, K., Ktistakis, N.T., and Yu, S. (1999). Phospholipase D as an effector for ADP-ribosylation factor in the regulation of vesicular traffic. Chem Phys Lipids *98*, 141-152.

Roux, A., Cappello, G., Cartaud, J., Prost, J., Goud, B., and Bassereau, P. (2002). A minimal system allowing tubulation with molecular motors pulling on giant liposomes. Proc Natl Acad Sci U S A *99*, 5394-5399.

Roux, A., Uyhazi, K., Frost, A., and De Camilli, P. (2006). GTP-dependent twisting of dynamin implicates constriction and tension in membrane fission. Nature *441*, 528-531.

Rual, J.F., Venkatesan, K., Hao, T., Hirozane-Kishikawa, T., Dricot, A., Li, N., Berriz, G.F., Gibbons, F.D., Dreze, M., Ayivi-Guedehoussou, N., Klitgord, N., Simon, C., Boxem, M., Milstein, S., Rosenberg, J., Goldberg, D.S., Zhang, L.V., Wong, S.L., Franklin, G., Li, S., Albala, J.S., Lim, J., Fraughton, C., Llamosas, E., Cevik, S., Bex, C., Lamesch, P., Sikorski, R.S., Vandenhaute, J., Zoghbi, H.Y., Smolyar, A., Bosak, S., Sequerra, R., Doucette-Stamm, L., Cusick, M.E., Hill, D.E., Roth, F.P., and Vidal, M. (2005). Towards a proteome-scale map of the human protein-protein interaction network. Nature *437*, 1173-1178.

Sacher, M., Barrowman, J., Schieltz, D., Yates, J.R., 3rd, and Ferro-Novick, S. (2000). Identification and characterization of five new subunits of TRAPP. Eur J Cell Biol *79*, 71-80.

Sacher, M., Jiang, Y., Barrowman, J., Scarpa, A., Burston, J., Zhang, L., Schieltz, D., Yates, J.R., 3rd, Abeliovich, H., and Ferro-Novick, S. (1998). TRAPP, a highly conserved novel complex on the cis-Golgi that mediates vesicle docking and fusion. Embo J *17*, 2494-2503.

Sahlender, D.A., Roberts, R.C., Arden, S.D., Spudich, G., Taylor, M.J., Luzio, J.P., Kendrick-Jones, J., and Buss, F. (2005). Optineurin links myosin VI to the Golgi complex and is involved in Golgi organization and exocytosis. J Cell Biol *169*, 285-295.

Sannerud, R., Saraste, J., and Goud, B. (2003). Retrograde traffic in the biosynthetic-secretory route: pathways and machinery. Curr Opin Cell Biol *15*, 438-445.

Sato, T., Mushiake, S., Kato, Y., Sato, K., Sato, M., Takeda, N., Ozono, K., Miki, K., Kubo, Y., Tsuji, A., Harada, R., and Harada, A. (2007). The Rab8 GTPase regulates apical protein localization in intestinal cells. Nature *448*, 366-369.

Schekman, R., and Orci, L. (1996). Coat proteins and vesicle budding. Science *271*, 1526-1533.

Sciorra, V.A., Audhya, A., Parsons, A.B., Segev, N., Boone, C., and Emr, S.D. (2005). Synthetic genetic array analysis of the PtdIns 4-kinase Pik1p identifies components in a Golgi-specific Ypt31/rab-GTPase signaling pathway. Mol Biol Cell *16*, 776-793.

Shaw, M.A., Brunetti-Pierri, N., Kadasi, L., Kovacova, V., Van Maldergem, L., De Brasi, D., Salerno, M., and Gecz, J. (2003). Identification of three novel SEDL mutations, including mutation in the rare, non-canonical splice site of exon 4. Clin Genet *64*, 235-242.

Shemesh, T., Luini, A., Malhotra, V., Burger, K.N., and Kozlov, M.M. (2003). Prefission constriction of Golgi tubular carriers driven by local lipid metabolism: a theoretical model. Biophys J *85*, 3813-3827.

Shin, H.W., and Nakayama, K. (2004). Dual control of membrane targeting by PtdIns(4)P and ARF. Trends Biochem Sci *29*, 513-515.

Stinchcombe, J.C., Nomoto, H., Cutler, D.F., and Hopkins, C.R. (1995). Anterograde and retrograde traffic between the rough endoplasmic reticulum and the Golgi complex. J Cell Biol *131*, 1387-1401.

Tarricone, C., Xiao, B., Justin, N., Walker, P.A., Rittinger, K., Gamblin, S.J., and Smerdon, S.J. (2001). The structural basis of Arfaptin-mediated cross-talk between Rac and Arf signalling pathways. Nature *411*, 215-219.

Thomas, G. (2002). Furin at the cutting edge: from protein traffic to embryogenesis and disease. Nat Rev Mol Cell Biol *3*, 753-766.

Tooze, S.A. (1998). Biogenesis of secretory granules in the trans-Golgi network of neuroendocrine and endocrine cells. Biochim Biophys Acta *1404*, 231-244.

Traub, L.M., and Kornfeld, S. (1997). The trans-Golgi network: a late secretory sorting station. Curr Opin Cell Biol *9*, 527-533.

Trucco, A., Polishchuk, R.S., Martella, O., Di Pentima, A., Fusella, A., Di Giandomenico, D., San Pietro, E., Beznoussenko, G.V., Polishchuk, E.V., Baldassarre, M., Buccione, R., Geerts, W.J., Koster, A.J., Burger, K.N., Mironov, A.A., and Luini, A. (2004). Secretory traffic triggers the formation of tubular continuities across Golgi sub-compartments. Nat Cell Biol *6*, 1071-1081.

Turnbull, A.P., Kummel, D., Prinz, B., Holz, C., Schultchen, J., Lang, C., Niesen, F.H., Hofmann, K.P., Delbruck, H., Behlke, J., Muller, E.C., Jarosch, E., Sommer, T., and Heinemann, U. (2005). Structure of palmitoylated BET3: insights into TRAPP complex assembly and membrane localization. Embo J *24*, 875-884.

Ullrich, O., Reinsch, S., Urbe, S., Zerial, M., and Parton, R.G. (1996). Rab11 regulates recycling through the pericentriolar recycling endosome. J Cell Biol *135*, 913-924.

Van Valkenburgh, H., Shern, J.F., Sharer, J.D., Zhu, X., and Kahn, R.A. (2001). ADP-ribosylation factors (ARFs) and ARF-like 1 (ARL1) have both specific and shared effectors: characterizing ARL1-binding proteins. J Biol Chem *276*, 22826-22837.

Vuong, T.T., Prydz, K., and Tveit, H. (2006). Differences in the apical and basolateral pathways for glycosaminoglycan biosynthesis in Madin-Darby canine kidney cells. Glycobiology *16*, 326-332.

Wang, Q.J. (2006). PKD at the crossroads of DAG and PKC signaling. Trends Pharmacol Sci *27*, 317-323.

Weigert, R., Silletta, M.G., Spano, S., Turacchio, G., Cericola, C., Colanzi, A., Senatore, S., Mancini, R., Polishchuk, E.V., Salmona, M., Facchiano, F., Burger, K.N., Mironov, A., Luini, A., and Corda, D. (1999). CtBP/BARS induces fission of Golgi membranes by acylating lysophosphatidic acid. Nature *402*, 429-433.

Williger, B.T., Ostermann, J., and Exton, J.H. (1999). Arfaptin 1, an ARF-binding protein, inhibits phospholipase D and endoplasmic reticulum/Golgi protein transport. FEBS Lett *443*, 197-200.

Yeaman, C., Ayala, M.I., Wright, J.R., Bard, F., Bossard, C., Ang, A., Maeda, Y., Seufferlein, T., Mellman, I., Nelson, W.J., and Malhotra, V. (2004). Protein kinase D regulates basolateral membrane protein exit from trans-Golgi network. Nat Cell Biol *6*, 106-112.

Yu, S., Satoh, A., Pypaert, M., Mullen, K., Hay, J.C., and Ferro-Novick, S. (2006). mBet3p is required for homotypic COPII vesicle tethering in mammalian cells. J Cell Biol *174*, 359-368.

Zhong, J., Zhang, H., Stanyon, C.A., Tromp, G., and Finley, R.L., Jr. (2003). A strategy for constructing large protein interaction maps using the yeast two-hybrid system: regulated expression arrays and two-phase mating. Genome Res *13*, 2691-2699.

Zimmerberg, J., and Kozlov, M.M. (2006). How proteins produce cellular membrane curvature. Nat Rev Mol Cell Biol *7*, 9-19.

Aknowledgements

I would like to thank my two supervisors Antonella De Matteis and Alberto Luini, this last being my Director of Studies, for their support and helpful discussions during the course of this work and for their help in writing this thesis. I would like to thank also my External Supervisor Gillian Griffiths for helpful discussions and for thesis reviewing.

I would like to thank also Cathal Wilson for many stimulating conversations during the course of these investigations.

I am particularly grateful to Chris Berrie for his intensive support during the writing of this thesis.

Thanks go to Giuseppe Di Tullio and Michele Santoro for their technical assistance and critical discussions about several methodologies used in this work.

Thanks also to Roberto Buccione and to Rosanna Tucci for their assistance and management during the PhD course and to all my colleagues that helped me in different ways in different aspects of this work.